The Columbia River estuary and plume: natural variability, anthropogenic change and physical habitat for salmon

Michela Burla

Laurea (M.Sc.), Civil and Environmental Engineering, Polytechnic of Milan (Milan, Italy), 1997

A dissertation presented to the faculty of the
Department of Science and Engineering, School of Medicine,
at Oregon Health & Science University
in partial fulfillment of the
requirements for the degree of
Doctor of Philosophy
in
Environmental Science and Engineering

December 2009

The dissertation “The Columbia River estuary and plume: natural variability, anthropogenic change and physical habitat for salmon” by Michela Burla has been examined and approved by the following Examination Committee:

_____

Dr. António M. Baptista, Professor

Dissertation Research Advisor

NSF Center for Coastal Margin Observation and Prediction

Oregon Health and Science University

_____

Dr. Tawnya Peterson

NSF Center for Coastal Margin Observation and Prediction

Oregon Health and Science University

_____

Dr. Edmundo Casillas

Northwest Fisheries Science Center

NOAA Fisheries Service

_____

Daniel L. Bottom, M. Sc.

Northwest Fisheries Science Center

NOAA Fisheries Service

DEDICATION

To all those who have given me the gift of their friendship,

their time and words of wisdom, making this journey possible

ACKNOWLEDGMENTS

Due to its interdisciplinary nature, this research would have not been possible without the advice and collaboration of so many people. First of all, I would like to thank my advisor, Prof. António M. Baptista, for his continuous guidance and support of many years. I am also extremely grateful to Dr. Edmundo Casillas, for many insightful comments and questions, and for giving me access to other NOAA researchers and data; Daniel L. Bottom, from whom I have learned, through illuminating discussions, about salmon ecology and resilience; Dr. John G. Williams, for his constructive and attentive feedback during my investigation of the potential relationships between the Columbia River plume environment and salmon survival; and Charles A. Simenstad, whose feedback helped me improve the analysis of salmon habitat opportunity in the Columbia River estuary. It is thanks to them that I have been able to integrate the biological perspective into the research.

I would also like to acknowledge Dr. Yinglong Zhang, who, with Prof. Baptista, has led the development of the current CORIE/SATURN modeling capabilities, and the generation of the multi-year simulation databases, without which none of my work would have been possible; and Charles Seaton and Paul Turner, for their contributions to generating the CORIE/SATURN circulation databases and related information products. Charles has also been instrumental in generating the model grids that have allowed the comparison of modern and historical bathymetric conditions in the Columbia River estuary in the study of salmon habitat opportunity, but I am especially thankful to him for the many invaluable discussions on data processing and visualization. I am thankful as

well to Dr. Sergey Frolov, not only for developing the algorithmic solution that made it possible for me to perform an EOF analysis of the large CORIE/SATURN simulation datasets, but also for sharing our years as doctoral students with Prof. Baptista.

Finally, I would like to thank Douglas M. Marsh (NOAA Northwest Fisheries Science Center), who generated and made available the smolt-to-adult return rate data that made it possible to pursue the research presented in Chapter 3; Jen Burke (School of Aquatic and Fisheries Science, UW), for providing the data for the reconstructed historical bathymetry used in the scenario comparison in Chapter 4; and Mike Wilkin and other field crew for their effort in maintaining CORIE/SATURN observational network.

Funding for this research was provided in part by the National Oceanic and Atmospheric Administration (AB133F-04-CN-0033) and the National Science Foundation (ACI-0121475; OCE-0622278; OCE-0424602).

TABLE OF CONTENTS

List of Tables

List of figures

Chapter 1

Introduction

1.1 The Columbia River estuary and salmon

At the center of the human and economic development of the U.S. Pacific Northwest region, the Columbia River (CR) and its tributaries drain a basin that is about the size of France, and covers major portions of the states of Oregon, Washington and Idaho, as well as extending into the Canadian Province of British Columbia, into western Montana and small parts of Nevada, Utah, and Wyoming (Lichatowich 1999; Williams 2006). Discharging into the Northeast Pacific, the CR effluent forms a plume of waters fresher than ocean salinity that influences ocean circulation and biological productivity off the Oregon and Washington coasts, from the California border to the Strait of Juan de Fuca (Barnes et al. 1972; Hickey et al. 1998; Hickey and Banas 2003; Hickey et al. 2005). The CR estuary, from the head of the tide, 234 km upstream of the river mouth, to the near-field of the plume, forms a physical continuum that is also believed to provide a continuum of habitats critical to support salmon populations in their transition from the freshwater to the marine environment (Fresh et al. 2005).

Salmon is an essential part of the cultural fabrics of the U.S. Pacific Northwest. The CR basin historically produced the largest runs of Chinook salmon (*Oncorhynchus tshawytscha*) of all rivers in the world (Van Hyning 1973). In the past 150 years, though, the CR system has experienced dramatic change due to development pressures. After decades of habitat degradation from mining, logging and irrigation, and salmon overfishing, development of the CR hydropower system started in the early 1930's, as President Franklin D. Roosevelt launched the "New Deal" to promote economic recovery out of the Great Depression (Lichatowich 1999). By the time the dam system was completed in the 1970's, 211 dams had been constructed in the river and its tributaries to exploit the hydropower and irrigation potential in the basin and to control flow for floods and navigation (Williams 2006). Navigational improvements also modified the morphology of the estuary. The 10 to 16 million adult salmon returning to the river to spawn before the development era suffered a steady decline, and had fallen to 2.5 million by the 1980's (NPPC 1986).

Scientists have recently questioned the paradigm that has informed salmon recovery strategies in the CR for the past century, which have proven ineffective to reverse the precipitous decline (Lichatowich 1999; Bottom et al. 2005; Williams 2006). Relying on hatcheries and technological fixes, the approach has failed to consider and understand the ecological processes that are needed to ensure the health of the overall ecosystem. A shift, however, is under way. Policy has, in the last decade (NPPC 1997; 1998; NPCC 2009), started to recognize that the estuary and river plume are an integral part of the CR ecosystem and that the continuum of marine, estuarine and riverine environments is critical to preserve the diversity of life history characteristics that enable salmon populations from the CR to withstand environmental fluctuations (Bottom et al. 2005). The science is tasked to further the understanding of the role of estuarine and near-shore habitat conditions in the recovery of Pacific salmon, of their response to local habitat change and management activities upstream, in the context of natural variability and climate shifts, and inform the choices the Pacific Northwest region is faced with for a sustainable development.

1.2 CORIE/SATURN: A Coastal-Margin Observatory for the U.S. Pacific Northwest

The U.S. Commission on Ocean Policy, in its report "An Ocean Blueprint for the 21st Century", recognized that, while "*new scientific understanding has taught us that natural systems are complex and interconnected, our decision-making and management systems have not been updated to address that complexity and interconnectedness*" (U.S. Commission on Ocean Policy 2004). The Commission recommended an ecosystem-based management approach to "*overcome the challenges inherent in addressing complex issues that cross traditional jurisdictional boundaries*" and "*continually adapt to new scientific information and improved management tools*". The Commission emphasized that moving toward an ecosystem-based approach will inevitably grow managers' requirements for scientific information and will also make even more pressing the need to translate that information into timely and relevant products for managers and policy makers. High-quality, accessible information critical to making wise decisions about ocean and coastal resources and their uses requires an adequate infrastructure for data collection and management. In its response to the Commission's recommendations (2004), the Bush Administration embraced the vision of the Commission to provide such infrastructure through implementation of a national Integrated Ocean Observing System (IOOS), based on a backbone of coordinated, interconnected U.S. regional ocean observing systems and linked to the international Global Ocean Observing System.

The CORIE/SATURN coastal-margin observatory, developed over the last decade for the CR estuary-plume-shelf system (Baptista 2006), contributes modeling and observational capabilities to the regional ocean observing system for the Pacific Northwest (NANOOS). Since its inception CORIE/SATURN's goal had been to deliver quantifiably reliable environmental information, at the right time and in the right form to the right users. An observation network and a modeling system, integrated by an information management system, provide the infrastructure and tools to pursue this goal. The evolving observation network is made of an array of estuarine stations and two offshore buoys, with all stations but the farthest offshore buoy linked via spread-spectrum radio telemetry that allows real-time access to data. The modeling system relies on two

numerical models to simulate the cross-scale 3D baroclinic circulation in the CR estuary-plume-shelf system: ELCIRC (Zhang et al. 2004; Baptista et al. 2005) and SELFE (Zhang and Baptista 2008). This computational engine is used to generate daily forecasts, multi-year circulation databases and on-demand products.

By including the estuary-plume-shelf continuum, the capabilities offered by the CORIE/SATURN coastal-margin observatory will best help pursue some of the scientific questions posed by the paradigm shift needed for salmon recovery strategies in the Columbia River system.

1.3 Research Objectives and Structure of the Dissertation

An overarching question that motivated this research is how in the years to come coastal observatories could be used in the context of ecosystem-based approaches to address scientific questions posed by management needs. This entails making accessible to the decision-making process a 'best available science' that relies upon the diagnostic and predictive capabilities of complex mechanistic modeling tools. The suitability of complex models that simulate the physical environment to provide credible and useful answers to the decision makers has been questioned (Reckhow 1999). The complex decisions facing natural resource managers also need to be taken in the context of natural variability. Back when we started this research, high-resolution numerical models, like ELCIRC and SELFE, were perceived as not optimal to address the time scales (seasons to years to over a century) relevant to separate the impact of anthropogenic activities from natural variability and climate change, and to inform management of riparian and coastal ecosystems (Walters 1997; Kukulka and Jay 2003).

While aiming at overcoming these perceived shortcomings, the research pursued the following specific objectives:

- To what extent is the CORIE/SATURN modeling system capable to reproduce known dynamics of the CR plume off the Oregon and Washington coasts (Barnes et al. 1972; Hickey et al. 1998; Garcia-Berdeal et al. 2002; Hickey et al. 2005; Thomas and Weatherbee 2006)? Can we rely on multi-year simulation databases

of circulation in the CR estuary-plume-shelf system to further our understanding of the seasonal and inter-annual variability of the plume in its response to river, ocean and atmospheric forcings?

- Does the CR plume play a role in the survival of juvenile salmon migrating from the Columbia River to the ocean? Through what mechanisms? Do inter-annual variability and climate and ocean regimes modulate that role?
- Using the high-resolution modeling capabilities of CORIE/SATURN, can we investigate the impact of natural variability and anthropogenic change on habitat opportunity for salmon in the CR estuary, as determined by the physical environment? Can we inform restoration strategies and management upstream?

The modeling of the physical continuum from river to ocean afforded by CORIE/SATURN enabled to investigate different species and life history types of salmon (yearling and subyearling Chinook; juvenile steelhead) in their response to variability in the physical environment at a couple of different life stages (i.e., the plume and estuary). In the last chapter, we discuss how the results of this investigation relate to the paradigm shift (from a production to a population perspective) needed for salmon recovery strategies in the CR that are aimed at promoting salmon resilience by preserving the diversity of salmon life history characteristics. The range of life history options is dependent upon habitat diversity in the continuum of marine, estuarine and riverine environments (Waples et al. 2009). Our modeling approach provides a tool to investigate habitat response (from a physical standpoint) to natural and anthropogenic variability and opportunities for life history expression.

The chapters of this dissertation are journal articles accepted or being submitted for publication. Chapter 2, which was accepted for publication in the Journal of Geophysical Research-Oceans, as part of a special issue on the project “River Influences on Shelf Ecosystems” funded by the National Science Foundation, reports our findings on the study of seasonal and inter-annual variability of the CR plume. Chapter 3 and 4 respectively address the role of the CR plume and estuary as salmon habitat. Chapter 5 introduces another example where we are using the CORIE/SATURN modeling capabilities to investigate variability across regions, seasons and years of residence times

in the CR estuary-plume system, and summarizes the contributions of the entire body of research. It also discusses the management implications of the research for salmon recovery in the CR.

1.4 References

Baptista, A. M. 2006. CORIE: the first decade of a coastal-margin collaborative observatory. In: *Ocean '06*. Boston, MA: MTS/IEEE.

Baptista, A. M., Y. Zhang, A. Chawla, M. Zulauf, C. Seaton, E. P. Myers, J. Kindle, M. Wilkin, M. Burla and P. J. Turner. 2005. A cross-scale model for 3D baroclinic circulation in estuary-plume-shelf systems: II. Application to the Columbia River. *Continental Shelf Research* 25: 935-972.

Barnes, C. A., A. C. Duxbury and B.-A. Morse. 1972. Circulation and selected properties of the Columbia River effluent at sea. In: A. T. Pruter and D. L. Alverson, Eds. *The Columbia River estuary and adjacent ocean waters*. University of Washington Press, Seattle, WA**:** 41-80.

Bottom, D. L., C. A. Simenstad, A. M. Baptista, D. A. Jay, J. Burke, K. K. Jones, E. Casillas and M. H. Schiewe. 2005. *Salmon at River's End: The Role of the Estuary in the Decline and Recovery of Columbia River Salmon*, U.S. Dept. of Commerce NOAA Technical Memorandum NMFS-NWFSC-68.

Fresh, K. L., E. Casillas, L. L. Johnson and D. L. Bottom. 2005. *Role of the estuary in the recovery of Columbia River basin salmon and steelhead: an evaluation of the effects of selected factors on salmonid population viability.* U.S. Dept. Commerce, NOAA Tech. Memo NMFS-NWFSC-69, 105 pp.

Garcia-Berdeal, I., B. M. Hickey and M. Kawase. 2002. Influence of wind stress and ambient flow on a high discharge river plume. *Journal of Geophysical Research* 107 (C9): 3130.

Hickey, B. M. and N. S. Banas. 2003. Oceanography of the U.S. Pacific Northwest coastal ocean and estuaries with application to coastal ecology. *Estuaries* 26(48): 1010-1031.

Hickey, B. M., S. Geier, N. Kachel and A. MacFadyen. 2005. A bi-directional river plume: the Columbia in summer. *Continental Shelf Research* 25: 1631-1656.

Hickey, B. M., L. J. Pietrafesa, D. A. Jay and W. C. Boicourt. 1998. The Columbia River Plume Study: Subtidal variability in the velocity and salinity fields. *Journal of Geophysical Research* 103(C5): 10339-10368.

Kukulka, T. and D. A. Jay. 2003. Impacts of Columbia River discharge on salmonid habitat: 2. Changes in shallow-water habitat. *Journal of Geophysical Research* 108(C9): 3294, doi:10.1029/2003JC001829.

Lichatowich, J. A. 1999. *Salmon Without Rivers: A History of the Pacific Salmon Crisis.* Island Press, Washington, DC

NPCC. 2009. *Columbia River Basin Fish and Wildlife Program, Council Document 2009-02*. Northwest Power and Conservation Council, Portland, OR

NPPC. 1986. *Compilation of Information on Salmon and Steelhead Losses in the Columbia River Basin*. Northwest Power Planning Council, Portland, OR

NPPC. 1997. *Consideration of ocean conditions in the Columbia Basin Fish and Wildlife Program.* Northwest Power Planning Council, Portland, OR

NPPC. 1998. *Columbia River Basin Fish and Wildlife Program, fiscal year 1999 annual implementation work plan, documents 98-31, 98-31a.* Northwest Power Planning Council, Portland, OR

Reckhow, K. H. 1999. Water quality prediction and probability network models. *Canadian Journal of Fisheries and Aquatic Sciences* 56: 1150-1158.

Thomas, A. C. and R. A. Weatherbee. 2006. Satellite-measured temporal variability of the Columbia River plume. *Remote Sensing of Environment* 100: 167-178.

U.S. Commission on Ocean Policy. 2004. *An Ocean Blueprint for the 21st Century*. Final Report. Washington, DC.

U.S. Council on Environmental Quality. 2004. *U.S. Ocean Action Plan. The Bush Administration's Response to the U.S. Commission on Ocean Policy*. Online at http://ocean.ceq.gov/actionplan.pdf.

Van Hyning, J. M. 1973. Factors affecting the abundance of fall Chinook salmon in the Columbia River. *Research Reports of the Fish Commission of Oregon* 4: 1-87.

Walters, C. J. 1997. Challenges in adaptive management of riparian and coastal ecosystems. *Conservation Ecology* 1(2): 1. [Online: http://www.consecol.org/vol1/iss2/art1/].

Waples, R. S., T. Beechie and G. R. Pess. 2009. Evolutionary history, habitat disturbance regimes, and anthropogenic changes: what do these mean for resilience of Pacific salmon populations? *Ecology and Society* 14(1): 3 [online].

Williams, R. N., Ed. 2006. *Return to the River: Restoring Salmon to the Columbia River*, Elsevier Academic Press.

Zhang, Y. and A. M. Baptista. 2008. SELFE: A semi-implicit Eularian-Lagrangian finite-element model for cross-scale ocean circulation, with hybrid vertical coordinates. *Ocean Modelling* 21(3-4): 71-96.

Zhang, Y., A. M. Baptista and E. P. Myers. 2004. A cross-scale model for 3D baroclinic circulation in estuary-plume-shelf systems: I. Formulation and skill assessment. *Continental Shelf Research* 24: 2187-2214.

Chapter 2

Seasonal and inter-annual variability of the Columbia River plume: A perspective enabled by multi-year simulation databases

Authors: Michela Burla, António M. Baptista*, Yinglong Zhang, Sergey Frolov

Accepted in the Journal of Geophysical Research: Oceans

Abstract:

As integral capability within an end-to-end observatory for the Columbia River estuary-plume-shelf system, we routinely create simulation databases of 3D baroclinic circulation with unstructured-grid models SELFE and ELCIRC. Here, 1999-2006 SELFE simulations are used to study plume variability at multiple temporal scales: inter-annual, seasonal, and event scale. Time series of plume metrics, together with climatology and anomalies of surface salinity, suggest that simulations usefully capture key features of plume dynamics. In particular, simulations capture seasonal variability around two known trends: a coastally-attached northward winter plume and a detached southward summer plume. Results show significant inter-annual variability of the plume orientation and extent, with potential implications on the variability of productivity in the system. An EOF analysis confirms that a bi-directional plume is prevalent in summer, showing that the result holds true regardless of inter-annual variability. Short-term bi-directional plumes, previously observed or modeled only in summer, can occasionally develop also in winter as a result of episodically strong upwelling-favorable winds. Across years, the predominantly coastal-attached northward plume in late fall and winter is found to separate frequently from the coast, during wind relaxation events or weak wind reversals. Multiple skill scores are used to evaluate the quality of the simulations against earlier circulation databases and data. Analysis of RMSE and bias suggests overall superiority of SELFE- generated over ELCIRC-generated simulation databases, but the generality of the conclusions is limited by (a) models not being the only difference between simulation databases, and (b) no model prevailing across all error metrics.

2.1 Introduction

The Columbia River (CR) is the major freshwater source on the US west coast entering the Eastern North Pacific Ocean (Figure 2.1), accounting for 77% of the drainage between San Francisco and the Strait of Juan de Fuca (Barnes et al. 1972). The freshwater plume formed by the CR off the Oregon and Washington coasts constitutes a major oceanographic feature, modifying regional coastal circulation patterns (Hickey et al. 2005). CR plume intrusions also affect the dynamics of other estuaries along the coast, in particular Washington estuaries like Willapa Bay and Grays Harbor (Hickey and Banas 2003). Hickey et al. (2005) presented evidence that suggests that the CR plume can inhibit the onset of upwelling along the Washington inner shelf. They further suggested that the seaward front of the CR plume likely provides a barrier to the onshore transport of harmful algal blooms in summer and early fall.

The presence of the CR plume may also have important ecological implications. Biological studies (Pearcy 1992; Casillas 1999; De Robertis et al. 2005; Morgan et al. 2005; Bottom et al. 2006; Burla et al. In review) have hypothesized that the CR plume provides habitat for Pacific salmon. Hickey and Banas (2003) speculated that the influence of the CR plume may be a contributing factor to the higher biological productivity off the Washington coast relative to the Oregon coast, a gradient in productivity that is opposite to the gradient in upwelling wind forcing. Improving understanding of how the CR plume may influence biological productivity over the Washington and Oregon shelf is the goal of the RISE (River Influences on Shelf Ecosystems) program, a 5-year interdisciplinary study funded by the National Science Foundation.

The CR plume is forced by daily river discharges that range, during a typical year, from 3,200 to 10,500 $m^3 s^{-1}$ (USGS, http://waterdata.usgs.gov/or/nwis, last accessed September 27, 2006), with sustained peaks during the spring snowmelt freshet and more episodic peaks generated by winter storms (Thomas and Weatherbee 2006). Evidence of the inter-annual variability superimposed onto this seasonal variability are the recent extremes of 1,800 $m^3 s^{-1}$ in September 2001 and of 24,500 $m^3 s^{-1}$ in February 1996. Inter-annual variability in the intensity of the winter storms and in the timing and intensity of

the freshet –although the latter is reduced relative to pre-development levels by hydropower regulation– is reflected in the time series of river discharge (Figure 2.2).

The classical view is of a bi-modal CR plume, generally oriented northward and attached to the Washington shelf in winter, and by contrast extending to the southwest and crossing the shelf off the Oregon coast in summer (Barnes et al. 1972; Hickey et al. 1998). This view reflects the prevailing seasonal winds: to the north, downwelling-favorable during winter and to the south, upwelling-favorable during summer. Northerly winds and coastal near-surface currents to the north generally reinforce in winter the Coriolis-induced rotational tendency of the plume to the north. The onshore Ekman transport resulting from the downwelling-favorable winds pushes the plume to hug the Washington coast. In summer, offshore Ekman transport results from the prevailing southward wind forcing and advects the plume seaward, where the mean California Current further advects it to the south. Recent observational and modeling studies, however, suggest that there is significant variability of the plume around that historical seasonal pattern (Hickey et al. 1998; Yankovsky et al. 2001; Garcia-Berdeal et al. 2002; Hickey et al. 2005). To characterize seasonal and inter-annual variability, Fiedler and Laurs (1990) and Thomas and Weatherbee (2006) explored the use of satellite imagery. With sea surface temperature and phytoplankton pigment images, Fiedler and Laurs (1990) provided additional evidence of the seasonal basic patterns of the plume, but also observed rapid changes in the orientation and shape of the plume resulting from brief reversals of the prevailing seasonal winds. Using six years of multispectral ocean color satellite data, Thomas and Weatherbee (2006) observed summer interannual variability in the plume pattern, dominated by variability in river discharge. They instead identified a clear association of interannual variability of the plume in winter with wind forcing.

In the present study we used multi-year retrospective simulations (hindcasts) to investigate the variability in the CR plume structure at multiple temporal scales (inter-annual, seasonal, and several-day/event scale). Using multiple strategies, we build progressively towards a systematic description of seasonal and inter-annual variability of the CR plume, which we accompany with a comprehensive evaluation of the skill of the simulations to represent different features of the dynamical behavior of the plume that are

well documented in the literature (Hickey et al. 1998; Yankovsky et al. 2001; Hickey et al. 2005; Thomas and Weatherbee 2006).

2.2 Methods

2.2.1 Analysis of variability of the plume

Multi-year simulations (1999-2006) of baroclinic circulation in the CR estuary-plume-shelf system, generated as an integral part of the CORIE/SATURN coastal-margin observatory (Baptista 2006), enabled our study of seasonal and inter-annual variability of the CR plume. Simulations were generated using the 3D numerical model SELFE (Zhang and Baptista 2008) and archived in the simulation database DB14.

From the 8-year long database, we first computed monthly and seasonal (winter and summer) climatologies for the surface salinity field, as well as anomalies for each year relative to the monthly climatologies.

To describe plume structure in a synthetic way, we integrated over space the 3D salinity field from model output and we generated time series of plume volume, area of the surface plume, and average depth of the plume from the simulation database that spanned from 1999 to 2006. We also computed the coordinates of the centroid of the surface plume, in the State Plane Coordinate System, as follows:

$$\vec{x}_p = \frac{\int_{S<S_{ref}} \vec{x}_c dA}{\int_{S<S_{ref}} dA}$$

where $\mathbf{x_c}$ are the coordinates of the centroid of each element in the grid.

In all cases, we defined the plume using a cutoff salinity (S_{ref}) of 28 psu, a conservative choice to distinguish the body of CR plume waters from ambient ocean salinity and from other freshwater sources. This value proved to be a suitable cutoff to track the evolution of the plume and its response to changes in the external forcings (tides, river discharge, winds). Zhang et al (In review) used similar metrics in providing context to their assessment of SELFE forecasts, although they adopted a definition that relates more closely to the notion of "freshness". Under their definition, an element in the grid contributes to the total volume proportionally to the difference between its salinity

and the cutoff salinity. In the work we present here, an element contributes its entire volume (or area) to the integration when its salinity is below the cutoff salinity. To follow changes in structure and orientation of the plume relative to the river mouth in response to wind shifts, we examined time series of plume depth in the model simulations (along with average depth of the plume), at three locations in the computational domain (Figure 2.1): *effn1*, located ~17 km to the north of the river mouth on the Washington inner shelf, ~4 km offshore, in ~24 m of water; *ogi02*, located in the very near-field ~10 km to the south of the mouth, in ~ 40 m of water; and *ogi01*, located ~30 km to the southwest of the river mouth, along the 100m isobath. Locations *ogi01* and *ogi02* coincide with two actual buoys of the CORIE/SATURN observation network.

To identify the dominant modes of variability in the simulated salinity off the Oregon and Washington coast, as affected by the CR plume, we performed an empirical orthogonal function (EOF) analysis (Storch and Zwiers 1999). An EOF analysis identifies an orthogonal vector basis that optimally represents the variability in the data. Vectors of the EOF basis represent a progressively smaller percentage of variability in the data, with the first vector aligned with the direction of the highest variability.

Since computing a direct EOF decomposition of a large (~4 Tb of binary data) simulation database is impractical, we computed an approximate EOF decomposition (Frolov et al. 2009). We first computed the spanning space for the EOF using 1000 random samples drawn from ~280,000 realizations of the simulated field in the 8-year-long database (output of the model available at 15-minute intervals). Once we determined the spanning EOF space of 120 vectors, we then computed the exact EOF in this subspace. We tested our EOF approximation on data not used in the computation of the spanning space and verified that the approximation captured 99% of variability in the data. A similar method was first used in Xue et al (1997).

We related variability in the plume structure to variability in river discharge (Figure 2.2) and local winds (Figure 2.3), using time series from the same data sources used to force the models. Data sources and strategies adopted in the CORIE modeling system to characterize external forcings are described in (Baptista et al. 2005). Information is also provided in Table 2.1.

2.2.2 Evaluation of model skills

To evaluate the quality of the model simulations upon which our analysis of variability of the CR plume structure is based (DB14), we used multiple strategies that involved model-data comparisons and inter-model comparisons.

Comparisons were based upon duplicative realizations of the multi-year databases of circulation: DB14, DB11, and DB13. While DB14 and DB13 were generated with SELFE, ELCIRC (Zhang et al. 2004; Baptista et al. 2005) was used to generate DB11. Both SELFE and ELCIRC are semi-implicit, unstructured grid models that solve the 3D barotropic shallow water equations. The difference between the two models lies in the numerical algorithms used to discretize the governing equations and in the approach adopted for the vertical discretization of the computational domain. ELCIRC uses a finite difference/finite volume method, and unstretched z-coordinates in the vertical, while SELFE adopts a finite element framework, with terrain-following S-coordinates (Song and Haidvogel 1994) placed on top of (optional) z-coordinates. For more detail on the CORIE/SATURN modeling system used to generate the simulations, and associated models, we refer the reader to Zhang et al (In review). In their parallel study, they looked at the performance of the SELFE model in producing reliable forecasts, as opposed to the retrospective hindcasts that are the subject of this work.

Besides the differences in the formulation of the two models used to generate them, DB14 and DB11 also differed in terms of the numerical solution for the transport equations of salinity and temperature. DB14 used a conservative upwind algorithm, as opposed to the non-conservative Eulerian-Lagrangian (ELM) framework of DB11. To isolate the effect of adopting an upwind algorithm to treat scalar transport, we looked at an earlier database (DB13) that was generated –like DB14– with SELFE, but that still used the ELM solution as in DB11. In addition to algorithmic differences, DB11 and DB14 were also generated with partially different atmospheric forcings, as summarized in Table 2.1. Differences in atmospheric forcings may prevent drawing unequivocal conclusions about what the relative merits of the two simulation databases should be attributed to. Nonetheless, the effect of partially different forcings was deemed comparatively small relative to the differences in algorithmic solutions.

Observational datasets used for the model-data comparisons were from 3 buoys deployed as part of the RISE program (all three very near to the 72 m isobath, respectively north, south and westward of the CR mouth: *risen*, *rises* and *risec*); and two buoys belonging to the CORIE network (*ogi01*, which is southwest of the river mouth, on the 100 m isobath, and *ogi02*, in the very near-field, immediately southwest of the river mouth, in ~ 40 m of water). All locations are shown in Figure 2.1. Table 2.2 summarizes the periods covered by each datasets from these stations.

To assess the skill of our models and to appreciate the relative merits of different skill scores, we used the root mean squared error (RMSE) and an array of other scores (Table 2.3). The mean squared error (MSE) represents the expected (i.e. long-term average) squared error (Storch and Zwiers 1999):

$$MSE = \mathrm{E}\left((M-O)^2\right) = \frac{1}{n}\sum\left(m_i - o_i\right)^2$$

where m_i and o_i are, respectively, the model prediction and the verifying observation at time i (realizations of the random variables M and O). The Brier skill score uses the MSE to measure the performance of a model forecast relative to a reference forecast (typically a naïve forecast like climatology or persistence) (Murphy 1992; Storch and Zwiers 1999; Oke et al. 2002):

$$B = 1 - \frac{MSE}{MSE_R}$$

We computed the Brier skill score to compare DB13 and DB14, using DB11 as the reference, to evaluate merits of SELFE versus ELCIRC and of the upwind transport scheme versus ELM. At each location and for each year covered by the available datasets we also computed the correlation skill score, ρ_{MO}, between model and observations; the (unconditional) model bias, MB, which we normalized by the standard deviation in the observations, σ_O:

$$MB = \frac{\mathrm{E}(M) - \mathrm{E}(O)}{\sigma_O};$$

and the normalized standard deviation for the model predictions, σ_M/σ_O. In Table 2.2, we show the range (minimum and maximum value) and the mean for the salinities observed at each location.

We must note that skill scores, by measuring the quality of a hindcast system, are parameters that characterize some aspect of the distribution of the bivariate random variable (M, O) (Storch and Zwiers 1999). Since we derived the skill parameters from a finite number of model-data comparisons, the parameters are only an estimate of the true skill.

To complete our assessment of model skills, we plotted the distributions of modeled salinity, conditional on the value of the observed salinity, at the different locations and for the periods covered by the observational datasets. To this end, we modified the graphical representation that was suggested in Storch and Zwiers (1999), which they originally proposed to show the distribution of observations conditional on the respective forecasts. Details for interpreting this graphical representation are in the legend of Figure 2.19.

2.3 Results and Discussion

2.3.1 Analysis of variability of the plume

2.3.1.1 Climatologies and anomalies of surface salinity

Climatologies of the surface salinity field, generated from our simulations covering the 8-year period from 1999-2006, are consistent with the prevailing seasonal patterns known for the CR plume (Barnes et al. 1972): a plume oriented northward and attached to the coast in winter (Figure 2.4, left), and mostly southward of the river mouth and detached from the coast in summer (Figure 2.4, right). Monthly climatologies show how the mean salinity field varies throughout the year, not only in response to the transition between prevailing seasonal wind regimes but also to the seasonality in river discharge (Figure 2.5, leftmost column). They show much larger plumes in February and May resulting from winter precipitation and spring snowmelt, and smaller plumes with the weakening of the signal towards the end of the summer, which reaches its lowest in September. Similarly to what Thomas and Weatherbee (2006) reconstructed in their study of the CR plume variability based upon multi-year data (1998-2003) of water-leaving radiance measured by ocean color satellites, in September our simulated plume also shows little

evidence of bias either to the north or the south. Yet, the monthly distribution of the plume centroid coordinates described in the next section also suggests some appreciable variability around this mean.

Anomalies computed relative to these monthly climatologies are useful for capturing the interannual variability in the CR plume structure superimposed onto the seasonal means (Figure 2.5). The anomaly maps generated from DB14 simulations reveal a plume more strongly oriented to the north and more tightly hugging the coast in February 1999 than in any other year of the series. Such orientation was also shown in the monthly means of water-leaving radiance (nLw at 555 nm) reconstructed by Thomas and Weatherbee (2006) from ocean color satellite data. The strongly enhanced downwelling explains the structure of the plume in February 1999. The storms responsible for this onshore transport also generated a maximum in river discharge, higher than in any other year of the series (Figure 2.2). While capturing the close attachment of the plume to the coast and its deep penetration to the north, the DB14 anomaly map does not reflect the stronger plume signal that was consequently expected in February 1999 than in February 2000, and which is confirmed in the higher nLw 555 values in the monthly mean of Thomas and Weatherbee (2006) for February 1999.

Similarities with the results of Thomas and Weatherbee (2006) validate other patterns found in our anomaly maps built from DB14 and give confidence to draw additional considerations. In our simulations, the positive salinity anomaly along the Washington coast in February 2003, suggestive of a more westward and southwestward orientation of the CR plume, is consistent with the weak northward wind forcing for the period. The extremely high discharge at the beginning of February 2003 is responsible for the negative salinity anomaly off the river mouth. Anomalies for February 2001 show not only the low occurrence of plume waters to the north determined by weak northward wind forcing, but also the weakest plume signal determined by the very low discharge of 2001. The sharp decrease in winter river discharge during February 2006 and the shift to upwelling winds explain the strong positive salinity anomaly in particular along the Washington coast. Inter-annual variability in May, for the 8 years considered, appears to be mostly determined by the variability in CR discharge. In 2000, however, the structure of the strong negative anomaly generated by the extremely high river discharge also

reveals the lack of southward displacement of the plume. In contrast, in May 1999 the strong plume signal appears both north and southwest of the mouth. May 2002 and 2004 exhibit fairly similar conditions relative to each other, with a positive anomaly outside the bulge region of the plume, in the outer field both off the Washington coast and to the southwest of the mouth. This may translate in a lower frequency of occurrence of the type of bi-directional plumes observed by Hickey et al (2005) in the summer and in a more modest influence of the plume on the Washington shelf. In May 2003 a fairly average plume exhibits a slight tendency to extend to the southwest rather than turning north to hug the Washington coast. Opposite tendency is revealed by the anomaly map in May 2005, due to strong downwelling events for that period. In September of most years, the plume signal is at its lowest and weakest in 2001 and 2003. Higher-than-average river discharge in September 1999 and 2004 show as negative anomalies in the surface salinity, but with opposite structure, hence opposite orientation of the plume: to the southwest in 1999, due to consistently upwelling-favorable, southward winds; prevalently northward and attached to the coast in 2004, due to prevailing downwelling favorable winds. Summer 2004 and 2005, years within the RISE field program, do not show strong anomalies between June and August (Figure 2.6), mainly due to the moderate flows reached early in the season. The late spring and late summer/early fall of the same years, however, deviate from average conditions as already noted above. In summer 2006 (another year of the RISE field program), by contrast, the freshet continued through June, determining the negative anomaly in the surface salinity field shown in the map. The structure of the anomaly is compatible with the occurrence of bi-directional plumes.

Although monthly climatologies and anomalies proved useful to investigate the inter-annual and seasonal variability of the surface salinity field generated by the CR plume, the structure of the plume exhibits strong variability at timescales of a few days (Hickey 1989; Hickey et al. 1998). This variability is largely driven by wind fluctuations, to which the plume responds nearly instantaneously (Hickey et al. 1998). Daily averages of the simulated surface salinity field for May 1999 (Figure 2.7) provide an example of the variability at this scale, which was averaged out in the monthly climatology (shown at the top right in Figure 2.7a). In addition to the response to shifts in wind stress, these daily averages also capture the effect on the plume of sub-inertial variability in river

discharge. Increases and subsidence of the inflow during the first half of May 1999, when the plume was oriented northward, determined in our simulations the development of a bulge and the subsequent formation of a secondary bulge propagating northward. In our simulations we did not observe, however, the partial detachment of the bulge further postulated by Yankovsky et al (2001) in the event of river discharge subsiding after a high runoff.

2.3.1.2 Time series of metrics of plume structure

Time series reconstructed from our 8-year model simulations showed that the total volume (and surface area) of plume waters within a 28 psu salinity isoline responded with a delay to increases in discharge from the CR (Figure 2.8). The largest volumes formed following the freshet season of 1999 and 2000, with seasonally larger volumes characterizing, in most years, the stormy winter season and the spring. The drought of the winter of 2000-2001 and the low flows of the melting season in spring 2001 are evident in the plume volume time series. Maximum volume of plume waters within the 28 psu isoline ranged from 21 to 69 km^3 in the years between 1999-2006. As noted in the Methods section, we chose here a salinity cutoff of 28 psu to better track the evolution of the plume in our simulations and its response to changes in external forcings. However, the volume within a 28 psu isoline does not represent the total volume of plume waters, because waters saltier than 28 psu still maintain a plume signature. Volume of water within the 30 psu isoline in our DB14 simulations (not shown) varied, in average-flow years, within a range comparable to the 20-110 km^3 reported in Hickey et al (1998) for total plume volume, but exceeded 110 km^3 in the highest discharge periods (freshet of 1999, 2000 and 2002).

The ratio of plume volume to its surface area (average depth) in DB14 simulations captures the prompt response of the plume to wind reversals (Figure 2.9; see, for example, the isolated downwelling event at the end of May 2002). The time series for this metric show the much higher thickness that characterizes the plume when it is pushed to hug the Washington coast by a strong wind stress to the North (downwelling favorable), prevailing during winter storms. Within the 8 years covered by our

simulations, February 1999 had the strongest wind forcing to the north (Figure 2.3). Consistently with known plume dynamics during downwelling, both the average depth of the simulated plume (Figure 2.9) and the depth at the *effn1* location (Figure 2.10a) –to the north of the mouth on the Washington inner shelf– reflect a plume most strongly oriented northward and closely attached to the coast. Thomas and Weatherbee (2006) similarly reported a plume most strongly oriented northward in February 1999, which is also apparent in our salinity anomaly maps. In our simulations, depth of the 28 psu isoline for the same month at the *effn1* location reached a maximum of 25 m. The depth of the 28 psu isoline at the same location fell below 10-15 m during winter months when winds turned for some time westward or southward. This is consistent with the two basic structures demonstrated for the CR plume during the fall and winter season by the observational study of Hickey et al (1998): a thicker, weakly stratified plume oriented northward and attached to the coast during periods of strong northward winds and a thin, strongly stratified plume oriented west to northwestward during relaxation periods or when wind stress turns to the south. February 2003 best exemplifies the transition between these structures in our simulations. During the first half of the month, wind stress turned from northward to southwestward (Figure 2.3), and the depth of the 28 psu isoline at *effn1* dropped in DB14 simulations from 20 m to about 5-7 m (Figure 2.10a). A plume extending westward during this period was also reported in Thomas and Weatherbee (2006). During the following downwelling event, our simulation captured the reattachment of the plume to the Washington coast, with a thickness, at the 28-psu isoline, again approaching 20 m. With the subsequent shift of wind stress to the south, the plume disappeared at *effn1*, having moved offshore, still off the Washington coast, but separated from it (as shown by animations of the simulated results accessible at http://www.ccalmr.ogi.edu/CORIE/hindcasts/database/base_frame.html).

In each year covered by our simulations, when wind stress became consistently upwelling favorable (to the south) during the summer season (Figure 2.3), the 28-psu plume from the CR was in DB14 seen on the Washington inner shelf at *effn1* only as occasional thin lenses in response to brief wind reversals. At the *ogi01* location (on the outer Oregon mid-shelf), as expected, a plume was seen under upwelling conditions and was strongest during the freshet season, in particular in 1999 and 2000 (Figure 2.10b).

This plume was generally much thinner (5-10 m at the 28 psu isoline) than the one detected, still in our DB14 simulations, at the northern location during winter. This is in agreement with observed shallow summertime plumes and deeper wintertime plumes (Hermann et al. 1989; Hickey et al. 1998; Horner et al. 2000; Hickey et al. 2005). Summer months of 1999 were characterized by decreasing flows relative to the freshet but higher than average for the season, and by winds most consistently toward the south than in any other year covered by this study, even through September. During this period, the 28-psu plume was consistently present at *ogi01*. In low and moderate discharge years like 2001 and 2003, with frequent wind reversals during the summer, the plume had only occasional appearances at *ogi01* in DB14 simulations.

Our simulations indicated that the bi-directionality observed by Hickey et al. (2005) for the CR summer plume may apply at times to the winter plume as well. Time series of the depth of the 28-psu isoline at *effn1*, *ogi01* and *ogi02* (Figure 2.10a-c), show an example of this behavior in February 2000. While the 28-psu plume was absent from *ogi01* for most of January 2000, the plume appeared at this station, which is southwestward relative to the river mouth on the outer Oregon mid-shelf, at the end of January and then again in mid-February, in response to a shift in wind stress to the south. At both times when the plume appeared at *ogi01*, the plume was still present at the northern location (*effn1*) on the Washington inner shelf, as well as at the Oregon near-field location *ogi02*, immediately south of the river mouth. Previous idealized numerical experiments (Garcia-Berdeal et al. 2002) suggested that, given that in winter the natural rotational tendency of the plume to the north due to Coriolis is reinforced by a mean ambient flow in the same direction, very significant upwelling wind events would be required to develop a reversal of the winter plume to the south. Early observations of the CR plume in winter (Hickey et al. 1998) did not identify any shift to a southwestward direction despite periods of persistent upwelling during their field campaign in the winter of 1990-1991. Nonetheless, while we do not have observations to the north of the river mouth in winter to verify bi-directionality, CORIE/SATURN observations provide evidence of plume reversals in winter with plume presence at *ogi01* (which is 30 km to the southwest of the river mouth) on several occasions during the years covered by the study (time series are available online at

http://www.stccmop.org/CORIE/data/publicarch/ogi01/): December 1999; February and December 2001; January 2002 and again mid-late February of the same year; and February 2005. In all these instances, Figure 2.10b shows that the model correctly captured these winter reversals of the plume to the south. DB14 simulations also suggest the plume to be present at *ogi01* in December 2000, in this case contrary to the observations. We conclude that, during the years covered by our study, there were upwelling wind events strong enough in winter to counter both ambient mean flow and rotational tendency, but possibly not enough to fully erode the northward plume and transport away aged plume waters off the Washington shelf, leading to the possibility of bi-directional plumes, as seen in our model simulations. Nonetheless, based upon the frequency of "sightings" of the plume at the *ogi01* buoy, these conditions can only be occasional events in winter and much reduced in scale. On the contrary in summer, the most typical conditions are 'upwelling-favorable with a downwelling event a few days in the past' (Banas et al. 2008) and the simulations of Liu et al (2009a) for summer 2004 would suggest that summer plumes may be bi-directional 70-80% of the time (although with different strength and extent), with important implications on the productivity off the Washington coast.

Upwelling (downwelling) events evident in the wind time series (Figure 2.3) are in clear correspondence with the centroid of the surface plume being located south (north) of the river mouth (Figure 2.11). The high variability shown in the centroid time series during low-discharge summer months (in particular in 2001 and 2003) is due to the small extent of the 28-psu plume off the river mouth and its consequent sensitivity to incoming and outcoming tides. The time series in Figure 2.11 shows, however, that during these periods the centroid of the plume was generally found either in front or to the south of the river mouth. To refer to examples already highlighted in the above discussion, we can see that, during February 1999, the centroid of the CR plume was more consistently to the north of the river mouth than in any other year for the same month. We can also see that the centroid shifted southward in mid-February 2000; however the ultimate westward location of the centroid in this case is an artifact of the bi-directionality of the plume. We cannot discern this bi-directionality by looking at the centroid time series alone, but we were able to infer it by also looking at the depth of the

plume at the three locations (*effn1*, *ogi01*, and *ogi02*) in the above discussion. The effect of the strong downwelling events of mid-May 2005 on the orientation of the plume is clearly captured in the position of its centroid distinctively to the north of the mouth.

Monthly distributions of the x and y coordinate of the plume centroid (in the State Plane Coordinate System) provide a useful synthesis of the prevailing orientation of the CR plume –and its variability– relative to the Washington and Oregon shelf in different years (Figure 2.12) and seasons (Figure 2.13). The limitations noted above in the presence of a bi-directional plume, however, apply. Tighter distributions around the median generally characterize the late summer and early fall, in particular for the alongshore position of the centroid relative to the mouth, as a consequence of the lower seasonal discharge. The alongshore position of the centroid exhibits large excursions in June, with frequent excursions both south and north of the river mouth in June 1999. The higher variability relative to the mouth in June 1999 seems more a consequence of a large plume and weaker wind stress to the south –unable to fully erode plume waters formed by the high river discharge turning north in response to the rotational tendency– than a consequence of full reversals. Years 2001 and 2004 constitute exceptions to the large along-shore excursions of the centroid in June. The distance from shore of the centroid in June 2004, however, exhibits significant variability. Strong variability in the alongshore position of the centroid relative to the mouth as well as in its distance from shore is exhibited in the spring, with clear interannual variability as a result of the different timing of the spring transition. Banas et al (2008) found evidence for a mechanistic hypothesis that sees the CR plume as a cross-shelf exporter but a semi-permeable along-shelf barrier, contributing to heterogeneity of the Washington-Oregon coastal upwelling system. The seasonal and interannual variability of the plume orientation and extent over the Washington and Oregon shelf would then have implications on the variability of productivity in the system.

2.3.1.3 EOF analysis

EOF analysis of the surface salinity field off the Oregon and Washington coasts, simulated for the years 1999-2006 with the SELFE model in DB14, identified two

dominant modes of variability that together explain 64% of the total variance in the data. The spatial pattern of the first mode (Figure 2.14, top left) and its time variation (Figure 2.14, top right) clearly captures the variability in the salinity field modulated by variability in the CR discharge, coupled with the rotational tendency due to Coriolis. The high correlation of this first mode with river discharge is evident in Figure 2.14 (top right), where both time series are shown. The correlation weakens during extreme events in river discharge, in particular in the early months of 1999 (bringing the overall correlation to a value of 0.72, significant at the 99% level of confidence). Such weakening may be due to poorer skill of the model to estimate salinity at high-discharge regimes. We had already noticed in the salinity anomaly map (Figure 2.5) generated for February 1999 that DB14 simulations missed the stronger plume signal relative to 2000. Also Zhang et al (In review) reported lower RMS errors in the presence of lower river discharges for the version of SELFE used to generate DB14. We will return to these considerations in evaluating model skills in the next section.

The first mode alone accounts for 43% of the variance in the modeled salinity. The variance in the second mode is 21%. The second mode from an EOF analysis is typically bimodal, being constrained to be orthogonal to the first mode. The bi-modality of the second mode in our analysis, however, has a clear physical interpretation: the pattern (Figure 2.14, bottom left) captures the oscillation between the two dominant orientations of the CR plume –northward along the coast and southwestward separated from the coast– in response to the seasonal shift in prevailing winds. The EOF time series (Figure 2.14, bottom right) confirms that the plume signal to the north is strong during the winter storms, with the pattern reversing sign in the springs and summers. The strong correlation of the second EOF with the wind series (0.63, significant at the 99% level) indicates that the temporal evolution of this pattern is further modulated by the inter-annual variability in seasonal wind forcing.

An EOF analysis limited to the winter months (November-March of all years from 1999-2006) identified two dominant modes of variability for the surface salinity field simulated in DB14 (Figure 2.15) that resemble the dominant modes identified in Hickey et al. (1998). Their EOF analysis of 1 m salinity survey data for the period October 25-November 28, 1990, produced a first mode that accounted for 57% of the

variance and described the CR plume when separated from the coast and oriented northward of the mouth. Their second mode (18%) described the plume again to the north but hugging the coast. Our EOF analysis, using 8 years of model data and including, for each year, all winter months through March, identified a first mode that accounted for 42% of the variance and that described the plume oriented northwestward and separate from the coast (which is the orientation of the plume during relaxation events). In the associated time series representing the temporal variation for this spatial pattern (Figure 2.15, top right), the higher values for the first months of 1999 and 2000 are associated with the strong river discharge in those periods. The second mode (15%) describes the CR plume when attached to the coast. The sign and amplitude in the associated time series (Figure 2.15, bottom right) –positive, hence reinforcing the sign and pattern in the map– shows the tendency of the plume to hug the coast during the winters of 1999 and 2000. It also shows a plume less frequently hugging the coast in later years, as already seen in the salinity anomaly maps.

An EOF analysis limited to the summer months (June-August of all years from 1999-2006) for the same salinity field simulated in DB14 identified as leading mode of variability a pattern associated with a bi-directional plume, which alone explains 51% of the variance (Figure 2.16). This result would confirm that a bi-directional structure for the CR plume in summer (Hickey et al. 2005) is prevalent in that season. Liu et al (2009a) demonstrated this result with a Self-Organizing Map (SOM) analysis of simulations limited to summer (June-August) 2004, generated for the CR plume with the Regional Ocean Modeling System (ROMS). Our work extends the result to the eight years 1999-2006, showing that it holds true regardless of inter-annual variability. According to the time modulation of the first EOF mode (Figure 2.16, top right), our analysis also indicates that the bi-directional pattern was dominant during the entire summer of 1999 (as indicated by the consistently and distinctly positive sign in the EOF time series during 1999), while in other years it tended to be stronger in June and weakening in July and August. The second summer EOF captures, instead, a pattern where the plume does not contribute freshwater to the Washington shelf by turning northward and is instead fully extended to the southwest. This second mode accounts for 16% of the variance. The SOM analysis of Liu et al (2009a) provides a finer resolution of

possible bi-directional patterns in summer, which an EOF analysis cannot achieve because of the orthogonality constraints. However, the leading mode in our analysis is consistent with their 'transitional' patterns and their relative frequency of occurrence, while our second mode captures the type of variability described by the remaining SOM patterns identified in Liu et al (2009a).

2.3.2 Evaluation of model skills

To evaluate the quality of the simulations used to analyze the seasonal and inter-annual variability of the CR plume, we used duplicative realizations of the multi-year database of circulation. The CORIE/SATURN modeling system has progressively relied upon the development of two models: ELCIRC and SELFE. While the evaluation of ELCIRC year-long simulations, archived in database DB11, was the focus of an earlier publication (Baptista et al. 2005), this is the first time we report on SELFE skills in the context of a multi-year simulation of the CR estuary-plume-shelf system (DB14). A comparison against earlier realizations of the multi-year database of circulation allows insights into the merits and shortcomings of the modeling solutions adopted in generating DB14. Looking at the structure of the plume in the two sets of simulations archived in DB14 and DB11, DB14 simulations appear to better capture features such as a deeper penetration of the plume into the north along the coast with the coastal jet and the formation of a bulge, and of a secondary bulge, in response to pulses in river discharge. Time series for the plume metrics computed from both simulation databases (Figures 2.17) indicate a stronger freshwater plume in DB11 simulations than in DB14. We present evidence below of a bias towards freshness of DB11. This bias affects the anomaly maps of surface salinity generated from ELCIRC simulations (DB11, Figure 2.18), which also generally show a more limited penetration of the CR plume to the north with the coastal jet. The weaker northward penetration of the plume simulated in DB11 was possibly due to excessive nudging of ocean conditions from NCOM (Navy Coastal Ocean Model, Barron et al. 2006). DB11 anomaly maps, however, show variability patterns similar to those identified in SELFE simulations (DB14). Time series of the ratio of plume volume to its surface area (average depth) from ELCIRC simulations capture, similarly to SELFE

simulations, the prompt response of the plume to wind reversals (Figure 2.17). In fact, on occasions, we noticed the response of the plume to wind forcing as simulated in DB11 to match observations more closely than in DB14 simulations: we noticed earlier, for example, that DB14 simulations suggested the plume to be present at *ogi01*, on the outer Oregon mid-shelf, in late December 2000, contrary to the observations and also to DB11. The salinity anomaly maps also show that ELCIRC simulations in DB11 captured the stronger plume signal of February 1999 relative to February 2000, in agreement with the results of Thomas and Weatherbee (2006). DB14 failed to reproduce this result, consistently with the idea of lower skills in the presence of high river discharges. Lower skills at high river discharges, we noted, may be also responsible for the weaker correlation of the first mode from the all-season EOF of DB14 salinity field with river discharge during extreme events. Hence, despite the evident improvements brought by SELFE and the modeling choices adopted in DB14 relative to ELCIRC and DB11, such improvements may not be consistent across the board.

In the following paragraphs, we present a more systematic evaluation of the individual and relative skills of the two models used to generate DB14 and DB11 simulations, respectively. We limited our analysis to salinity, which is the variable upon which we based our computation of integrative plume metrics.

The skill scores computed relative to the available observational datasets –both scores and datasets that were described in the Methods Section– indicate an overall superiority of SELFE simulations archived in DB14 and a strong bias towards freshness of ELCIRC in DB11 (Table 2.3). The RMSE is in most cases substantially reduced in DB14, except at deeper stations (at 5 and 20 m depth at the three RISE buoys), in which case DB11 simulations scored similarly to DB14, if not slightly better. We must note that estimates of salinity in the deeper layers are more strongly affected by the biases introduced through the imposition of boundary and initial ocean conditions from NCOM. The surface layer is instead locally modified by atmospheric forcing and river outflow, as also noted by Liu et al (2009b), who reported similar biases inherited through boundary conditions in their ROMS simulations of the CR plume. The unconditional normalized bias is consistently negative for DB11, and markedly larger, in absolute value, than the bias in DB14, providing evidence of the excessive freshness in ELCIRC simulations. The

deeper stations at the RISE buoys constitute, also with respect to this score, an exception: at a 5-m depth, biases are comparable for the two databases at the central (*risec*) and south RISE mooring (*rises*), while at a 20-m depth, at all three RISE buoys it is DB14 that shows a somewhat larger negative bias in its simulations. Experimental simulation runs (not shown) suggest that the larger biases at depth in DB14 are due to the use of terrain-following coordinates.

Despite the clear overall superiority of SELFE in DB14, the correlation skill score ρ_{MO} (Table 2.3) reveals instances where DB14 simulations perform worse than DB11 in reproducing the variability in observed salinity. ELCIRC simulations (DB11) show a higher correlation with the salinity observations at *ogi01* (-0.8 m depth), on the outer Oregon mid-shelf, in 2001; at the south (*rises* at -1 m) and at the north RISE moorings (*risen*, both at -1 and -5m depth) in the summer of 2004. In a few cases, both simulation databases DB11 and DB14 correlate poorly with observed salinities, particularly at the central RISE mooring (*risec*, -1 and -5m depth), which is located west, just off the mouth of the CR. The poorer skill of CORIE/SATURN simulations to capture the finer variability in the region frequently occupied by the bulge of the plume was confirmed in the evaluation of CORIE/SATURN forecasts in Zhang et al (In review). The negligible correlation with salinities observed at *ogi01* in 2004 is due to the very small dataset available at that station for that year.

The normalized standard deviation (Table 2.3) shows that, in the ELCIRC simulations archived in DB11, the variability in modeled salinity is generally distinctively higher than the variability in observed salinity ($\sigma_M>\sigma_O$); the opposite is true for DB14 ($\sigma_O>\sigma_M$). To a certain extent, for comparable and weaker phase association than DB11 (i.e., comparable or smaller ρ_{MO} with respect to DB11), SELFE in DB14 achieves better predictions in terms of RMSE and unconditional bias by predicting salinity values that are conservatively less variable than the observations.

The conditional distributions of modeled salinity graphically depicted in Figures 2.19 and 2.20 provide a clear confirmation of the strong biases in the salinities simulated in DB11: the median curve of DB11 distributions tends to be below the diagonal that represents a perfect match of model predictions to observations (Figure 2.20). The higher accuracy of DB14 simulations is evident in their much tighter distributions around

observed values, and in the proximity of the distribution median to the diagonal representing a perfect match of model predictions to observations (Figure 2.19). Nonetheless, the plots in Figure 2.19 also show that DB14 consistently fails to reach the minimum observed salinities (congruently with the fact that the first EOF of DB14 surface salinity did not correlate with extremes in river discharge), and modeled values in DB14 exhibit a smaller variance than observed salinities (as confirmed by computed standard deviations). In fact, the slope of the quantile curves for DB14 simulations tend to be consistently less than 1. The slope of the median distributions confirms the better correlation scores that we obtained for DB11 at the south (*rises* at -1 m) and at the north RISE mooring (*risen*, both at -1 and -5m depth), respectively on the Oregon and Washington mid-shelf, in the summer of 2004, and at *ogi01* (-0.8 m depth), on the outer Oregon mid-shelf, in 2001. In particular, the conditional distributions of modeled salinity at *risen* would suggest that DB14 simulations failed to capture reversals of the plume to the north that were observed in the summer of 2004, while DB11 simulations captured them. Despite seemingly missing these events of plume shifting to the north, DB14 simulations still exhibit a somewhat smaller RMSE because of the high variability of modeled values in DB11 around the observed salinity. MacCready et al (2008) and Liu et al (2009b) reported also for their ROMS simulations of the CR plume an underperformance at the north RISE mooring (*risen*), with the model under-predicting the amount of time that the plume was present at the mooring. Liu et al (2009b) noted that skill evaluation based on point mooring observations may suffer from the fact that a slight difference in the plume position may result in a large difference in salinity for a mooring like *risen*, often located at the northern edge of the CR plume. Examination of animations of our simulations in DB14 and DB11 (available at http://www.stccmop.org/CORIE/hindcasts/database/base_frame.html) reveal that, when the plume in DB14 simulations responded to shifts in winds to the north during summer 2004, reversals were modest and, because of the limited size of the plume, did not extend to the mid-shelf location of *risen*. The plume in DB11 recurrently occupied that location during reversals to the north, because of its larger extent. It must be noted that, for this period, the bias towards freshness typically affecting DB11 simulations was modest at this location, as shown in Table 2.3.

Despite the higher accuracy of the SELFE higher-order solution and of the upwind transport scheme, the slope of the median distributions for DB14 simulations in Figure 2.19, which tends to be consistently flatter than the diagonal that represents a perfect match with the observations, may lead to think that the model solution adopted in DB14 is too diffusive. This fact would increase the weight that river discharge has as a forcing versus wind, as a consequence of plume water being mixed away before it can be advected by the Ekman transport. In fact, the EOF analysis described in the previous section suggests a leading role for the river over winds in forcing the variability in the surface salinity field generated by the CR plume off the Washington and Oregon coasts in the DB14 simulations. In contrast, the leading mode of variability for the simulations in DB11 (not shown), which were generated with the ELCIRC model, appears to capture the seasonal oscillation between upwelling- and downwelling-favorable wind regimes. Nonetheless, while the upwind scheme adopted in DB14 to treat scalar transport is more diffusive than the ELM framework used in DB11, we do not believe this to be the likely reason for river discharge being dominant in forcing plume variability in DB14. We would otherwise expect a larger freshwater plume in DB14. Calibration experiments are underway to further explore the issue and improve DB14 skills.

As summarized in Table 2.1, DB11 and DB14 simulations were generated using different models (ELCIRC and SELFE, respectively) as well as a different approach to the solution of scalar transport for salinity and temperature. To isolate the effect of adopting an upwind algorithm to treat scalar transport from the different algorithmic solutions of SELFE and ELCIRC, skill scores were also computed for a third realization of the multi-year database of circulation, DB13. DB13 was generated with the SELFE model, but it still adopted the ELM framework to solve the transport equation. The Brier skill score, which we computed using DB11 simulations as a reference, confirms the improved predictive skills of DB14 simulations relative to the predictive skills of the DB11 simulations, except at larger depths, as already-noted. It must be noted that the computation of the Brier skill score is based on the MSE. The Brier skill score, with consistently higher values for DB14 than for DB13, also manifests the improvement achieved in adopting an upwind method in place of ELM to solve the transport equation – an improvement that is generally confirmed by all other scores (Table 2.3).

2.4 Summary and Conclusions

In this paper we offer a systematic approach to investigate seasonal and inter-annual variability in the structure of the CR plume. Multi-year simulations of baroclinic circulation in the CR estuary-plume-shelf system from 1999-2006, generated as an integral part of the CORIE/SATURN coastal-margin observatory with the SELFE model (and archived in simulation database DB14), enabled the study.

The generation of climatologies and anomalies of surface salinity from the multi-year simulations provided a systematic way to look at the inter-annual variability that overlapped with climatological seasonal conditions. The identified patterns agreed with the results of Thomas and Weatherbee (2006). In addition, the anomaly maps provided indication of the differential influence of the CR plume on the Washington shelf across the years. Recognizing that the structure of the CR plume exhibits strong variability at finer timescales –a few days (Hickey 1989; Hickey et al. 1998)–, we used daily averages of surface salinity in order to identify an example of such variability and verify that it is also well reproduced by the model. These daily averages were also useful in capturing the effect of sub-inertial variability in river inflow on the plume (Yankovsky et al. 2001).

To represent concisely key features of the modeled plume structure, we used a suite of metrics: plume volume, average depth, position of the centroid of the surface plume relative to the river mouth, and depth at three locations: (1) north of the river mouth, on the Washington inner shelf; (2) 30 km southwest of the river mouth, off the Oregon coast, along the 100 m isobath; and (3) again south but in the very near-field of the plume, within 10 km of the river mouth. While the RISE field program in 2004 focused on resolving variability of the plume along the 72 m isobath, we picked the three locations above to provide the ability, in particular, to identify the detachment of the plume from the Washington shore as well as conditions during which the CR plume fully extends to the southwest on the Oregon shelf.

These metrics proved valuable in capturing the evolution of the CR plume in its response to: the seasonal variability in river discharge, from the high flows during the winter storm season and during the spring freshet, to the low flows of the late summer and fall; the inter-annual variability in river discharge, with record-high flow years such

as in 1999 and drought years such as 2001; and the shifts between downwelling-favorable (northward) winds that prevail during winter, and upwelling-favorable (southward) winds that prevail during spring and summer. Monthly distribution of the location of the plume centroid provided an indication of the degree of seasonal and interannual variability of the plume orientation and extent over the Washington and Oregon shelf with potential implications on the variability of productivity in the system.

Our results proved consistent with those reported in observational studies (Hickey et al. 1998; Hickey et al. 2005; Thomas and Weatherbee 2006), confirming the ability the SELFE model to reproduce important features of the behavior of the CR plume. Our simulations were able to reproduce the variability around the two basic structures traditionally known for the CR plume (Barnes et al. 1972; Hickey et al. 1998; Hickey et al. 2005): a winter plume oriented northward and hugging the coast, and a summer plume oriented southwestward and extending offshore, separated from the Oregon coast. We identified, and confirmed through a EOF analysis, the two basic structures described in Hickey et al. (1998) for the plume during fall and winter: a thicker, weakly stratified plume that orients northward and is attached to the coast during periods of strong winds to the north; and a thin, strongly stratified plume oriented west to northwestward during wind relaxation periods or when wind stress turns to the south. The extent to which each pattern explains the winter variability of the plume in the eight years we analyzed closely matched what found by Hickey et al (Hickey et al. 1998) during only one winter season (1990-1991), indicating the generality of that result. We also showed, with an EOF analysis of the salinity field in the summer months, that the result of a prevalent bi-directional structure for the CR plume in that season (Hickey et al. 2005; Liu et al. 2009a) holds true regardless of inter-annual variability.

We further found that a bi-directional plume, with branches both north and south of the river mouth, can occur also in the winter season. In their analysis of CR plume variability from multispectral satellite data, Thomas and Weatherbee (2006) concluded that CR plume waters south of the river mouth are a relatively rare occurrence in winter. García-Berdeal et al. (2002) suggested, with numerical experiments, the difficulty for the plume to reverse direction during winter because of an ambient flow having the same direction as the natural rotational tendency due to Coriolis. Nonetheless, our simulations

would suggest that, during the 8-year period we considered, there were wind events that were capable of generating in winter the same bi-directional plume observed by Hickey et al (2005) in summer. Observations at the *ogi01* buoy, which is located on the Oregon mid-shelf along the 100-m isobath about 30 km southwest of the river mouth, confirmed reversals of the CR plume during winter.

An EOF analysis of the surface salinity field off the Oregon and Washington coast was further used to identify the leading modes of variability of the CR plume. The orthogonal spatial patterns identified through an EOF analysis are data modes of variability, not necessarily physical modes of variability, being constrained to be orthogonal to each other (Storch and Zwiers 1999). Yet, the low-order EOFs can sometimes be interpreted as natural modes of variation of the system, associated with a physical process. Indeed, the first two modes from the EOF decomposition of the surface salinity field in DB14 simulations were clearly related to the two key forcing mechanisms of seasonal and inter-annual variability of the CR plume: variability in river discharge and shifting wind regimes. The relative importance of the two forcing mechanisms in the SELFE simulations archived in DB14 continues to be subject of investigation, to verify whether it is determined by specific modeling choices.

Duplicative realizations of the multi-year simulations enabled the evaluation of skills of our modeling approach to study seasonal and inter-annual variability of the CR plume. These duplicative realizations were generated using two 3D numerical models: SELFE (Zhang and Baptista 2008) –simulations archived in database DB14– and ELCIRC (Zhang et al. 2004; Baptista et al. 2005) –simulations archived in DB11. All three approaches used to investigate variability in the plume –climatologies and anomalies in surface salinity, time series of metrics of plume structure, and an EOF analysis of the same salinity field– provided some indication of the individual and relative merits of SELFE and ELCIRC. We further illustrated the usefulness of aggregated scores to evaluate systematically the skills of the two models. We also proposed a graphical representation (modified from Storch and Zwiers 1999) of the distribution of modeled salinities, conditional on the value of observed salinity, as an effective way to synthesize many aspects of individual and relative model skills.

Zhang and Baptista (2008) showed results suggesting the superior skills of SELFE over ELCIRC. Our study confirmed the overall superiority of SELFE in the multi-year DB14 simulations, as shown in the small RMSE and bias, and the excessive freshness of DB11 simulations (ELCIRC). We also demonstrated the ability of SELFE to capture important features of plume behavior, including its deeper penetration along the Washington coast with the coastal jet and the formation of a bulge developing into a secondary bulge in response to subinertial variability in river discharge (Yankovsky et al. 2001). We also showed, however, that SELFE, to a certain extent, achieves better performance in terms of RMSE –even when its simulations exhibit a weaker correlation with the observations than ELCIRC simulations– by producing results that are conservatively less variable than the corresponding observations.

We conclude that no one score is adequate by itself to fully evaluate the skill of a model. We also conclude that only through a holistic approach that uses multiple but integrated strategies, not limited to skill scores, can we adequately evaluate the ability of a model to reproduce the complex features of the CR estuary-plume-shelf system, and its variability at multiple temporal and spatial scales. We note that this study focused on simulated salinity, hence a more comprehensive evaluation is required extending to modeled velocity and temperature.

The availability of long-term, multi-year databases of simulated circulation opens unparalleled data mining opportunities to continue investigating the behavior of the CR plume at multiple scales. The only other long-term simulation of the circulation in the CR estuary-plume-shelf system (Liu et al. 2009a; Liu et al. 2009b; MacCready et al. 2008) covered a period of solely three months (June-August) of 2004 and could only look at intraseasonal variability. With hindcasts that already extend even beyond the eight years covered by the present study, CORIE/SATURN simulations allow investigating variability of the CR plume across seasons and years and its implications to the coastal productivity off the Washington and Oregon coast. They therefore provide an invaluable context to the questions posed by the RISE program. This study also provides a rationale for using metrics of CR plume structure from simulations to investigate the ecological implications of plume dynamics, in particular as they relate to the survival of CR salmon. For example, we are currently using our simulations to explore existing hypotheses that

attribute a role for the CR plume as salmon habitat (Casillas 1999; De Robertis et al. 2005; Morgan et al. 2005; Bottom et al. 2006; Burla et al. In review).

2.5 Acknowledgments

The National Science Foundation (OCE-0622278; OCE-0424602) provided financial support for this research. The study relied on results from the CORIE/SATURN modeling system. Thanks are due to the following members of the CORIE/SATURN team: to Paul Turner and Charles Seaton for their contributions to generating the circulation databases and related information products, and generation of Figure 2.1; and to Mike Wilkin and other field crew for their effort in maintaining CORIE observational network. We also thank Barbara Hickey and Ed Dever for providing the observational datasets from the RISE buoys, and two anonymous reviewers and an associate editor whose comments helped to improve this manuscript. Any statements, opinions, findings, conclusions or recommendations expressed in this material are those of the authors and do not necessarily reflect the views or policies of the federal sponsors, and no official endorsement should be inferred.

2.6 References

Banas, N. S., P. MacCready and B. M. Hickey. (2008) The Columbia River plume as cross-shelf exporter and along-coast barrier. *Continental Shelf Research* doi: 10.1016/j.csr.2008.03.011.

Baptista, A. M. (2006). CORIE: the first decade of a coastal-margin collaborative observatory. In: *Ocean '06*. Boston, MA: MTS/IEEE.

Baptista, A. M., Y. Zhang, A. Chawla, M. Zulauf, C. Seaton, E. P. Myers, J. Kindle, M. Wilkin, M. Burla and P. J. Turner. (2005). A cross-scale model for 3D baroclinic circulation in estuary-plume-shelf systems: II. Application to the Columbia River. *Continental Shelf Research 25:* 935-972.

Barnes, C. A., A. C. Duxbury and B.-A. Morse. (1972). Circulation and selected properties of the Columbia River effluent at sea. In: A. T. Pruter and D. L. Alverson, Eds. *The Columbia River estuary and adjacent ocean waters*. University of Washington Press, Seattle, WA**:** 41-80.

Barron, C. N., A. B. Kara, P. J. Martin, P. J. Rhodes and L. F. Smedstad. (2006). Formulation, implementation and examination of vertical coordinate choices in the Global Navy Coastal Ocean Model (NCOM). *Ocean Modelling 11:* 347-375.

Bottom, D. L., B. E. Riddell and J. A. Lichatowich. (2006). The estuary, plume, and marine environments. In: Richard N. Williams, Ed. *Return to the River. Restoring Salmon to the Columbia River.* Elsevier Academic Press**:** 507-569.

Burla, M., A. M. Baptista, E. Casillas and J. G. Williams. (In review). The influence of the Columbia River plume on the survival of steelhead (*Oncorhynchus mykiss*) and chinook salmon (*O. tshawytscha*): a numerical exploration. *Submitted to Canadian Journal of Fisheries and Aquatic Sciences*.

Casillas, E. (1999). Role of the Columbia River estuary and plume in salmon productivity. In: *Ocean Conditions and the Management of Columbia River Salmon*, (Proc. Symposium, Portland, OR, 1 July 1999). Gustavo A. Bisbal (Ed.) Portland, OR: Northwest Power Planning Council, pp. 55-64.

De Robertis, A., C. A. Morgan, R. Schabetsberger, R. W. Zabel, R. D. Brodeur, R. L. Emmett, C. M. Knight, G. K. Krutzikowsky and E. Casillas. (2005). Columbia River plume fronts. II. Distribution, abundance, and feeding ecology of juvenile salmon. *Marine Ecology Progress Series 299:* 33-44.

Fiedler, P. C. and R. M. Laurs. (1990). Variability of the Columbia River plume observed in visible and infrared satellite imagery. *International Journal of Remote Sensing 11(6):* 999-1010.

Frolov, S., A. M. Baptista, Z. Lu, R. van der Merwe and T. K. Leen. (2009). Fast data assimilation using a nonlinear Kalman filter and a model surrogate: an application to the Columbia River estuary. *Dynamics of Atmosphere and Oceans*. doi:10.1016/j.dynatmoce.2008.10.004.

Garcia-Berdeal, I., B. M. Hickey and M. Kawase. (2002). Influence of wind stress and ambient flow on a high discharge river plume. *Journal of Geophysical Research 107 (C9):* 3130.

Hermann, A., B. M. Hickey, M. R. Landry and D. Winter. (1989). Coastal upwelling dynamics. In: Michael R. Landry and B. M. Hickey, Eds. *Coastal Oceanography of Washington and Oregon*. Elsevier Science, New York**:** 211-253.

Hickey, B. M. (1989). Patterns and processes of circulation over the Washington continental shelf and slope. In: Michael R. Landry and B. M. Hickey, Eds. *Coastal Oceanography of Washington and Oregon*. Elsevier Science, New York**:** 41-115.

Hickey, B. M. and N. S. Banas. (2003). Oceanography of the U.S. Pacific Northwest coastal ocean and estuaries with application to coastal ecology. *Estuaries* 26(48): 1010-1031.

Hickey, B. M., S. Geier, N. Kachel and A. MacFadyen. (2005). A bi-directional river plume: the Columbia in summer. *Continental Shelf Research 25:* 1631-1656.

Hickey, B. M., L. J. Pietrafesa, D. A. Jay and W. C. Boicourt. (1998). The Columbia River Plume Study: Subtidal variability in the velocity and salinity fields. *Journal of Geophysical Research 103(C5):* 10339-10368.

Horner, R., B. M. Hickey and J. R. Postel. (2000). *Pseudo-nitzschia* blooms and physical oceanography off Washington State. *African Journal of Marine Science 22:* 299-308.

Liu, Y., P. MacCready and B. M. Hickey. (2009a). Columbia River Plume Patterns as Revealed by a Hindcast Coastal Ocean Circulation Model in Summer 2004.*Geophysical Research Letters 36*, L02601, doi:10.1029/2008GL036447.

Liu, Y., P. MacCready, B. M. Hickey, E. P. Dever, P. M. Kosro and N. S. Banas. (2009b). Evaluation of a coastal ocean circulation model for the Columbia River plume in summer 2004. *Submitted to Journal of Geophysical Research*.

MacCready, P., N. S. Banas, B. M. Hickey, E. P. Dever and Y. Liu. (2008). A model study of tide- and wind-induced mixing in the Columbia River estaury and plume. *Continental Shelf Research* doi:10.1016/j.csr.2008.03.015.

Morgan, C. A., A. De Robertis and R. W. Zabel. (2005). Columbia River plume fronts. I. Hydrography, zooplankton distribution, and community composition. *Marine Ecology Progress Series 299:* 19-31.

Murphy, A. H. (1992). Climatology, persistence, and their linear combination as standards of reference in skill scores. *Weather and Forecasting 7:* 692-698.

Oke, P. R., J. S. Allen, R. N. Miller, G. D. Egbert, J. A. Austin, J. A. Barth, T. J. Boyd, P. M. Kosro and M. D. Levine. (2002). A modeling study of the three-dimensional continental shelf circulation off Oregon. Part I: Model-data comparisons. *Journal of Physical Oceanography 32:* 1360-1382.

Pearcy, W. G. (1992). *Ocean Ecology of North Pacific Salmon*. University of Washington Press, Seattle, WA

Song, Y. and D. Haidvogel. (1994). A semi-implicit ocean circulation model using a generalized topography-following coordinate system. *Journal of Computational Physics 115:* 228-244.

Storch, H. v. and F. W. Zwiers. (1999). *Statistical analysis in climate research*. Cambridge University Press

Thomas, A. C. and R. A. Weatherbee. (2006). Satellite-measured temporal variability of the Columbia River plume. *Remote Sensing of Environment 100:* 167-178.

Xue, Y., M. A. Cane and S. E. Zebiak. (1997). Predictability of a coupled model of ENSO using singular vector analysis. Part I: Optimal growth in seasonal background and ENSO cycles. *Monthly Weather Review 125:* 2043-2056.

Yankovsky, A. E., B. M. Hickey and A. K. Münchow. (2001). Impact of variable inflow on the dynamics of a coastal buoyant plume. *Journal of Geophysical Research 106(C9):* 19809-19824.

Zhang, Y. and A. M. Baptista. (2008). SELFE: A semi-implicit Eularian-Lagrangian finite-element model for cross-scale ocean circulation, with hybrid vertical coordinates. *Ocean Modelling 21(3-4):* 71-96.

Zhang, Y., A. M. Baptista, B. M. Hickey, B. C. Crump, D. A. Jay, M. Wilkin and C. Seaton. Daily forecasts of Columbia River plume circulation: a tale of spring/summer cruises. (In review). *Submitted to Journal of Geophysical Research*.

Zhang, Y., A. M. Baptista and E. P. Myers. (2004). A cross-scale model for 3D baroclinic circulation in estuary-plume-shelf systems: I. Formulation and skill assessment. *Continental Shelf Research 24:* 2187-2214.

Tables

Table 2.1 – Key differences between the three multi-year databases of circulation used in the study. Resolution for the forcing sources is indicated in parenthesis. ELM: Eulerian Lagrangian Method; NRL NCOM: Navy Coastal Ocean Model of the Naval Research Laboratory; GFS: NOAA National Centers for Environmental Prediction (NCEP)'s Global Forecast System; OSU ARPS: the Advanced Regional Prediction System developed at the University of Oklahoma, as modified and run at Oregon State University; NARR: NCEP North American Regional Reanalysis.

	Model	**Grid**	**Numerical solution for S, T transport**	**Ocean conditions**	**Atmospheric forcing**
DB11	ELCIRC	Horizontal grid: 50622 elements; ~2.1 mil faces; Vertical: 62 Z-levels (min & max equivalent radius= 11m, 12km)	ELM	NRL NCOM (1/8 degree; daily), with strong nudging in extensive shelf region	1999-2001: GFS re-analysis (1 degree; 3-hourly); 2002-2003: GFS + OSU ARPS (12km; hourly); 2004: ETA (12km; 3-hourly)
DB13	SELFE v1.3n2	Reduced ocean grid Horizontal grid: 39133 elements; ~2.5 mil. faces Vertical: 18 Z-levels + 37 S-levels, with transition depth between SZ hs=100m, and transition depth between S and sigma hc=30m	ELM	NRL NCOM (1/8 degree; daily), with weak nudging in extensive shelf region	NARRS (32 km resolution; 6-hourly)
DB14	SELFE v1.4a	Same as DB13 (min & max equivalent radius= 19m, 12km)	Finite-volume upwind method	NRL NCOM (1/8 degree; daily), with weak nudging in extensive shelf region	1999-2003: NARRS; 2004: ETA

Table 2.2 – Observational datasets used for the model skill evaluation

Year	Station	Total water depth		Sensor depth (m)	period	N of obs.	std dev	mean	Min	Max
1999	OGI01	100 m	outer Oregon mid-shelf	-0.8	7/8-12/30	8085	2.68	29.97	13.9	32.9
2000	OGI01	100 m		-0.8	1/1-12/29	13339	3.70	28.09	14.4	32.7
2001	OGI01	100 m		-0.8	1/1-12/30	17367	2.56	29.89	17.1	32.7
2002	OGI01	100 m		-0.8	1/1-12/14	18445	3.48	29.14	12.6	32.7
2004	OGI01	100 m		-0.8	7/8-7/20	1125	2.14	26.61	20.1	31.7
	OGI02	41 m	Oregon inner shelf – near field	-1	5/18-10/19	14627	3.09	27.55	9.4	32.2
	RISEC	72 m	Oregon mid-shelf – near field	-1m	6/21-9/9	15204	3.10	26.35	15.5	32.2
				-5m	6/21-9/9	15204	1.14	30.85	25.2	32.8
				-20m	6/21-9/9	15204	0.25	32.99	31.7	33.5
	RISES	72 m	Oregon mid-shelf	-1m	6/21-9/7	15135	2.31	28.78	18.8	32.3
				-5m	6/21-9/7	15135	1.00	31.07	24.6	32.8
				-20m	6/21-9/7	15135	0.25	32.93	31.4	33.5
	RISEN	72 m	Washington mid-shelf	-1m	6/22-9/8	15086	2.80	29.55	18.2	32.6
				-5m	6/22-9/8	15086	1.58	30.87	24.2	32.8
				-20m	6/22-9/8	15086	0.31	32.70	31.3	33.5
2005	OGI01	100 m	outer Oregon mid-shelf	-0.8	1/13-6/24	11693	4.04	28.93	15.0	33.0

Table 2.3 – Skill scores computed for the simulations in the three databases used in the study. Definition of each score is presented in the Methods. In case of perfect predictive skills, each score takes the value shown in parenthesis. The Brier skill score for DB13 and DB14 is computed using DB11 as reference hindcast.

Year	**Station**	**Depth, m**	**RMSE (0)**			**correlation skill score (1)**			**unconditional (normalized) bias (0)**			**normalized standard deviation (1)**			**Brier skill score (1)**	
			db11	db13	db14	db11	db13	db14	db11	db13	db14	db11	db13	db14	db13	db14
1999	OGI01	-0.8	9.79	5.77	2.85	0.43	0.58	0.62	-2.88	-1.67	-0.57	2.49	1.67	1.06	0.65	0.92
2000	OGI01	-0.8	7.94	5.38	3.01	0.47	0.59	0.6	-1.48	-1.08	-0.10	1.74	1.15	0.71	0.54	0.86
2001	OGI01	-0.8	7.51	5.26	2.51	0.54	0.44	0.46	-2.11	-1.56	-0.26	2.40	1.42	0.79	0.51	0.89
2002	OGI01	-0.8	5.70	4.70	2.89	0.56	0.58	0.57	-0.84	-0.98	-0.12	1.70	1.02	0.65	0.32	0.74
2004	OGI01	-0.8	6.63	3.38	3.25	0.02	0.08	-0.04	-1.21	-0.97	0.89	2.69	0.82	0.68	0.74	0.76
	OGI02	-1	11.00	6.89	2.56	0.36	0.50	0.6	-2.93	-1.90	-0.17	2.15	1.29	0.72	0.61	0.95
	RISEC	-1m	10.26	7.04	3.11	0.29	0.28	0.29	-2.59	-1.87	0.10	2.11	1.13	0.57	0.53	0.91
		-5m	2.61	3.02	2.10	-0.1	0.03	0.04	-1.49	-2.17	-1.32	1.33	1.17	0.83	-0.34	0.35
		-20m	1.01	1.45	1.25	0.43	0.57	0.59	-3.68	-5.69	-4.88	1.84	1.11	1.00	-1.06	-0.53
	RISES	-1m	7.31	4.44	2.19	0.46	0.39	0.36	-2.58	-1.64	-0.05	2.06	0.78	0.52	0.63	0.91
		-5m	2.18	2.73	1.57	0.21	0.37	0.18	-1.43	-2.51	-1.12	1.53	0.91	0.68	-0.57	0.48
		-20m	1.01	1.36	1.13	0.46	0.63	0.67	-3.48	-5.36	-4.44	2.32	1.35	1.00	-0.82	-0.25
	RISEN	-1m	4.00	3.12	3.20	0.54	0.14	0.47	-0.39	0.49	0.65	1.64	0.29	0.15	0.39	0.36
		-5m	1.52	1.56	1.56	0.59	0.22	0.47	-0.28	0.11	0.36	1.04	0.34	0.20	-0.06	-0.05
		-20m	0.75	1.17	0.97	0.44	0.19	0.58	-2.23	-3.63	-3.03	0.87	0.50	0.48	-1.42	-0.67
2005	OGI01	-0.8	5.17	5.45	3.40	0.56	0.68	0.66	-0.57	-1.09	-0.33	1.35	0.97	0.52	-0.11	0.57

Figures

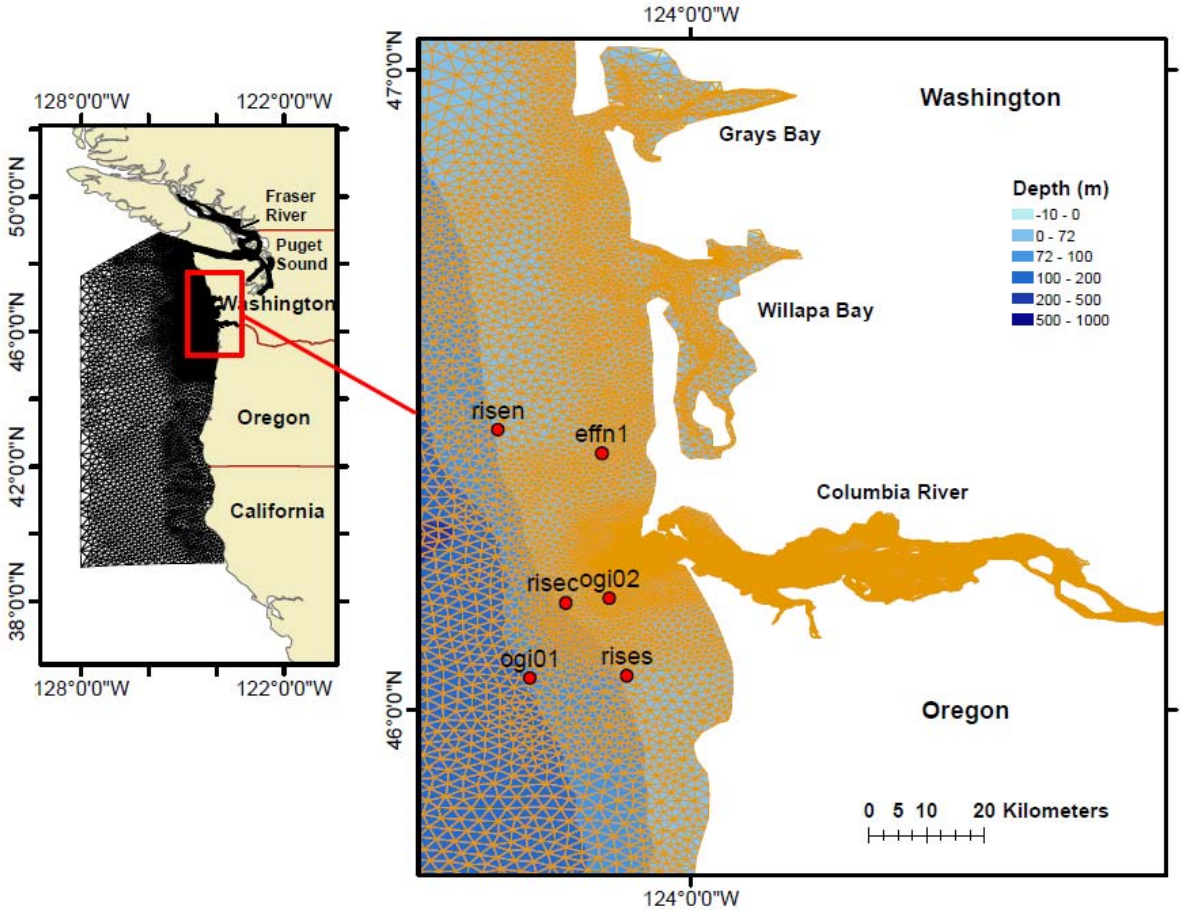

Figure 2.1 - Left: Model domain showing the computational grid. Right: Zoom of the study area with location of the model stations used for the analysis and the buoys to which the observational datasets refer.

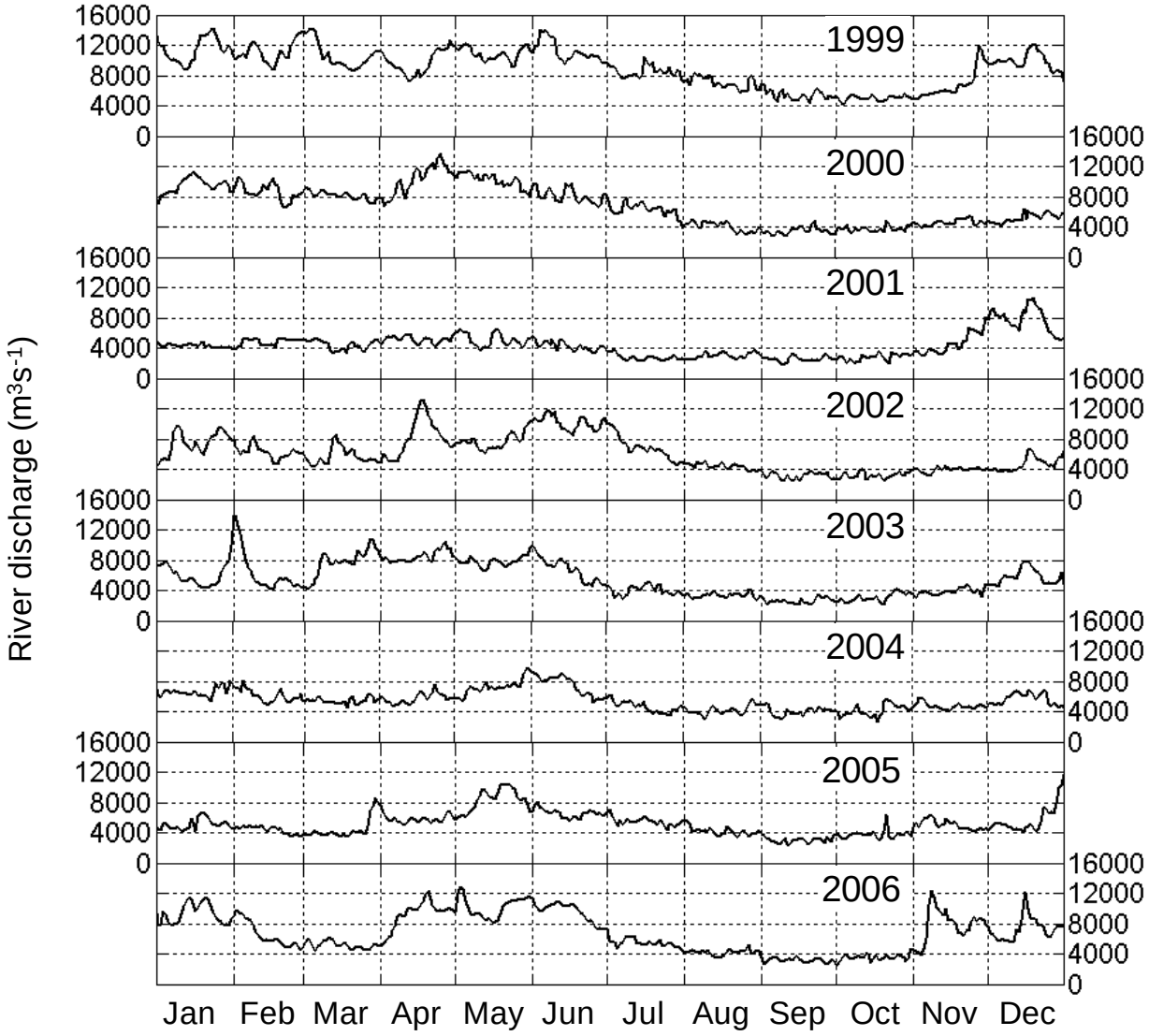

Figure 2.2 - Columbia River discharge (m^3/s) at the US Geological Survey station at Beaver Army Terminal, Quincy, Oregon (daily averages).

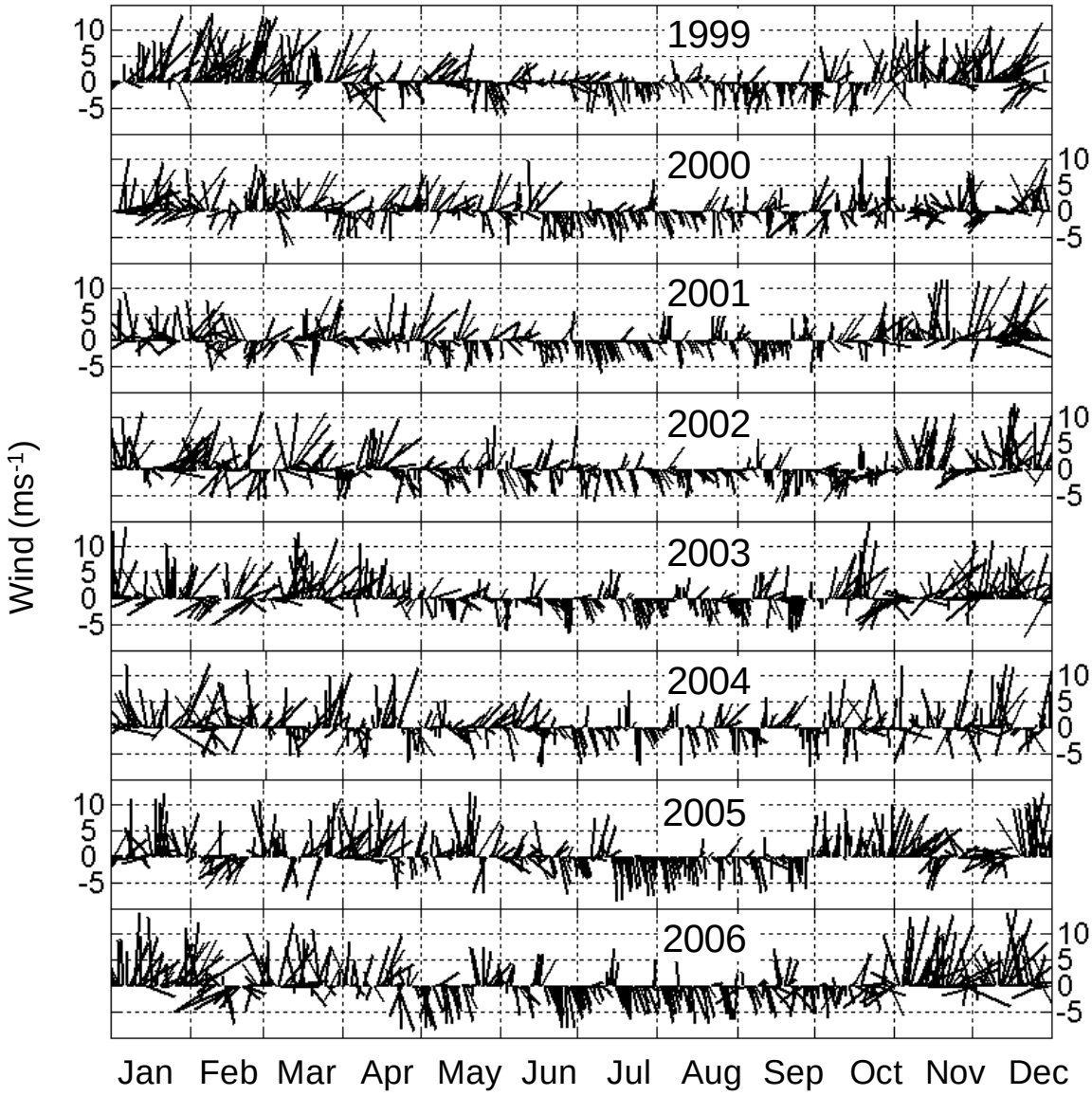

Figure 2.3 - Vector wind time series, for winds off the Columbia River mouth; in the north-south-east-west reference frame used, vectors above the x-axis indicate downwelling-favorable (southerly) winds.

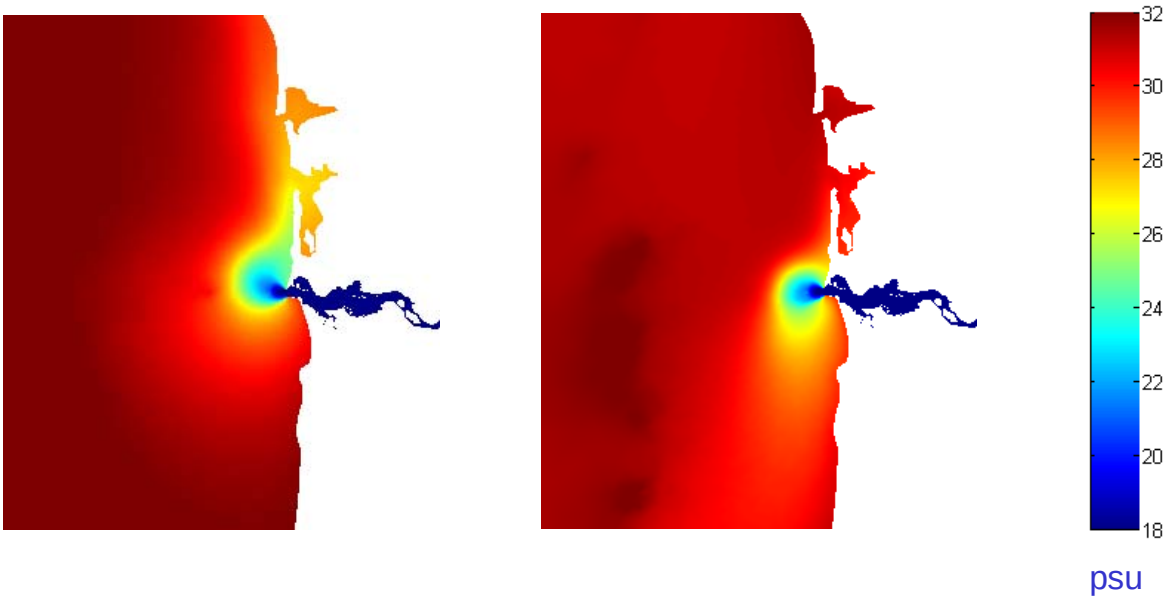

Figure 2.4 - 1999-2006 winter climatology (left) and 1999-2006 summer climatology (right) from DB14 simulations.

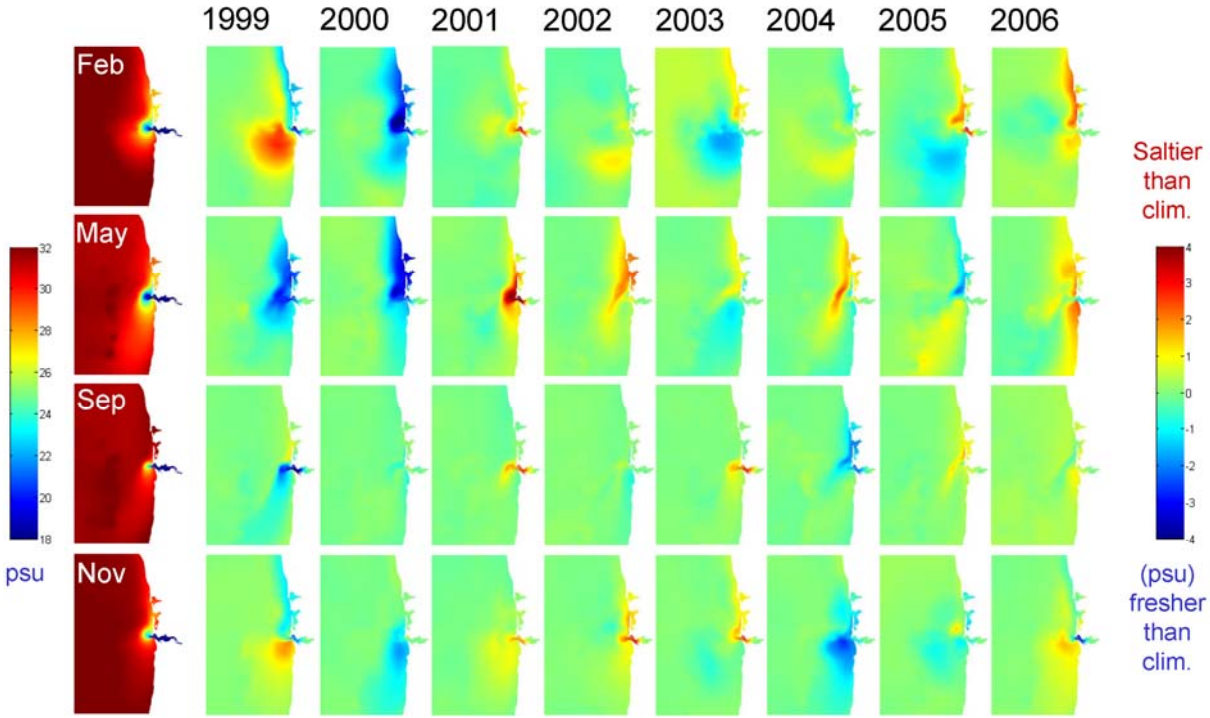

Figure 2.5 - Monthly climatologies and anomalies for the surface salinity field from 1999-2006 DB14 simulations

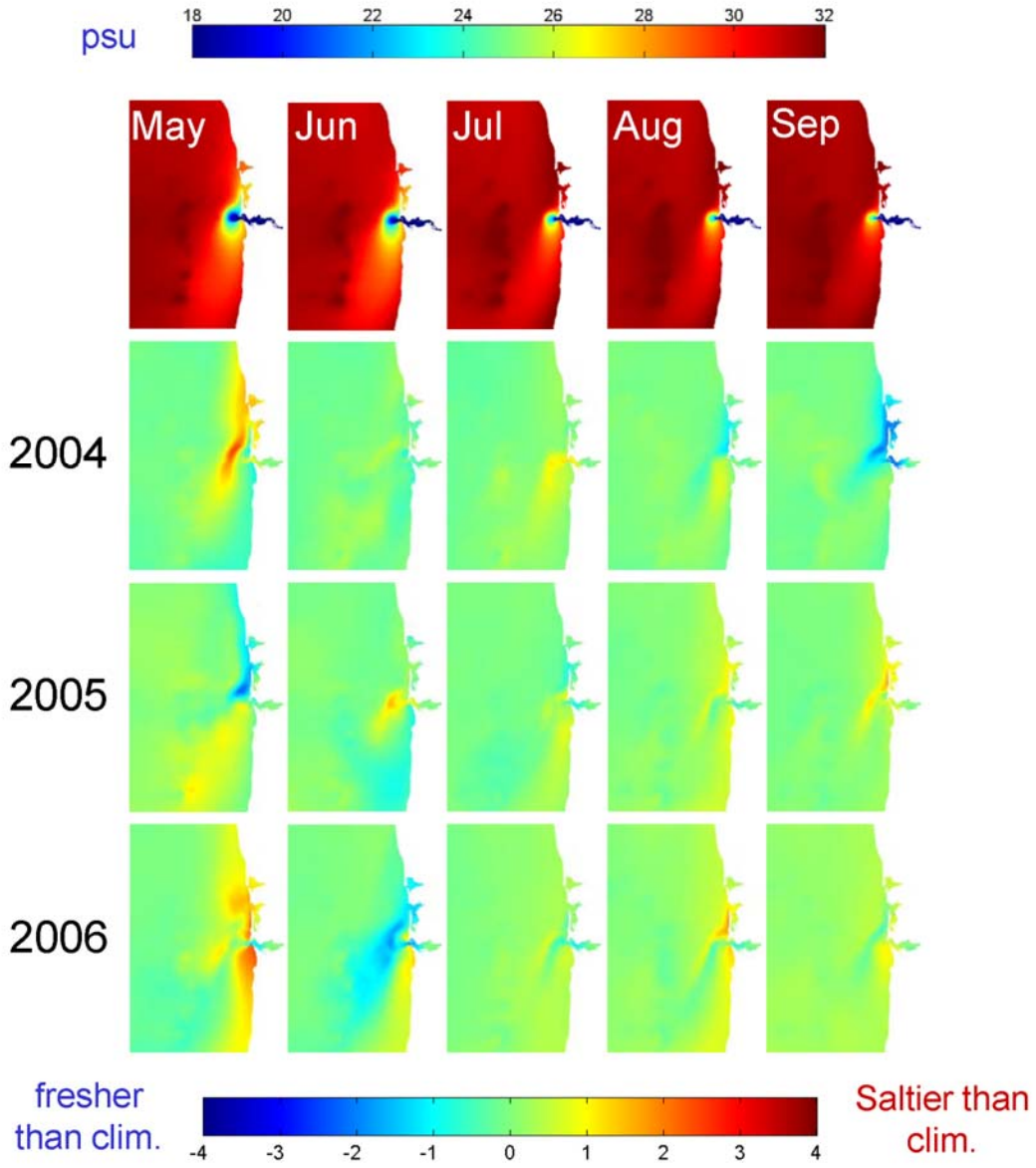

Figure 2.6 - Anomalies in the surface salinity field in the late spring and summer months of 2004, 2005 and 2006, field seasons for the RISE program. Anomalies are relative to the 1999-2006 climatologies constructed from DB14 simulations.

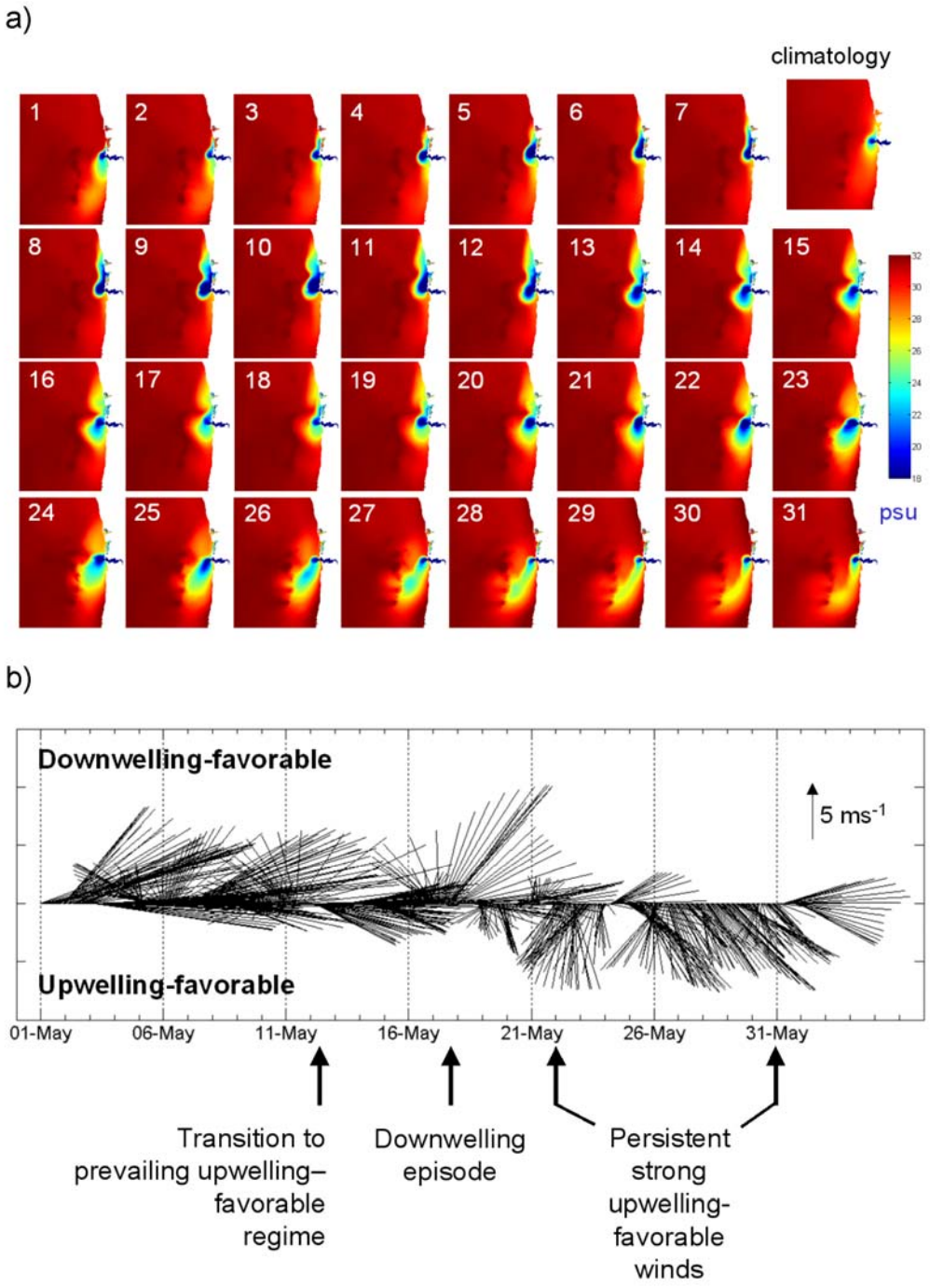

Figure 2.7 - a) Daily averaged surface salinity for May 1999 from DB14 simulations. The climatology for the same month is shown at the top left. b) Time series for the hourly wind off the river mouth. Increases and subsidence in river discharge were observed during the same period, with discharge ranging between 9000 and 12000 m^3s^{-1}.

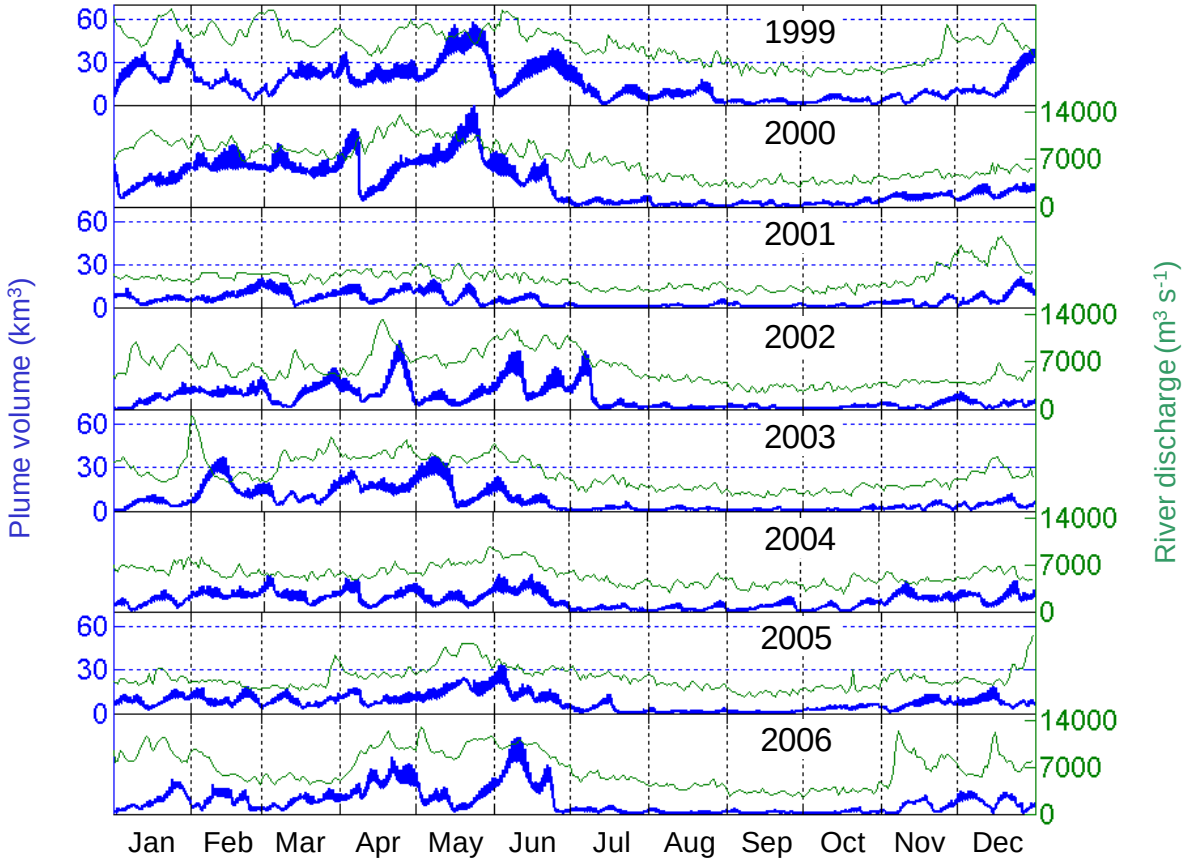

Figure 2.8 - Time series of the volume of the plume defined by the 28-psu isoline.

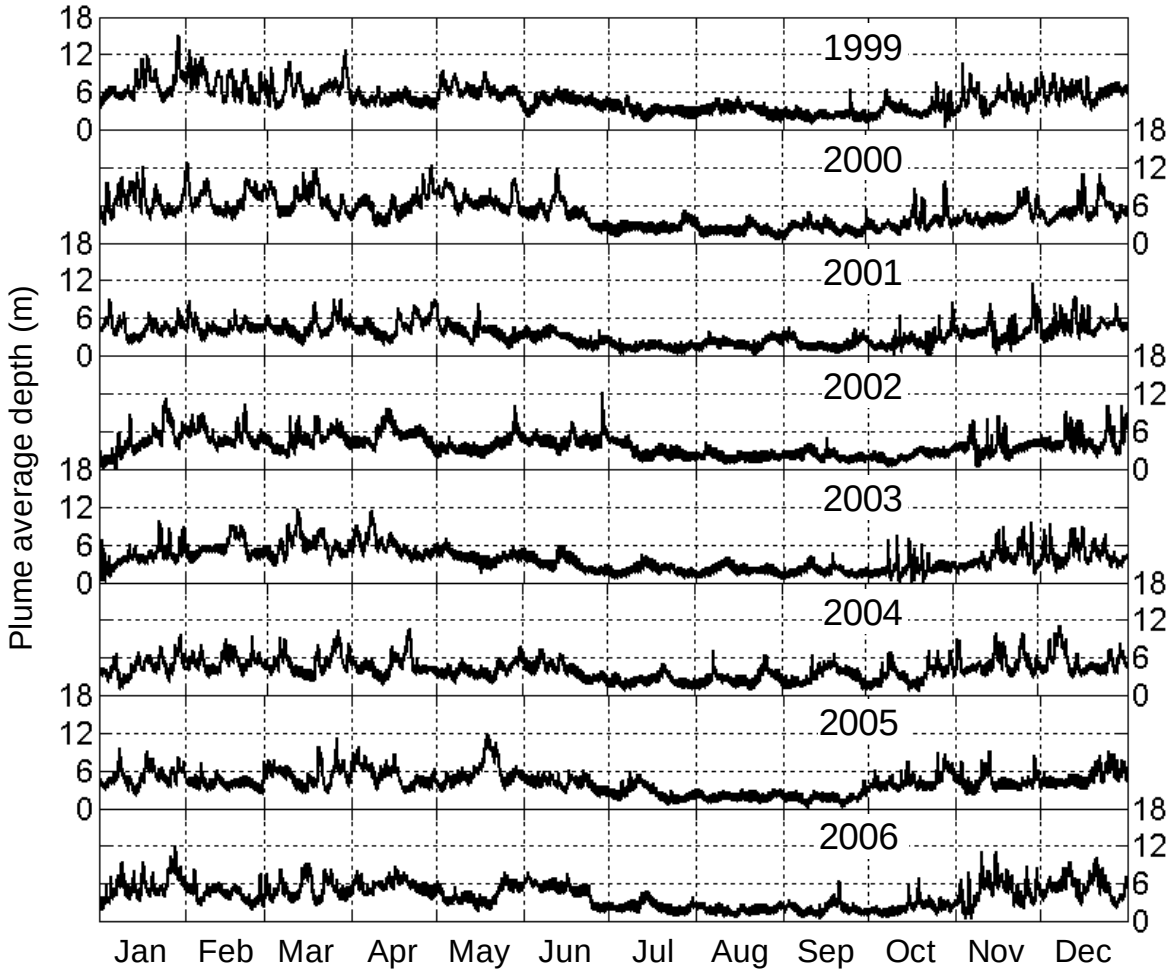

Figure 2.9 - Time series of the average depth of the plume defined by the 28-psu isoline.

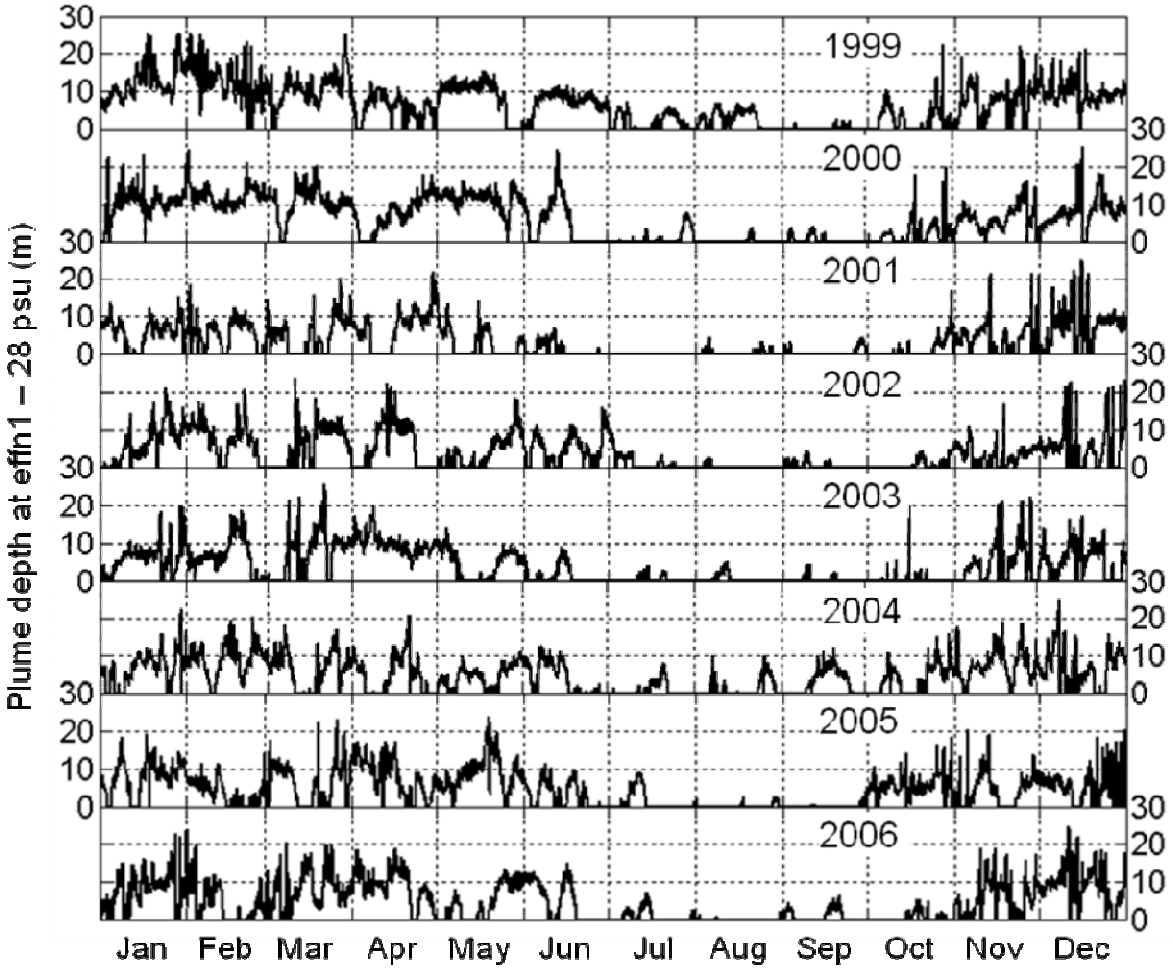

Figure 2.10a - Depth (m) below sea surface of the simulated plume at model station *effn1*.

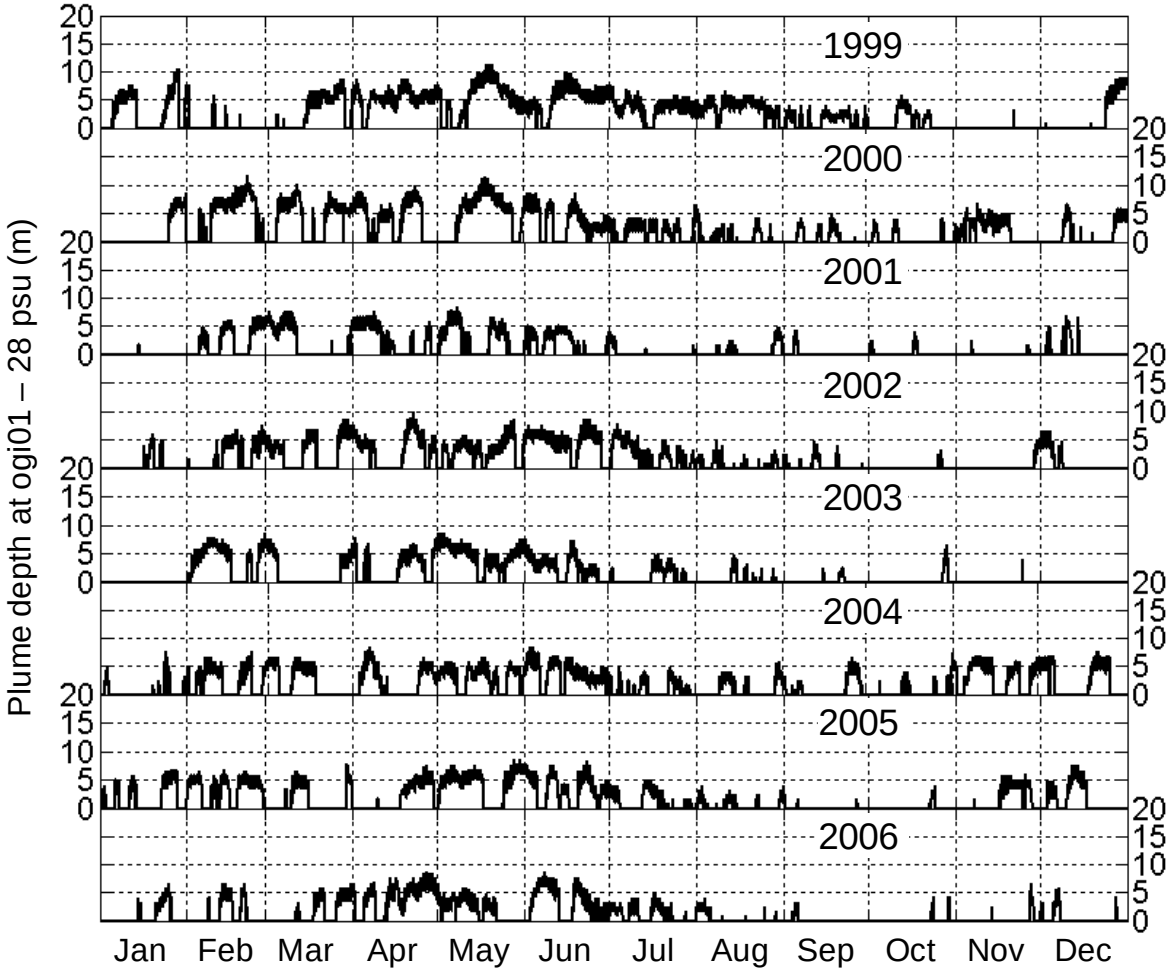

Figure 2.10b - Depth (m) below sea surface of the simulated plume at the *ogi01* location.

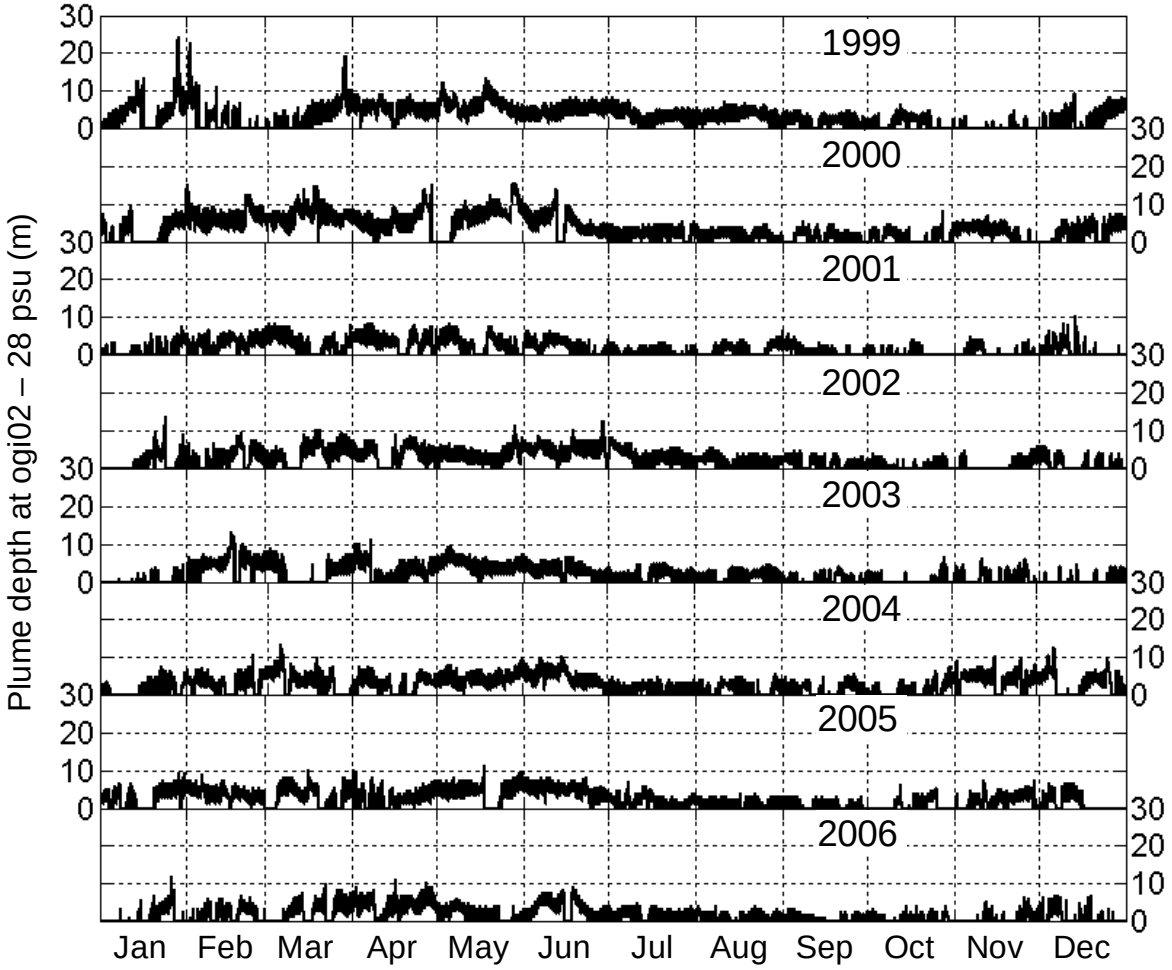

Figure 2.10c - Depth (m) below sea surface of the simulated plume at *ogi02* location.

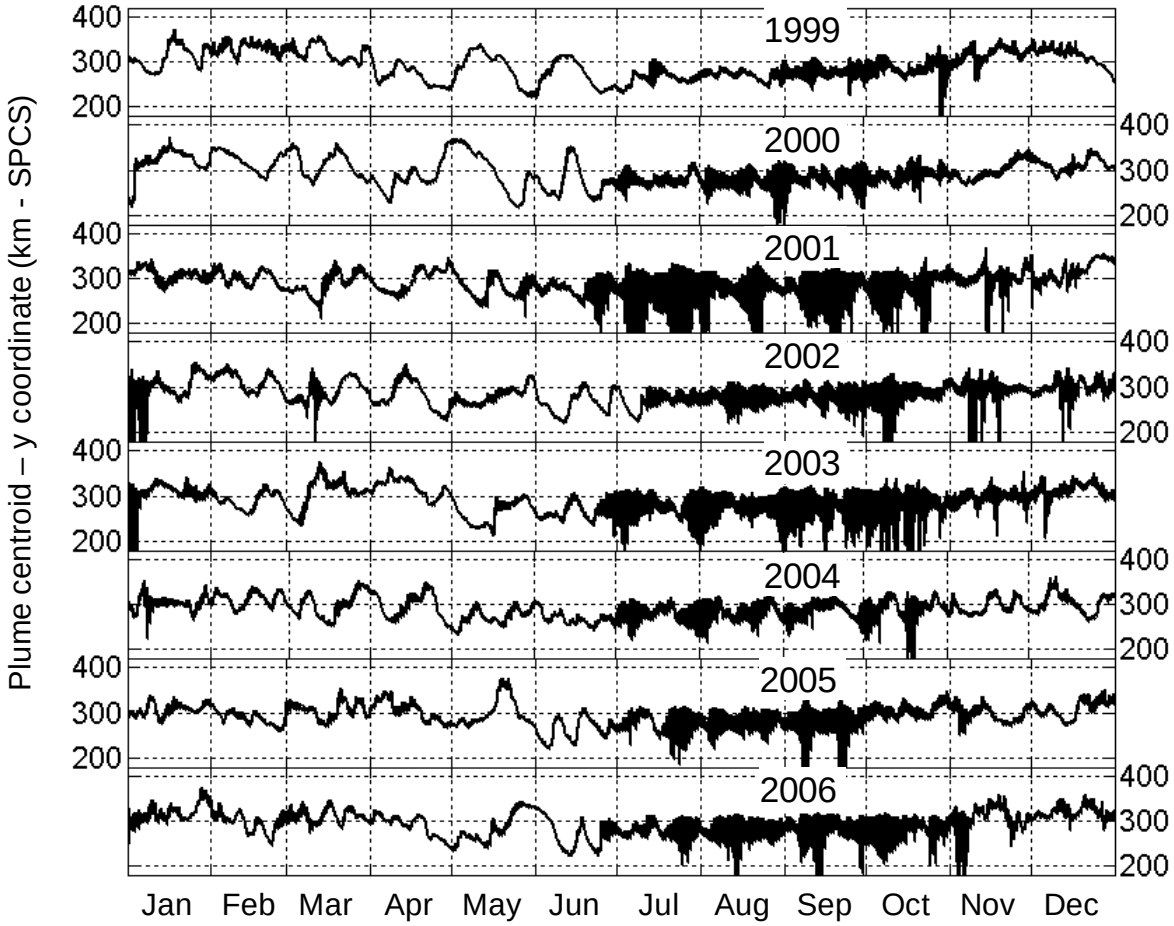

Figure 2.11 - Time series of the y-coordinate (in the State Plane Coordinate System) of the centroid of the plume. The river mouth is located just south of the 300 km mark.

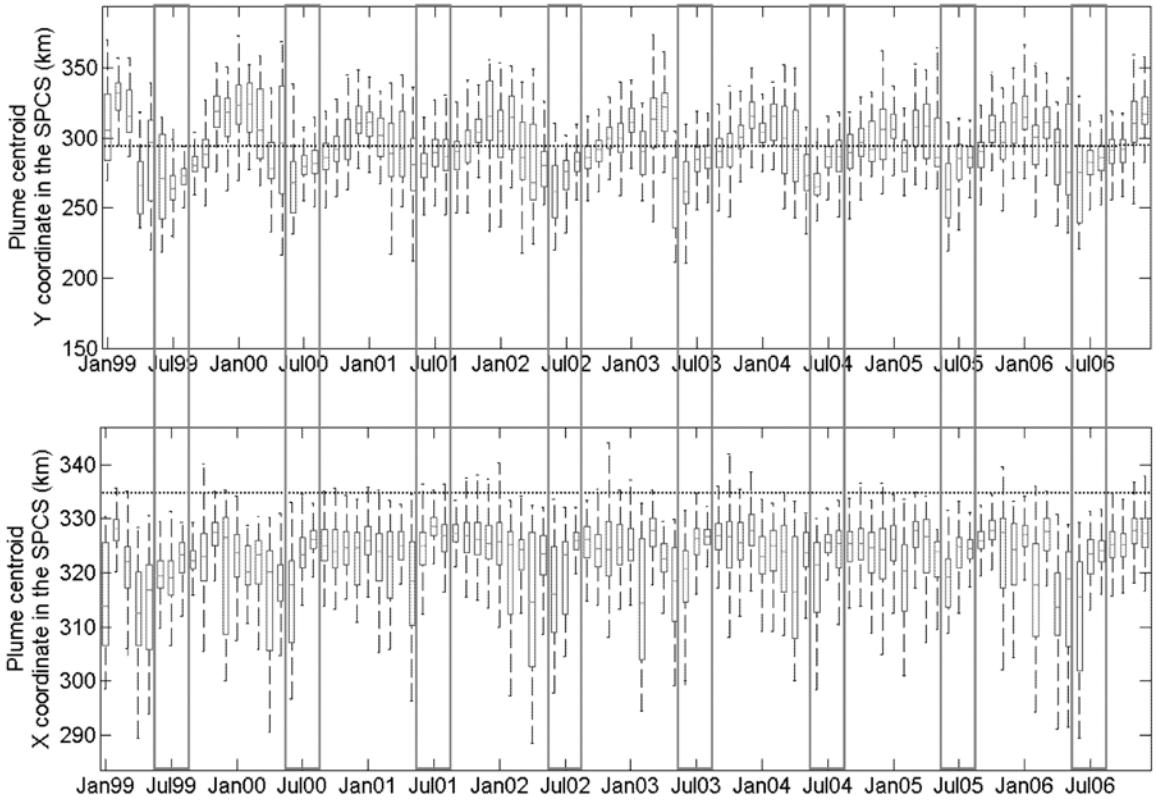

Figure 2.12 - Box plots of the monthly distributions of the y and x coordinates of the centroid of the surface CR plume (in the State Plane Coordinate System). Horizontal dotted lines indicate the location of the river mouth. Box plots represent the interquartile range of each distribution. The median is shown within each box. Whiskers extend out of the boxes to 1.5 the interquartile range, or stop at the farthest outlier.

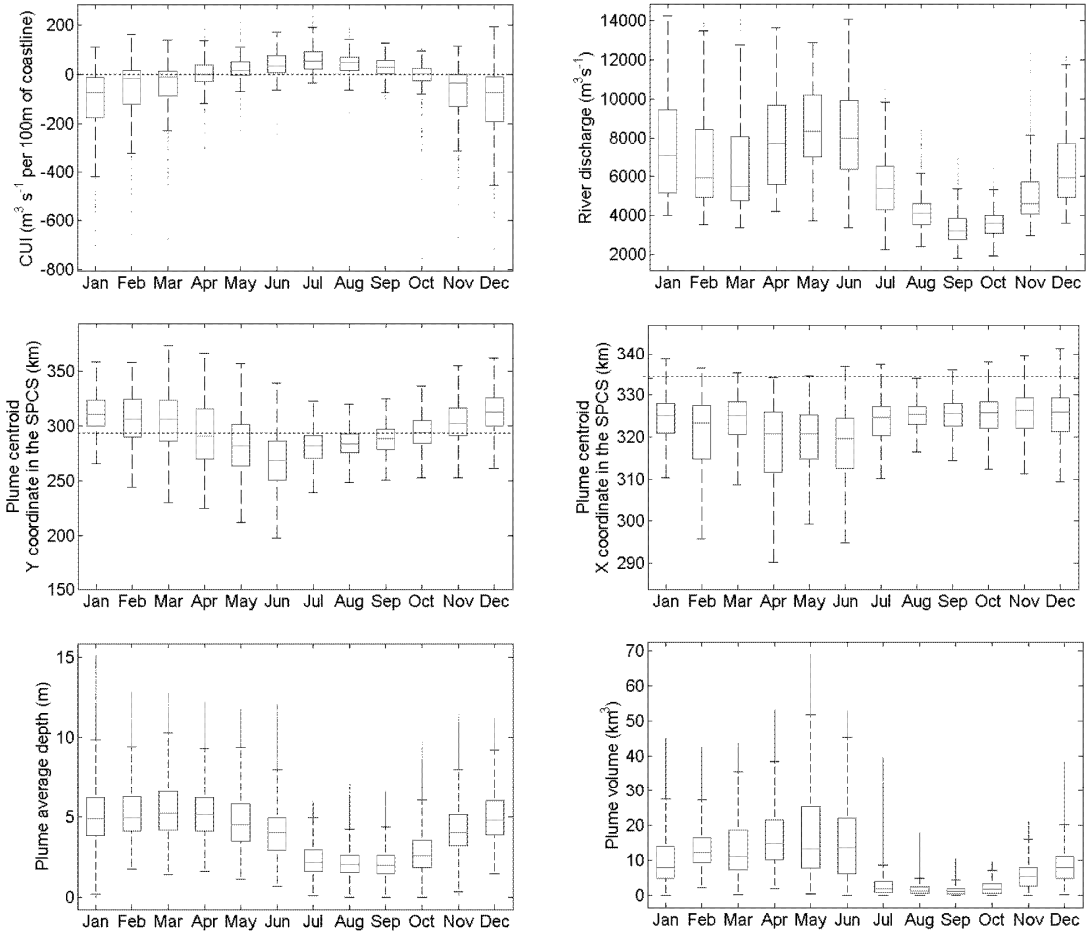

Figure 2.13 - Seasonal variability captured in the monthly distributions, over the 8-year period 1999-2006, of the plume metrics, framed by the variability in the forcings: (top left) Coastal Upwelling Index for location 45N 125W from NOAA's Pacific Fisheries Environmental Laboratory (PFEL, http://www.pfeg.noaa.gov, last accessed August 11, 2008); (top right) Columbia River discharge at Beaver Army terminal.

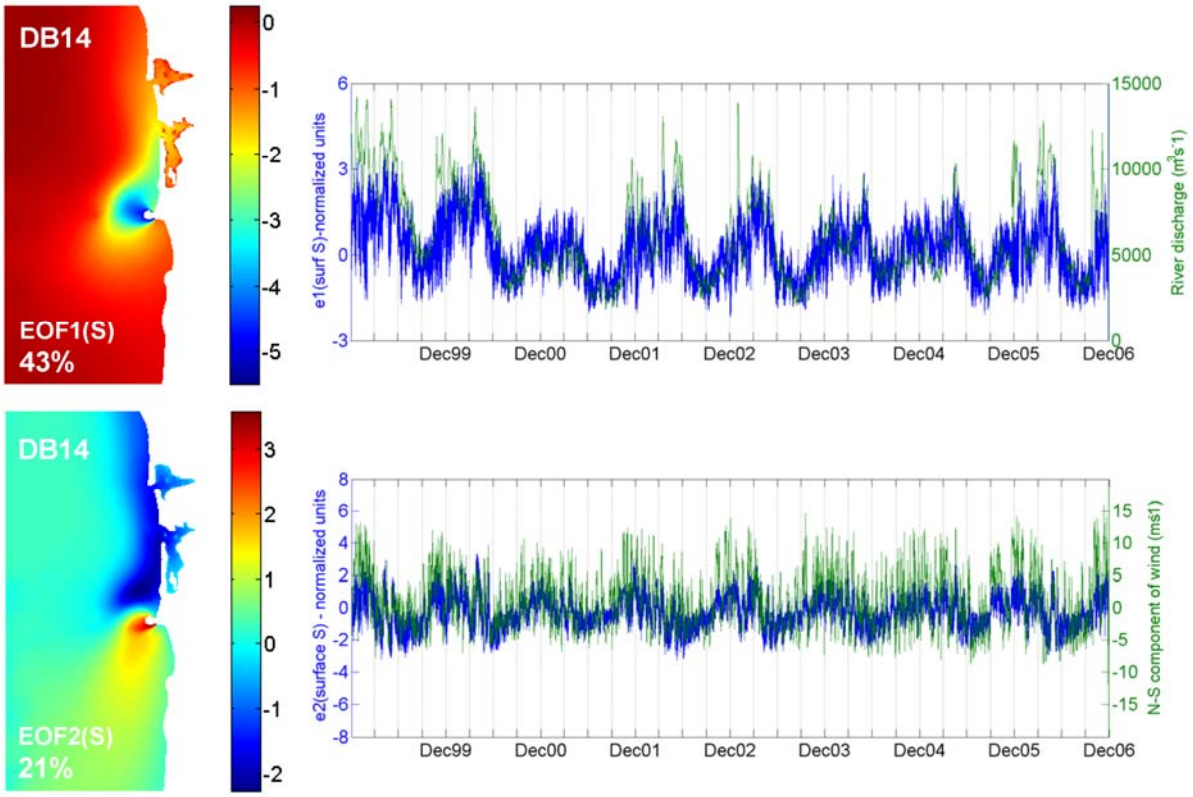

Figure 2.14 - EOF analysis of the 1999-2006 surface salinity field simulated with the SELFE model (database DB14). Maps to the left are the eigenvectors (EOFs) of the two leading modes of variability for the field and can be regarded as their spatial pattern. The time series on the right are obtained by projecting the original field (simulated surface salinity) onto the EOFs and they represent how each spatial pattern evolves with time. Amplitudes are normalized by the standard deviation. The first mode (top) accounts for 44% of the total variance in the data, the second mode (bottom) for 21%. Time series on the top also shows, in green, the time series for the Columbia River discharge at Beaver Army, used to force the model. Time series on the bottom shows in green the time series of the N-S component of winds. Note that the y-axis for this time series is reversed to show the match with the EOF time series. Positive values (shown below the x-axis) represent wind stress to the north.

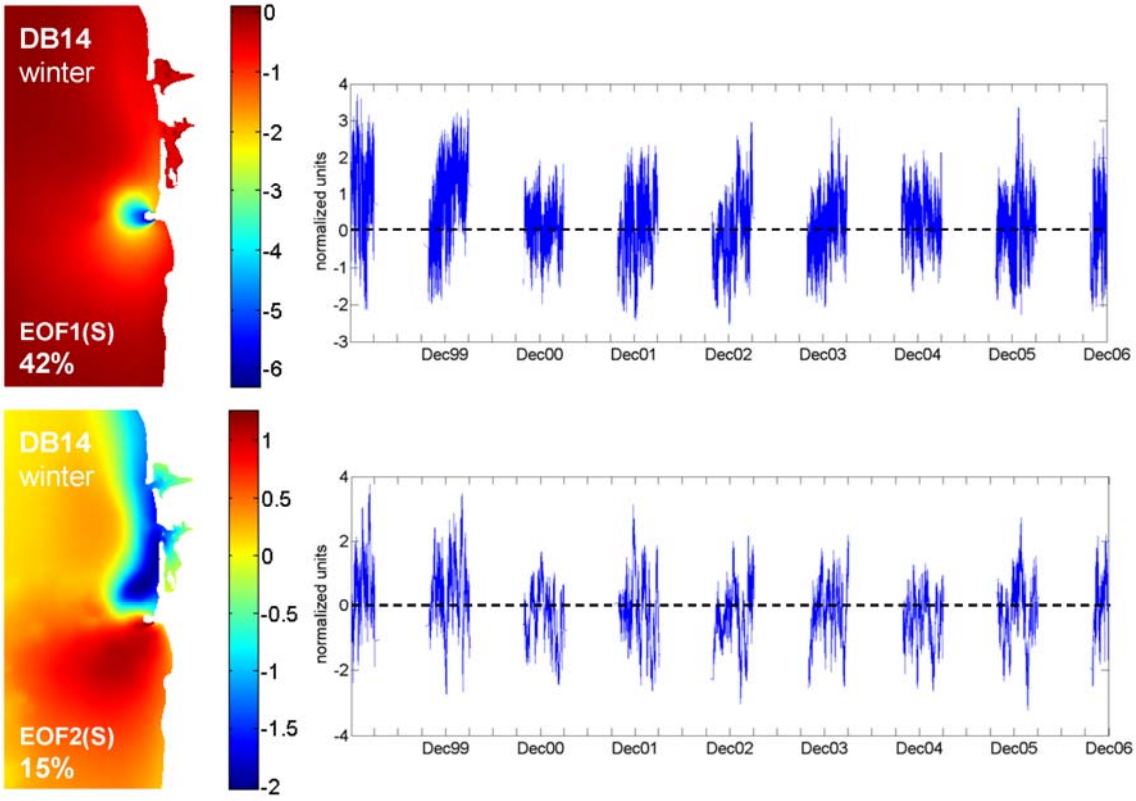

Figure 2.15 - EOF analysis of the 1999-2006 surface salinity field during the winter months only (November-March), simulated with the SELFE model (database DB14). In the time series of expansion coefficients of the two EOF modes, amplitudes are normalized by the standard deviation.

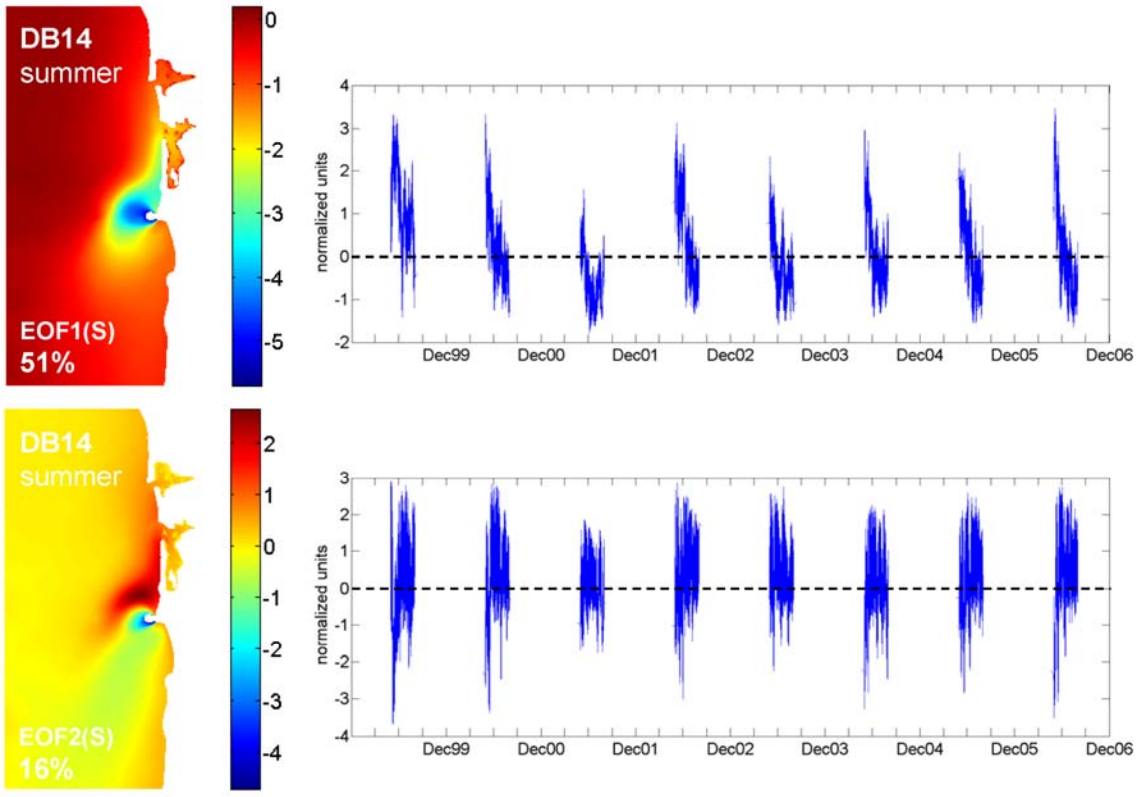

Figure 2.16 - EOF analysis of the 1999-2006 surface salinity field during the summer months only (June-August), simulated with the SELFE model (database DB14). In the time series of expansion coefficients of the two EOF modes, amplitudes are normalized by the standard deviation.

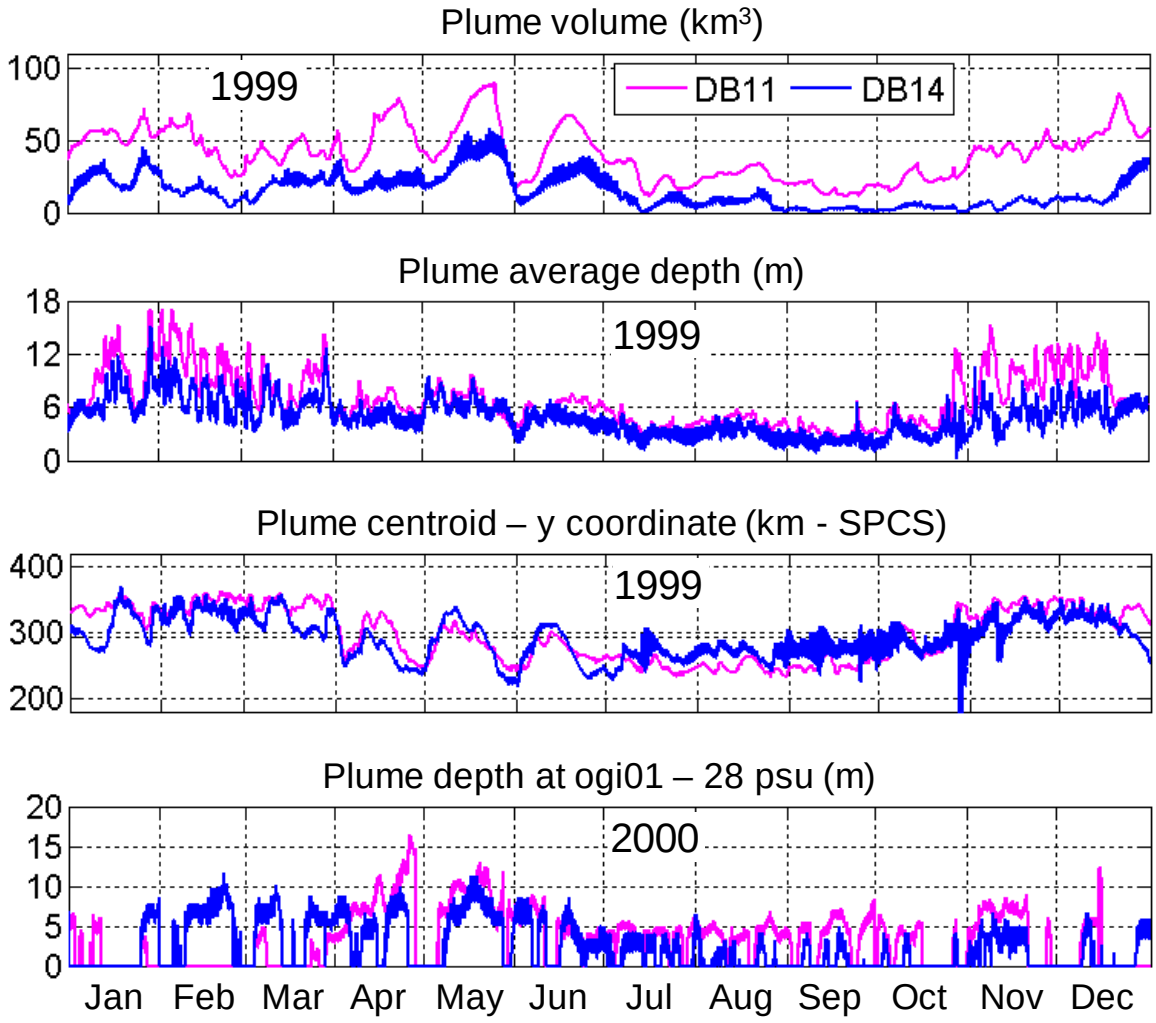

Figure 2.17 - Comparison of plume metrics computed from database DB14 and database DB11. From top to bottom: volume of the plume defined by the 28-psu isoline for the year 1999; average depth of the plume for the same year; y-coordinate (in the State Plane Coordinate System) of the centroid of the plume, again for 1999 (the river mouth is located just south of the 300 km mark); depth (m) below sea surface of the simulated plume at the *ogi01* station in 2000. The latter time series reveals, in particular, events when the two simulation databases disagree in estimating the presence of the plume in winter at this location, on the outer Oregon mid-shelf southwest of the mouth.

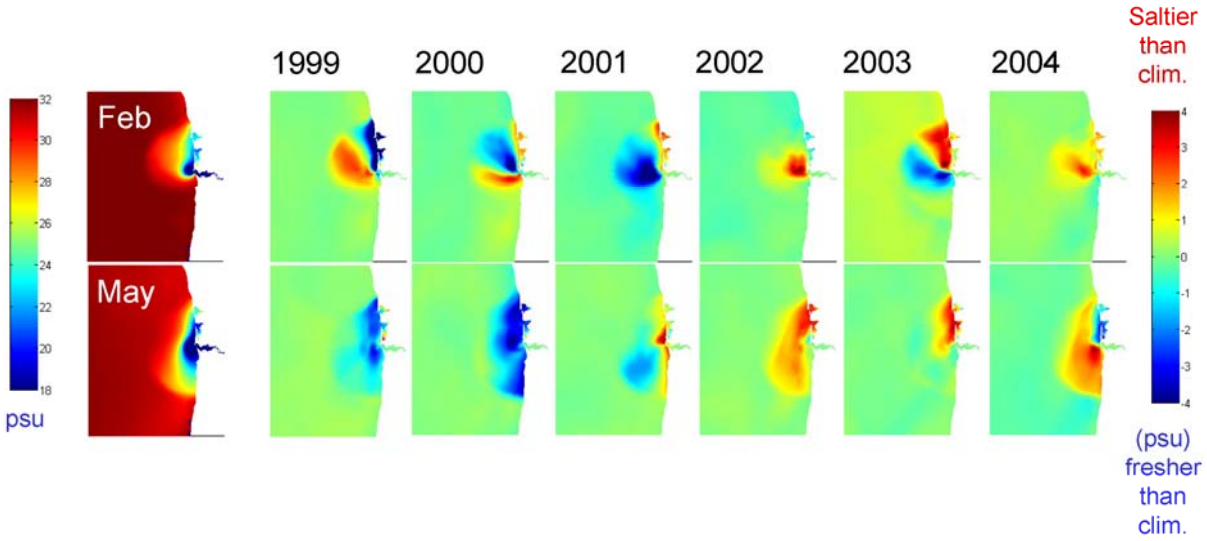

Figure 2.18 - February and May climatologies and anomalies for the surface salinity field from DB11 simulations

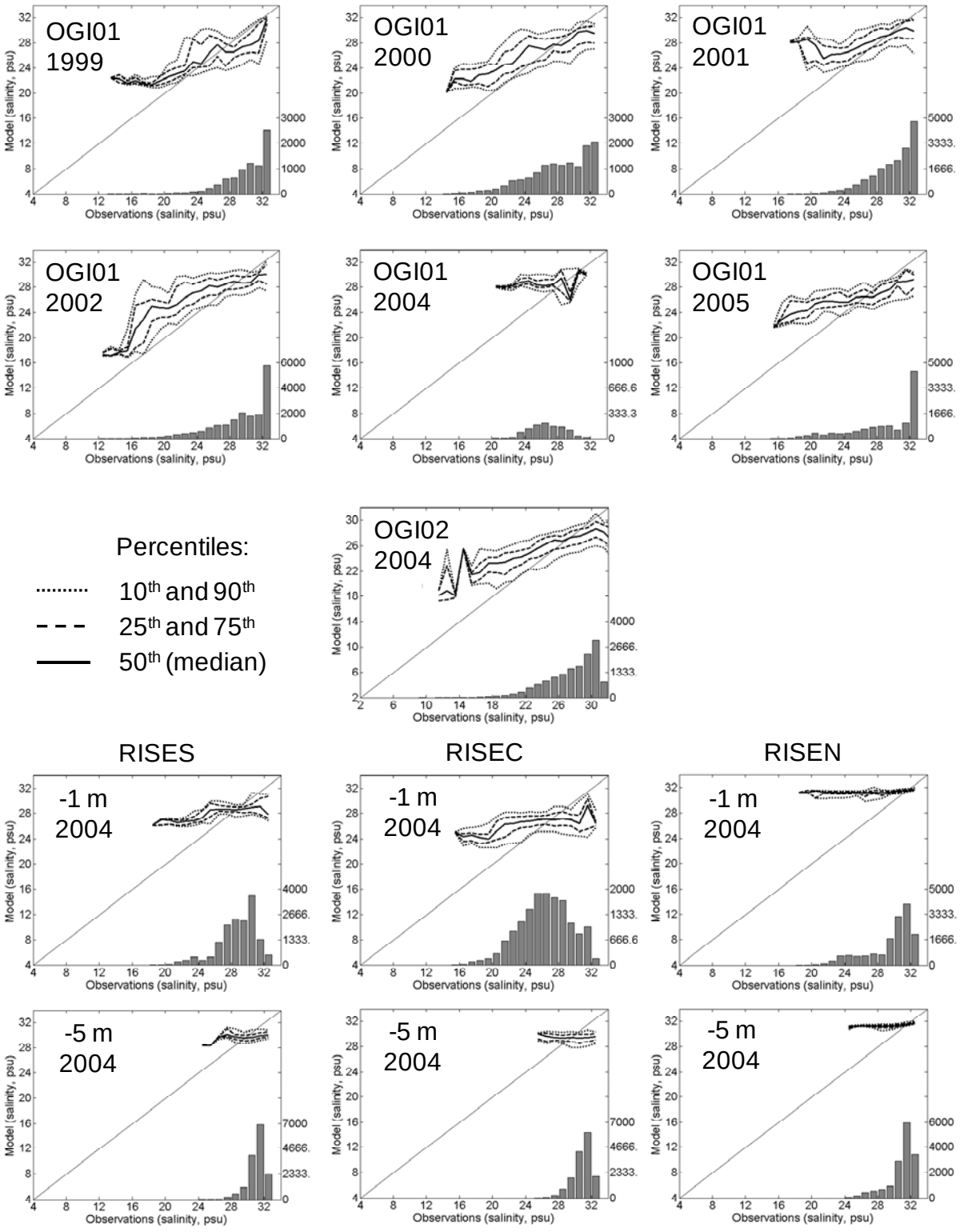

Figure 2.19 - Distributions of modeled salinity in DB14, conditional on the observed salinity value. The curves represent the quantiles of each conditional distribution, i.e. the distribution of salinity values predicted by the model

when the observation falls in a specific range (observations are binned in 1-psu ranges). The bar plot shows the marginal distribution of the observations. Besides providing information about how observations were distributed at each station for the period of coverage, the frequency of the observations in each value range allows to evaluate the credibility of each quantile.

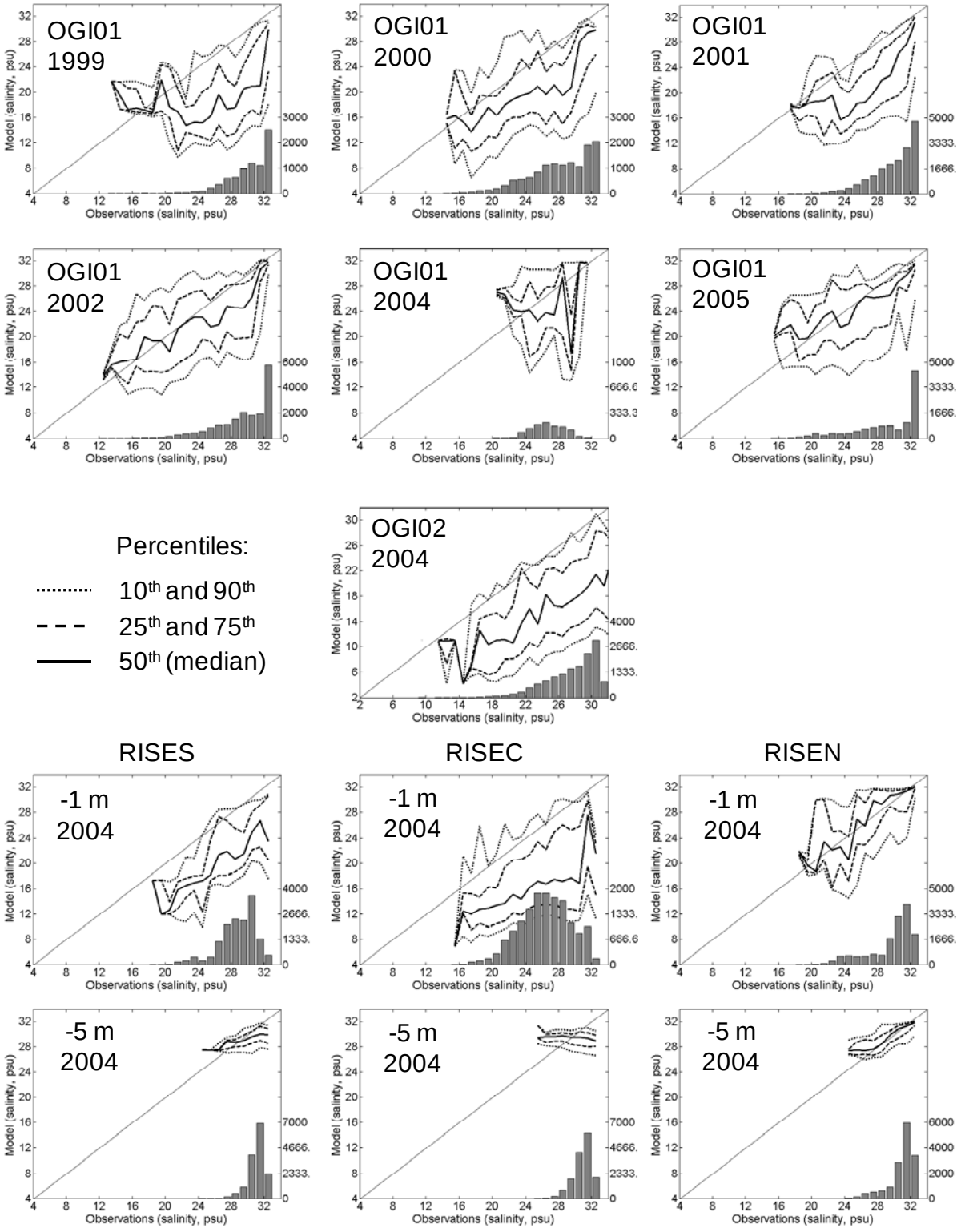

Figure 2.20 - Distributions of modeled salinity in DB11 conditional on the observed salinity value. See Figure 19 for further detail.

Chapter 3

The influence of the Columbia River plume on the survival of steelhead (*Oncorhynchus mykiss*) and Chinook salmon (*O. tshawytscha*): a numerical exploration.

Authors: Michela Burla, António M. Baptista, Edmundo Casillas, John G. Williams and Douglas M. Marsh

Submitted to the Canadian Journal of Fisheries and Aquatic Sciences

Abstract:

A coastal-margin observatory in the Pacific Northwest relies on 3D numerical models to systematically simulate and understand baroclinic circulation in the Columbia River estuary-plume-shelf system. We used multi-year databases of simulations to address the question of whether the intraseasonal variability in smolt-to-adult survival rates (SARs) for steelhead (*Oncorhynchus mykiss*) and Snake River spring/summer Chinook salmon (*O. tshawytscha*) related to changes in the Columbia River plume as the juvenile migrants entered the ocean. Lagged cross-correlations between SARs and metrics of plume size and location suggested that steelhead benefited from the plume environment at a narrow window of time around their ocean entry. When large-scale ocean conditions, however, turned unfavorable the contribution of local (plume) conditions to the overall variability in steelhead survival became modest. A similar evaluation revealed that the plume did not affect survival of Chinook salmon, at least at the fine scale of variability considered. The differential response between the two species is consistent with observed and previously reported behavioral characteristics they exhibit. We speculate that steelhead mainly use the plume to move quickly away from coastal habitats and the predation pressures associated with this environment, for a more direct migration to ocean habitats in the Gulf of Alaska.

3.1 Introduction

The Endangered Species Act (ESA) listing of many Evolutionarily Significant Units (ESUs) of eastern Pacific Ocean salmon (*Oncorhynchus* spp.) has prompted extensive research into possible causes for their declines. Although most research on salmon mortality historically focused on freshwater, both freshwater and ocean environments contribute substantially to egg-to-adult mortality, and they contribute roughly equally to the interannual variability in such mortality (Bradford 1995). Additionally, a considerable body of evidence exists that indicates that, for the ocean phase of salmon life history, most mortality occurs within the first few weeks or months of ocean residence (Pearcy 1992).

In recent years, more effort has gone into understanding the relationship between Pacific salmon production and climate variability patterns, such as the El Niño Southern Oscillation (ENSO) and the Pacific Decadal Oscillation (PDO) (Johnson 1988; Francis and Hare 1994; Mantua et al. 1997; Francis et al. 1998; Peterson and Schwing 2003). Local marine environments, as affected by ocean-shelf upwelling or infusion of freshwater from river plumes may play as large a role in the early marine survival of salmon as the regime shifts operating at broader, regional scales (Beamish et al. 1994; Peterman et al. 1998; Casillas 1999).

Recent field research has begun to develop information that provides an understanding of the mechanisms by which the plume of the Columbia River (CR) may influence juvenile salmon survival (Emmett et al. 2003; Schabetsberger et al. 2003; De Robertis et al. 2005; Morgan et al. 2005). Emmett et al. (2003) found that the highest densities of subyearling Chinook salmon off the CR were associated with the stronger currents emanating from the river mouth during ebb tide, while densities of yearling Chinook salmon were higher at lower water clarity. They also found that, in the study location, most juvenile salmon resided in the upper 12 m of the water column. They recognized the possibility that features associated with the plume (low salinities, high turbidity, fronts, and eddies) determined this distribution. De Robertis et al. (2005) confirmed these suggestions as they found a higher abundance of juvenile Pacific salmon in the coastal region off the CR associated with the low-salinity plume waters and frontal

zones compared to the surrounding, more saline ocean waters. They called for focused studies to determine if growth and survival of juvenile salmon are related to plume structure and, in particular, to changes in the timing and intensity of freshwater discharge from the CR into the coastal ocean. Morgan et al. (2005) focused on the hypothesis of plume fronts as feeding habitats for juvenile salmon. Fronts were found to be zones of increased zooplankton biomasses. However, based on stomach content analysis, juvenile salmon do not seem to take advantage of this valuable food resource, possibly due to the transience of the frontal features or to the small scale of the frontal regions compared to the size of the plume and ocean habitats. Research is starting to address the intra-annual variability in survival rates of steelhead and yearling Chinook salmon leaving the CR system (Scheuerell et al. 2009). The rapidity of change in survival suggested local conditions in the environments that connect the river migration corridor to the ocean were more likely a determinant of the observed variability than conditions farther away (in the ocean feeding areas of the gulf of Alaska or Bering Sea).

Initial results from this recent research suggest that the survival of outmigrating juvenile salmon varies at time scales consistent with changes in the CR plume. Such changes occur not just across seasons and years, but also on a time scale of days (Hickey et al. 1998; Hickey et al. 2005). With knowledge that the plume varies temporally within a migration season as well as inter-annually (Hickey et al. 1998; Hickey et al. 2005), and with multi-year databases of baroclinic circulation in the CR estuary-plume-shelf system from the CORIE (Columbia River Ecosystem) coastal-margin observatory (Baptista 2006), we undertook a correlation analysis to relate the variability in the physical plume environment to the variability in salmon survival.

3.2 Methods

3.2.1 Study area

The CR (Fig. 3.1) is the largest river on the U.S. Pacific coast, with daily discharges ranging, over a typical year, from 3,200 to 10,500 $m^3 s^{-1}$, with recent extremes of 1,800 $m^3 s^{-1}$ in 2001 and of 24,500 $m^3 s^{-1}$ during 1996 (USGS,

http://waterdata.usgs.gov/or/nwis, last accessed January 25, 2009). The CR plume is a dominant hydrographic feature off the Oregon and Washington coasts.

3.2.2 Model simulations of the CR plume physical environment

To characterize variability in the structure of the CR plume at the time juvenile salmon migrants enter the ocean, we used multi-year (1999-2006) simulations of the 3D salinity field from the CORIE coastal-margin observatory (Baptista 2006). Developed in 1996 for the CR estuary-plume-shelf system, CORIE integrates an observation network with the simulation capabilities of a modeling system and with a web-based information system. The modeling component of CORIE relies on two alternative numerical models that can be used to simulate 3D baroclinic circulation in the CR estuary-plume-shelf system: an older model - ELCIRC (Zhang et al. 2004; Baptista et al. 2005) and a more recent one – SELFE(Zhang and Baptista 2008). Because ELCIRC tends to predict salinities that are systematically lower than observations in the CR plume region (Fig. 3.2), we used SELFE as the default model for the highly resolved, long-term simulations and the bulk of the results presented in this paper used a circulation database (DB14) generated with SELFE. However, SELFE has not yet proven to outperform ELCIRC in all regards. So to explore the sensitivity of our results to model uncertainty arising from specific algorithmic solutions and model parameterizations, we repeated the correlation analysis (described below) using a realization of the circulation database (DB11) generated with ELCIRC.

Both models predict water levels, 3D velocities, salinity and temperature at each point in space and time of the computational domain. For the purpose of this study, we translated this output in terms of metrics of plume size (area of the surface plume and volume) and location (expressed in terms of coordinates of the centroid of the surface plume). We defined the plume using a cutoff-salinity of 28 psu because it provides a conservative choice to distinguish the body of CR plume waters from other freshwater sources and from ambient ocean salinity.

3.2.3 Salmon data

As an indicator of varying population performance in changing estuary, plume, and ocean-shelf conditions, we used smolt-to-adult return (SAR) rates computed from Passive Integrated Transponder (PIT-) tag data. We used PIT-tag data from Snake River spring/summer Chinook salmon (*O. tshawytscha*) and steelhead (*O. mykiss*), originally collected for studies designed for purposes other than this analysis. The SARs were computed by dividing the number of adult PIT-tagged fish returning to Lower Granite Dam (RKm 695) by the number of juveniles previously collected, tagged at, and transported from there on barges to a release site downstream of Bonneville Dam (RKm 234) (Fig. 3.1). The SARs are therefore a rate of survival over a period of time that encompasses the 2-4 years of ocean residence as well as the upriver migration when adult salmon return to spawn.

We used SARs from the 1999, 2001, 2002 and 2003 outmigrations of (yearling) wild Snake River spring/summer Chinook salmon and wild steelhead, both ESUs listed as threatened under the ESA. No data exist for the same transport group (fish collected, tagged and barged at Lower Granite) for 2000. The data in each year covered the salmon outmigration from the beginning of April through mid-June.

The data are referenced to the day the smolts are loaded on barges after tagging. Day of ocean entry of the juvenile migrants was estimated by adding 36-48 hours for barging the fish past the dam system, about two days for the smolts to migrate to Jones Beach (RKm 75) and then two more days to leave the estuary and enter the plume.

Pre-processing of the time series of SARs separately computed for the smolts tagged on each day was limited to filtering once with a 3-point median filter, to reduce gaps in the SAR series (which typically preceded or followed dates on which fish were barged early or late in the day) and to smooth the most extreme spikes.

3.2.4 Correlation analysis

We conducted a correlation analysis between daily values of SARs and plume metrics because the CR plume is a fast-changing hydrodynamic feature. It responds nearly instantaneously (within hours) to shifts in wind regimes – with wind fluctuations having

time scales of 2-10 days – while the plume response to river discharge is modulated by the semi-diurnal and diurnal tides (Hickey et al. 1998). Maps of the daily averaged simulated salinity field that capture the variability determined by the fast dynamics of the plume on the Washington and Oregon shelf can be found in Burla et al (In press).

Although models could produce highly resolved temporal scales for plume characteristics, we could only roughly estimate the time juvenile salmon left the estuary and entered the ocean as 5-6 days after the day on which fish were tagged and barged for transportation. To identify when the cross-correlation between SARs and plume metrics reaches its peak with respect to the time fish were tagged upriver and to the time of estimated ocean entry, we explored the cross-correlations at different time lags (lagging the plume time series by an increasing number of days relative to the SAR series).

To limit the linearity assumption that is implicit in a correlation analysis, we performed the analysis using anomalies - limiting the assumption to the relationship between the stochastic deviations in the variables (here from a baseline provided by a multiyear climatology), rather than between the variables themselves (Thiébaux 1994). Daily anomalies in the plume size and location, relative to climatologies (multiyear weekly averages) computed from the long-term computer simulations, were meant to capture how the variability in the plume structure relates to a similarly defined variability in salmon survival. Salmon survival data were available only for 1999, 2001, 2002 and 2003. Hence we constructed the climatologies based upon these four years only, not only for the SARs but also for the plume metrics.

3.2.5 Testing the statistical significance of the correlations accounting for the autocorrelation in the data

To test the significance of the cross-correlations between salmon survival rates and plume metrics and account for the autocorrelation in the data, we adopted a non-parametric method, from the climate and physical research literature (Prichard and Theiler 1994; Ebisuzaki 1997). The advantage of the non-parametric test lies in its simplicity, in avoiding the task of fitting a statistical model and, more importantly, in avoiding the assumptions other approaches rely upon or implicitly make (Pyper and Peterman 1998).

The shape of the autocorrelation (ACF) and partial autocorrelation (PACF) functions (Fig. 3.3) suggested that simple autoregressive models of the first order, often a good approximation in fisheries series, were not adequate to describe the plume metrics time series in our study. Hence, we could not remove autocorrelation by first-differencing. In addition, while we used a daily sampling frequency to be able to capture the fast-changing dynamics of the CR plume, we could not assume that lower frequencies of variability, which are removed by removing the autocorrelation, were unimportant. Because of the size of our SAR dataset and the non-stationarity exhibited by some of the plume metrics series (Fig.3.3), we also had concerns about the potential shortcomings of adjusting the procedure to test the null hypothesis of no correlation by replacing the sample size with the "effective" number of degrees of freedom (Pyper and Peterman 1998; Botsford and Paulsen 2000).

The non-parametric method we adopted consisted of determining the critical value for the significance of the cross-correlations between SARs and plume metrics, r_{crit}, by generating an empirical sampling distribution for the cross-correlation coefficients, "resampling" in the frequency domain. "Resampling" in the frequency domain exactly preserves the power spectrum, hence resampled series (surrogates) retain the autocorrelation structure of the original series (Ebisuzaki 1997), which traditional bootstrapping techniques may fail to replicate (Zwiers 1990).

To generate the surrogate time series that we used to estimate the empirical distribution for the cross-correlations in our analysis, we followed Prichard and Theiler (1994). We first obtained the Discrete Fourier Transform of the original time series *x(t)* from:

$$X(f) = F(x(t)) = \sum_{n=0}^{N-1} x(t_n) e^{2\pi i f n \Delta t} \quad (1)$$

for $t = t_0, t_1, \ldots, t_{N-1} = 0, \Delta t, \ldots, (N-1)\Delta t$. This can be rewritten as

$$X(f) = |X(f)| e^{i\phi(f)} \quad (2)$$

which is evaluated at the discrete frequencies $f = -N\Delta f/2, \ldots, -\Delta f, 0, \Delta f, \ldots, N\Delta f/2$, where $\Delta f = 1/(N\Delta t)$. We generated a "phase-randomized" Fourier transform by rotating the phase Φ at each frequency by an independent random variable φ, drawn from a uniform distribution in the range $[0,2\pi)$:

(3) $$\widetilde{X}(f) = |X(f)|e^{i[\phi(f)+\varphi(f)]}$$

To ensure that the inverse Fourier transform (IFT) was a time series of real values, φ was constrained to satisfy the symmetry property $\varphi(f) = -\varphi(-f)$.

The IFT gave the surrogate time series:

(4) $$\widetilde{x}(t) = F^{-1}\left\{\widetilde{X}(f)\right\}$$

We repeated steps (3-4) to generate 2000 surrogates of the time series for the plume metrics and to compute the critical value for the significance of the cross-correlations with the SARs, r_{crit}, as the 95-percentile (5-percentile for negative correlations) of the generated distribution. We applied the resampling to the time series of the plume metrics, which, contrary to the observed SARs, had no gaps, being computed from the simulations of the circulation model. Taking the 95-percentile corresponded to testing at the 0.05 significant level, in a one-tail test.

3.3 Results

Data from migration years 1999, 2001 and 2002 indicated a consistent pattern in the correlations between the anomalies predicted by the plume modeling and anomalies in the survival rates for steelhead. Data from 2003 did not. When plotted as a function of the lag between the two time series (with the plume metrics series trailing), the cross-correlations between anomalies in steelhead SARs and daily-averaged plume metrics (Fig. 3.4) consistently peaked shortly after the estimated time of ocean entry of the outmigrating juveniles. The cross-correlations with plume size were consistently positive, i.e. positive anomalies in plume volume and area (a larger plume, in particular a larger surface plume) correlated with increases in steelhead survival throughout each migration season. The cross-correlations with the plume location relative to the coast were consistently negative. The plume proximity to the coast was represented by the location in the East-West direction of the plume centroid. During the salmon outmigration season, the climatology showed a plume prevalently detached from the coast and oriented to the SW (but with variability around this known seasonal pattern). Small or negative anomalies in the centroid metric correlated with increases in steelhead survival.

Anomalies of this sign correspond to a plume which is either located where predicted by the climatology, or extending farther offshore.

The strength of the correlations, at the peak values, was moderate in the first three years of the study, leading to a proportion of variability in the steelhead SARs explained by the variability in plume structure that ranged from 16-40%, except for the plume proximity to the coast in 2001, in which case it amounted to only 5%. The strongest correlation was in 2001 with plume volume anomalies (0.63). Although in most cases correlations passed the non-parametric test for statistical significance, they did so convincingly only in 2001 with plume size and in both 1999 and 2002 with the plume proximity to the coast. However, the consistency in the correlation patterns was lost when we plotted the correlograms replacing the original plume time series with the surrogate time series, which we generated to construct the empirical distribution for the cross-correlation coefficients. This result indicates that the revealed patterns were not spurious and not merely due to the autocorrelation structure in the data, which the surrogate time series preserved.

In 2003, correlations still peaked around or after the time the juvenile steelhead were estimated to enter the ocean, with the same sign as in previous years. Correlations, however, were weak and not (or barely) statistically significant (weakly significant for the proximity to the coast).

Across all four years covered by the study, the cross-correlograms for Chinook SARs (Fig. 3.5) did not show the same distinct patterns, with weak, statistically non significant correlations, suggesting that the influence of the plume environment is not significant for the survival of Chinook salmon, at least at the scale of variability considered in the analysis.

A comparison of the above results based on database DB14 (SELFE model) to results from database DB11 (ELCIRC model) provided relatively consistent predictions in the occurrence of the anomalies in the plume metrics. They often differed, however, in the order of magnitude and duration of the predicted anomalies and in the relative magnitude of the anomalies across one season. Consistently, the patterns observed in the correlations between steelhead SARs and plume anomalies from DB14 (Fig. 3.4) were largely confirmed with DB11 (not shown) but with correlations generally weaker than

what obtained with DB14. We attribute both the consistency in the patterns and the different strength in the correlations with the SARs to the fact that ELCIRC systematically predicts overly fresh conditions in the plume region, a shortcoming that the algorithmic solutions in DB14 overcome (Fig. 3.2). Nevertheless, ELCIRC captures other important features of the plume behavior, in particular the plume response to shifts in wind regimes between upwelling- and downwelling-favorable conditions.

3.4 Discussion

3.4.1 Plume conditions and salmon survival

Observational studies have begun to address the question of whether the CR plume, which is a dominant feature off the Oregon and Washington coasts, constitutes local ocean conditions that affect Pacific salmon production (Emmett et al. 2003; Schabetsberger et al. 2003; De Robertis et al. 2005; Morgan et al. 2005). To explore relationships between salmon survival and plume conditions, here we used an approach that relies on the simulation capabilities of the CORIE coastal-margin observatory and on biological observations taken in river for the purpose of other studies. We have examined, in particular, whether the intraseasonal variability in SARs for steelhead and Snake River spring/summer Chinook salmon is dependent upon changes in the plume at the time the juvenile migrants enter the ocean.

Available observation and model datasets limited the study period to the years 1999, 2001, 2002 and 2003. Years 1999, 2001, and most of 2002 all fell within a short cool phase of the PDO that started at the end of the 1990's and ended in mid-late 2002 (Joint Institute for the Study of the Atmosphere and Ocean, Climate Impacts Group, http://jisao.washington.edu/pdo/PDO.latest, last accessed July 22, 2008). They were therefore years characterized by cooler ocean conditions and enhanced biological productivity off the US west coast (Mantua et al. 1997; Hare et al. 1999; Peterson and Schwing 2003). Thus, the outmigrating juveniles during the first three years of this study all entered the ocean under favorable large-scale ocean conditions, which however soon deteriorated for the 2002 migrants. The 2003 migrants, instead, entered the ocean during a warm phase of the PDO, facing poor large-scale ocean conditions.

The positive and significant correlation we found during the cool PDO phase (1999, 2001, 2002) between anomalies in the survival rates for steelhead and anomalies in the plume size (Fig. 3.4) suggests that a larger plume (in particular a larger surface plume) near the time of ocean entry of juvenile steelhead favored their survival. The negative correlation with anomalies in the location of the plume suggests that a plume extending farther offshore, rather than attached to the shoreline, also led to higher steelhead survival. We interpret, instead, the poor correlations between the same anomalies in 2003, after the transition to a warm PDO phase, as a consequence of a modest contribution –in a regime of poor ocean conditions– of local (plume) conditions to the overall survival compared to the impact of large-scale ocean conditions. In years of favorable large-scale ocean conditions, the effect of local conditions becomes appreciable.

The lack of similar consistent correlation patterns for Chinook salmon (Fig. 3.5) suggests that the CR plume plays a different role as habitat for steelhead and Chinook. This difference is consistent with the notion that Chinook salmon, even when they enter the ocean as yearlings, reach the ocean as smaller fish than steelhead and appear to reside for a longer time in the coastal waters, closer to shore (R.L. Emmett, National Marine Fisheries Service, Northwest Fisheries Science Center, Newport, OR, personal communication). In contrast, looking at the distinct peaks in the correlograms for steelhead, we speculate that steelhead benefit from the plume environment as they enter the ocean, but that they mainly use the plume to move quickly away from coastal habitats and the predation pressures associated with this environment. This postulate is consistent with the finding that steelhead in particular concentrate at the plume frontal regions (De Robertis et al. 2005) whereas yearling Chinook salmon tend to be associated with the overall plume habitat when compared to the ocean (more saline) habitat. Moreover, these findings are consistent with the migration patterns of yearling Chinook salmon and steelhead we can discern from our observations. Whereas we can track yearling Chinook moving north along the coastal shelf margin from May through July, we typically observe steelhead in May, but seldom catch any in our coastal surveys after May. These findings suggest that steelhead may make a more direct and rapid migration to ocean habitats in

the Gulf of Alaska, underlying the finding why plume structure may benefit their success more directly than for yearling Chinook salmon.

To what extent should the lack of a uniform response of steelhead and yearling Chinook salmon to plume structure serve as support for or against the putative relationships described herein? Although there may be a perceived notion that salmonids use essentially the same habitats, evidence suggests habitat use is species specific. Along with a general higher abundance of juvenile salmon in plume waters and frontal zones than in the surrounding more saline ocean waters, observations have shown a differential distribution of juveniles of different species in different habitats, although with variability across years. For example, Schabetsberger et al (2003) found yearling and subyearling Chinook salmon to be present in much higher numbers closer to shore and to be on average smaller than juvenile coho, which were caught farther offshore during their study. Bi et al (2007) confirmed these findings when evaluating a suite of physical and biological features that describe unique habitat features that differently influence the distribution and abundance of juvenile Chinook and coho salmon in coastal Pacific Northwest waters.

We further speculate that the stronger correlations of steelhead SARs with the 2001 plume volume can be explained by the much smaller plume formed by the CR in that drought year. A small plume would be particularly limiting and its variability in size more critical to juvenile steelhead trying to migrate offshore. In years of higher river discharge, like 1999 and 2002, a larger plume would be less limiting but its location relative to the coast in response to winds would become more critical (consistently with the more significant correlations of steelhead SARs with the plume proximity to the coast than with plume size in 1999 and 2002). Our results also suggest that, in a year like 2001, juvenile steelhead depended upon the plume environment for a period of the order of days following ocean entry.

The fact that the conditions that steelhead encounter in the plume at the time of ocean entry can explain only part of their overall survival (16-40% of its variability) does not surprise us. Most mortality of salmonids during their marine residence is hypothesized to occur shortly after they enter the ocean (Pearcy 1992). SARs are a metric, however, that encompasses several stages in the life history of the fish and

multiple years, and therefore likely reflects many compounding and confounding factors (Williams et al. 2005) over this period. At this stage our goal was not to predict survival and production based upon predicted physical conditions in the plume region, rather to infer possible cause-effect relationships between variability in the plume and variability in salmon survival.

3.4.2 Critical uncertainties

Our results are clearly not conclusive because of a number of limitations in the analysis. First, the study used estimates of salmon survival from PIT tags. The small numbers of returning adults upon which the SARs are based make their estimate fairly imprecise, even more so when, during the migration season, the SAR ratio is computed starting from a low number of PIT-tagged juveniles. Despite the imprecision in the estimates of salmon survival, which is expressed by the wide confidence intervals shown in Appendix A, we believe that the trends of within-season variability are correctly captured by the data.

Secondly, variability in the actual time of ocean entry may have weakened the strength of the correlations, where they peak shortly after estimated entry time of steelhead to the ocean. This variability makes the true lag between the correlated time series not necessarily unique within each year, since the lag is a function of the time of ocean entry. Nevertheless, quantifying how much the variability in the time of ocean entry impacts the strength of the correlations is not as critical to the conclusions of this study.

Despite our study could cover only four years of data, those years are representative of a wide range of the local-scale ocean conditions determined by the presence of the CR plume (Fig. 3.6). Those local conditions were the focus of our investigation. The monthly CR flow is only weakly correlated with the PDO (Keefer et al. 2008). During the three years in our study that precede the transition from a cold to a warm PDO phase, CR discharge ranged from the very high flows of 1999 to the record drought of 2001, both years also characterized by La Niña conditions. ENSO-neutral conditions and highly variable flows characterized the 2002 migration season. Moderate flows, but considerably higher than in 2001, were observed in 2003, a warm-PDO and El

Niño year. The volume and surface area of the CR plume computed from our simulations reflect this broad range of flow conditions (Fig. 3.6). Also in terms of proximity to the coast and South-North orientation relative to the river mouth, the plume structure varied over a wide range during the four years of the study. Both river flow and winds determined such variability across years as well as within each migration season. Our results were robust to the high inter-annual variability in local ocean (plume) conditions, till the regime shift in the large-scale ocean conditions occurred.

It must also be noted that all results from this study refer to transported fish. Given the dataset used, we had no means to infer differences/similarities with survival of in-river migrants.

3.4.3 Alternative interpretations

Is the plume environment the true causative agent for the fraction of the total variability in the SARs found to be correlated with changes in the plume structure? Plume conditions and steelhead survival rates could both be simply responding to local upwelling, which several studies have indicated as a potential factor affecting salmon survival through bottom-up forcing of the marine food web (see Scheuerell and Williams 2005 for an example addressing this hypothesis). However, attributing to this mechanism the intraseasonal variability in steelhead survival would not explain why a similar response to increased productivity in the coastal environment was not found also in Chinook survival rates in our analysis. The utilization of the plume environment that we have postulated earlier in the discussion instead discriminates between the two species. Besides, the stratification determined by the presence of the plume may locally hinder effective upwelling (Hickey et al. 2005). In addition, during our study period there were instances (such as at the beginning of the 2002 migration season) where the strength of the anomalies in the plume metrics could not be explained by a response to upwelling-favorable winds alone, rather by a concurrent increase in river discharge. Indeed, later upwelling events, which were not accompanied by increases in river discharge, did not generate plumes of comparable characteristics and neither were they accompanied by comparably high SARs for steelhead.

3.4.4 Final considerations

The need to account for ocean conditions when addressing salmon management and restoration has been widely recognized (e.g. Pearcy 1992; Kareiva et al. 2000; Scheuerell and Williams 2005). In most cases researchers have pointed to the ocean as a source of variability that needs to be isolated and eliminated from analyses, in order to correctly assess restoration efforts and inform adaptive management experiments in the freshwater environment (Anderson 1997; Hilborn and Coronado 1997; Casillas 1999). Recognizing the ocean as a source of variability does not imply shifting the focus from the freshwater to the ocean environment for bottlenecks to salmon production, and relieving management decisions upstream. On the contrary, management strategies directly guided by the knowledge of the conditions downstream (such as timing of transportation of smolts, hatchery releases, hydropower management) become available when we establish an impact for local ocean features like the CR plume on Pacific salmon survival (Williams et al. 2005). By predicting conditions off the river mouth, the simulation capabilities made available by CORIE potentially provide an effective approach both to timely support those management decisions and to learn about the mechanisms governing salmon survival success in the coastal margin ecosystems. In this study, we used CORIE simulations in a correlation analysis with available biological data to formulate the hypothesis of a role for the CR plume dynamics in the early marine survival of steelhead. We speculate that the lack of supportive evidence for a similar role of the plume in the early marine survival of juvenile Chinook, at least at the fine scale of variability considered in the study, is not contradictory and suggests means to explore how yearling Chinook salmon and steelhead may use these local ocean habitats differently. The hypotheses generated from this analysis should be further pursued through continuation of focused observational studies. Future studies should focus on validating the results in the context of interannual and interdecadal variability, using longer time series, and on investigating residence time of juvenile salmon in the plume and differential distribution of species against plume structure again in the context both of intraseasonal and interannual variability.

3.5 Acknowledgments

Funding for this research was provided in part by the National Oceanic and Atmospheric Administration (AB133F-04-CN-0033) and the National Science Foundation (ACI-0121475; OCE-0424602). The study relied on results of the CORIE modeling system. Within the CORIE team, thanks are due to Dr. Yinglong Zhang, Charles Seaton and Paul Turner for the generation of the circulation databases and related information products. Charles Seaton also drew the map of the study area. We thank Mark D. Scheuerell and two anonymous reviewers for their useful comments. We are finally grateful to Sandra Oster for editorial advice in the preparation of the manuscript. Any statements, opinions, findings, conclusions or recommendations expressed in this material are those of the authors and do not necessarily reflect the views or policies of the federal sponsors, and no official endorsement should be inferred.

3.6 References

Anderson, J. J. 1997. Decadal scale climate pattern and salmon survival: indicators, interactions, and implications. In: Robert L. Emmett and M. H. Schiewe, Eds. *Estuarine and ocean survival of Northeastern Pacific salmon: Proceedings of the workshop*. U.S. Dep. Commer., NOAA Tech. Memo. NMFS-NWFSC-29**:** 43-53. (Available online at: http://www.nwfsc.noaa.gov/publications/index/cfm).

Baptista, A. M. 2006. CORIE: the first decade of a coastal-margin collaborative observatory. In: *Ocean '06*. Boston, MA: MTS/IEEE.

Baptista, A. M., Y. Zhang, A. Chawla, M. Zulauf, C. Seaton, E. P. Myers, J. Kindle, M. Wilkin, M. Burla and P. J. Turner. 2005. A cross-scale model for 3D baroclinic circulation in estuary-plume-shelf systems: II. Application to the Columbia River. *Continental Shelf Research* 25: 935-972.

Beamish, R. J., C.-E. M. Neville, B. L. Thomson, P. J. Harrison and M. St. John. 1994. A relationship between Fraser River discharge and interannual production of Pacific salmon (*Oncorhynchus* spp.) and Pacific herring (*Clupea pallasi*) in the Strait of Georgia. *Canadian Journal of Fisheries and Aquatic Sciences* 51: 2843-2855.

Bi, H., R. E. Ruppel and W. T. Peterson. 2007. Modeling the pelagic habitat of salmon off the Pacific Northwest (USA) coast using logistic regression. *Marine Ecology Progress Series* 336: 249-265.

Botsford, L. W. and C. M. Paulsen. 2000. Assessing covariability among populations in the presence of intraseries correlation: Columbia River spring-summer chinook salmon (*Oncorhynchus tshawytscha*) stocks. *Canadian Journal of Fisheries and Aquatic Sciences* 57: 616-627.

Bradford, M. J. 1995. Comparative review of Pacific salmon survival rates. *Canadian Journal of Fisheries and Aquatic Sciences* 52: 1327-1338.

Burla, M., A. M. Baptista, Y. Zhang and S. Frolov. In press. Seasonal and interannual variability of the Columbia River plume: A perspective enabled by multi-year simulation databases. *Journal of Geophysical Research: Oceans*.

Casillas, E. 1999. Role of the Columbia River estuary and plume in salmon productivity. In: *Ocean Conditions and the Management of Columbia River Salmon*, (Proc. Symposium, Portland, OR, 1 July 1999). Gustavo A. Bisbal (Ed.) Portland, OR: Northwest Power Planning Council, pp. 55-64

De Robertis, A., C. A. Morgan, R. Schabetsberger, R. W. Zabel, R. D. Brodeur, R. L. Emmett, C. M. Knight, G. K. Krutzikowsky and E. Casillas. 2005. Columbia

River plume fronts. II. Distribution, abundance, and feeding ecology of juvenile salmon. *Marine Ecology Progress Series* 299: 33-44.

Ebisuzaki, W. 1997. A method to estimate the statistical significance of a correlation when the data are serially correlated. *Journal of Climate* 10: 2147-2153.

Emmett, R. L., R. D. Brodeur and P. M. Orton. 2003. The vertical distribution of juvenile salmon (*Oncorhynchus* spp.) and associated fishes in the Columbia River plume. *Fisheries Oceanography* 13(6): 392-402.

Francis, R. C. and S. R. Hare. 1994. Decadal-scale regime shifts in the large marine ecosystems of the Northeast Pacific: a case for historical science. *Fisheries Oceanography* 3: 279-291.

Francis, R. C., S. R. Hare, A. B. Hollowed and W. S. Wooster. 1998. Effects of interdecadal climate variability on the oceanic ecosystems of the NE Pacific. *Fisheries Oceanography* 7: 1-21.

Hanley, J. A. and A. Lippman-Hand. 1983. If nothing goes wrong is everything right? *Journal of American Medical Association* 249: 1743-1745.

Hare, S. R., N. J. Mantua and R. C. Francis. 1999. Inverse Production Regimes: Alaska and West Coast Pacific Salmon. *Fisheries* 24(1): 6-14.

Hickey, B. M., S. Geier, N. Kachel and A. MacFadyen. 2005. A bi-directional river plume: the Columbia in summer. *Continental Shelf Research* 25: 1631-1656.

Hickey, B. M., L. J. Pietrafesa, D. A. Jay and W. C. Boicourt. 1998. The Columbia River Plume Study: Subtidal variability in the velocity and salinity fields. *Journal of Geophysical Research* 103(C5): 10339-10368.

Hilborn, R. and C. Coronado. 1997. Changes in ocean survival of coho and chinook salmon in the Pacific Northwest. In: Robert L. Emmett and M. H. Schiewe, Eds. *Estuarine and ocean survival of Northeastern Pacific salmon: Proceedings of the workshop*. U.S. Dep. Commer., NOAA Tech. Memo. NMFS-NWFSC-29**:** 9-18.

Johnson, S. L. 1988. The effects of the 1983 El Niño on Oregon's coho (*Oncorhynchus kisutch*) and chinook (*O. tshawytscha*) salmon. *Fisheries Research* 6: 105-123.

Kareiva, P., M. Marvier and M. McClure. 2000. Recovery and management options for spring/summer chinook salmon in the Columbia River basin. *Science* 290(5493): 977-979.

Keefer, M. L., C. A. Peery and C. C. Caudill. 2008. Migration timing of Columbia River spring chinook salmon: effects of temperature, river discharge, and ocean envronment. *Transactions of the American Fisheries Society* 137: 1120-1133.

Mantua, N. J., S. R. Hare, Y. Zhang, J. M. Wallace and R. C. Francis. 1997. A Pacific interdecadal climate oscillation with impacts on salmon production. *Bulletin of the American Meteorological Society* 78(6): 1069-1079.

Morgan, C. A., A. De Robertis and R. W. Zabel. 2005. Columbia River plume fronts. I. Hydrography, zooplankton distribution, and community composition. *Marine Ecology Progress Series* 299: 19-31.

Pearcy, W. G. 1992. *Ocean Ecology of North Pacific Salmon*. University of Washington Press, Seattle, WA

Peterman, R. M., B. J. Pyper, M. F. Lapointe, M. D. Adkinson and C. J. Walters. 1998. Patterns of covariation in survival rates of British Columbian and Alaskan sockeye salmon (*Oncorhynchus nerka*) stocks. *Canadian Journal of Fisheries and Aquatic Sciences* 55: 2503-2517.

Peterson, W. T. and F. B. Schwing. 2003. A new climate regime in Northeast Pacific ecosystems. *Geophysical Research Letters* 30(17): 1896, doi: 10.1029/2003GL017528.

Prichard, D. and J. Theiler. 1994. Generating surrogate data for time series with several simultaneously measured variables. *Physical Review Letters* 73(7): 951-954.

Pyper, B. J. and R. M. Peterman. 1998. Comparison of methods to account for autocorrelation in correlation analyses of fish data. *Canadian Journal of Fisheries and Aquatic Sciences* 55: 2127-2140.

Schabetsberger, R., C. A. Morgan, R. D. Brodeur, C. L. Potts, W. T. Peterson and R. L. Emmett. 2003. Prey selectivity and diel feeding chronology of juvenile chinook (*Oncorhynchus tshawytscha*) and coho (*O. kisutch*) salmon in the Columbia River plume. *Fisheries Oceanography* 12(6): 523-540.

Scheuerell, M. D. and J. G. Williams. 2005. Forecasting climate-induced changes in the survival of Snake River spring/summer Chinook salmon (*Oncorhynchus tshawytscha*). *Fisheries Oceanography* 14(6): 448-457.

Scheuerell, M. D., R. W. Zabel and B. P. Sandford. 2009. Relating juvenile migration timing and survival to adulthood in two species of threatened Pacific salmon (*Oncorhynchus* spp.). *Journal of Applied Ecology*. doi: 10.1111/j.1365-2664.2009.01693.x

Thiébaux, H. J. 1994. *Statistical data analysis for ocean and atmospheric sciences*. Academic Press, Inc., San Diego, CA

Williams, J. G., S. G. Smith, R. W. Zabel, W. D. Muir, M. D. Scheuerell, B. P. Sandford, D. M. Marsh, R. A. McNatt and S. Achord. 2005. *Effects of the Federal Columbia River Power System on salmonid populations*. U.S. Dept. Commer., NOAA Tech. Memo. NMFS-NWFSC-63, 150 pp. (Available online at: http://www.nwfsc.noaa.gov/publications/index/cfm).

Zhang, Y. and A. M. Baptista. 2008. SELFE: A semi-implicit Eularian-Lagrangian finite-element model for cross-scale ocean circulation, with hybrid vertical coordinates. *Ocean Modelling* 21(3-4): 71-96.

Zhang, Y., A. M. Baptista and E. P. Myers. 2004. A cross-scale model for 3D baroclinic circulation in estuary-plume-shelf systems: I. Formulation and skill assessment. *Continental Shelf Research* 24: 2187-2214.

Zwiers, F. W. 1990. The effect of serial correlation on statistical inferences made with resampling procedures. *Journal of Climate* 3: 1452-1461.

Appendix A

SARs for PIT-tagged Snake River steelhead (Table A.1) and spring/summer Chinook salmon (Table A.2), before filtering. 95% confidence intervals are shown. Intervals are t-based estimates, except for cases where there were no adult returns. For such cases (shown in italics) the upper limit of the 95% confidence intervals for the zero survival rate was estimated with the 'rule of 3' (Hanley and Lippman-Hand 1983). Anomalously high values in the SARs relate to cases where the ratios were computed starting from a very low number of tagged juveniles: in such cases the return of just a few fish causes the SAR values to spike.

Table A.1

	Steelhead							
	1999		2001		2002		2003	
Date	SAR (%)	95% CI	SAR (%)	95% CI	SAR (%)	95% CI	SAR (%)	95% CI
8-Apr	0	*0÷9.38*	-	-	-	-	-	-
10-Apr	0	*0÷6.12*	-	-	10	0÷19.30	1.55	0÷3.29
12-Apr	0	*0÷37.50*	4.05	1.11÷6.99	7.77	2.60÷12.94	4.35	0÷9.16
14-Apr	4.35	0÷13.17	4.97	1.61÷8.33	14.58	4.60÷24.56	-	-
16-Apr	0	*0÷25.00*	-	-	2.56	0÷6.07	0	*0÷12.00*
18-Apr	1.96	0÷5.77	1.59	0÷3.37	2.69	0.37÷5.01	1.14	0÷3.35
20-Apr	0	*0÷5.77*	2.49	0.34÷4.64	2.72	1.05÷4.39	3.33	0.12÷6.54
22-Apr	1.19	0÷2.52	3.70	1.18÷6.22	-	-	2.00	0÷5.88
23-Apr	0.90	0÷1.91	-	-	1.69	0÷4.98	12.77	3.23÷22.31
24-Apr	1.55	0.20÷2.90	4.42	2.07÷6.77	1.37	0÷4.04	7.69	0÷23.79
25-Apr	1.75	0.46÷3.04	-	-	0	*0÷2.61*	0	*0÷23.08*
26-Apr	0	*0÷1.28*	3.75	1.75÷5.75	0	*0÷5.56*	0	*0÷50.00*
27-Apr	2.26	0.30÷4.22	-	-	3.64	0÷8.59	-	-
28-Apr	0.49	0÷1.44	5.19	3.80÷6.58	-	-	-	-
29-Apr	0.55	0÷1.62	3.30	1.91÷4.69	-	-	3.45	0÷10.39
30-Apr	0	*0÷1.72*	4.19	1.80÷6.58	4.76	0÷11.20	0	0÷18.75
1-May	2.43	0.33÷4.53	3.31	2.30÷4.32	1.92	0÷5.65	5.88	0÷17.98
2-May	0.81	0÷2.40	1.03	0.36÷1.70	6.67	0÷15.98	8.00	0÷19.20
3-May	0.82	0÷2.42	2.84	2.08÷3.60	0	*0÷6.82*	0	*0÷17.65*
4-May	1.56	0÷4.60	2.55	1.74÷3.36	0	*0÷6.38*	-	-
5-May	0.76	0÷2.24	1.22	0.38÷2.06	-	-	-	-
6-May	0.79	0÷2.34	2.01	1.00÷3.02	-	-	5.56	0÷16.95
7-May	1.59	0÷4.68	1.80	0.75÷2.85	4.17	0÷8.44	0	*0÷17.65*
8-May	2.70	0÷5.31	1.01	0÷2.15	2.56	0÷7.52	6.25	0.32÷12.18
9-May	0	*0÷3.30*	0.72	0.70÷2.14	1.56	0÷4.60	13.33	0÷32.16
10-May	-	-	1.42	0.03÷2.81	0	*0÷8.82*	1.71	0÷4.06
11-May	1.11	0÷3.28	1.00	0÷2.39	4.76	0÷6.44	-	-
12-May	2.25	0÷5.33	1.47	0÷3.12	-	-	-	-
13-May	2.44	0÷5.78	1.44	0÷3.42	-	-	1.25	0÷3.68
14-May	3.23	0.12÷6.34	-	-	4.08	0÷9.62	0	*0÷5.26*
15-May	2.56	0÷5.42	1.75	0÷4.16	0	0÷12.00	2.20	0÷5.21

16-May	-	-	0	*0÷1.92*	0	0÷8.82	2.50	0÷5.92
17-May	-	-	-	-	0	0÷10.71	0.81	0÷2.38
18-May	5.60	1.57÷9.63	-	-	2.63	0÷7.72	-	-
19-May	0.75	0÷2.22	0.99	0.20÷1.78	0	0÷7.69	-	-
20-May	3.60	0.50÷6.70	0.61	0÷1.30	0	0÷4.84	1.80	0.48÷3.12
21-May	4.92	1.08÷8.76	-	-	2.70	0.57÷4.83	-	-
22-May	0.85	0÷2.52	0.33	0÷0.97	0	*0÷3.37*	2.99	0.81÷5.17
23-May	-	-	0.70	0.02÷1.38	1.01	0÷2.40	1.17	0÷2.48
24-May	-	-	1.14	0÷2.43	1.61	0÷3.42	2.52	0.09÷4.95
25-May	-	-	-	-	3.56	1.99÷5.13	1.96	0÷4.65
26-May	1.45	0.45÷2.45	0	*0÷3.45*	-	-	-	-
27-May	0.34	0÷1.01	-	-	3.64	1.17÷6.11	2.15	0.07÷4.23
28-May	-	-	-	-	-	-	4.21	0.17÷8.25
29-May	-	-	-	-	3.91	0.55÷7.27	2.80	0÷5.93
30-May	-	-	1.56	0÷4.60	-	-	2.86	0÷6.76
31-May	-	-	0	*0÷6.00*	2.39	0.84÷3.94	0	0÷3.66
1-Jun	-	-	0	*0÷8.57*	1.45	0.03÷2.87	0	0÷5.56
3-Jun	-	-	0	*0÷7.69*	2.49	0.97÷4.01	2.08	0÷6.12
5-Jun	0	*0÷3.26*	0	*0÷37.50*	2.06	0.06÷4.06	0	*0÷3.06*
7-Jun	0	*0÷12.50*	0	*0÷23.08*	2.15	0÷5.10	0	*0÷3.13*
8-Jun	0	*0÷8.33*	-	-	-	-	-	-
9-Jun	0	*0÷18.75*	0	*0÷19.5*	0	*0÷9.38*	-	-
11-Jun	0	*0÷15.00*	-	-	0	*0÷8.57*	-	-

Table A.2

	Chinook							
	1999		2001		2002		2003	
Date	SAR (%)	95% CI	SAR (%)	95% CI	SAR (%)	95% CI	SAR (%)	95% CI
31-Mar	1.10	0÷2.61	-	-	-	-	-	-
2-Apr	0	*0÷2.0000*	-	-	-	-	-	-
4-Apr	3.77	0÷8.90	-	-	-	-	-	-
6-Apr	0	*0÷6.25*	-	-	-	-	-	-
8-Apr	0.89	0÷2.63	-	-	-	-	-	-
10-Apr	1.27	0÷3.73	-	-	0	*0÷8.57*	0.29	0÷0.85
12-Apr	0	*0÷16.67*	3.66	0÷7.72	1.05	0÷2.50	0	*0÷2.16*
14-Apr	2.08	0÷6.12	1.84	0÷4.36	0.82	0÷2.42	-	-
16-Apr	6.06	0÷14.20	-	-	0	*0÷2.03*	0.23	0÷0.68
18-Apr	0.42	0÷1.25	1.04	0÷3.05	0.38	0÷1.13	0.37	0÷1.09
20-Apr	0.65	0÷1.92	1.48	0÷3.50	1.44	0.18÷2.70	0	*0÷2.75*
22-Apr	0	*0÷0.52*	0	0÷2.24	-	-	0.51	0÷1.51
23-Apr	0.68	0÷1.44	-	-	0	*0÷5.08*	0	*0÷0.84*
24-Apr	1.03	0.03÷2.03	0.52	0÷1.53	0	*0÷4.22*	0	*0÷1.18*
25-Apr	3.47	1.68÷5.26	-	-	1.28	0÷3.04	0.36	0÷1.07
26-Apr	1.79	0.47÷3.11	0.91	0÷2.16	2.33	0÷4.93	0	*0÷2.33*
27-Apr	1.58	0.61÷2.55	-	-	1.59	0.05÷3.13	-	-
28-Apr	2.86	1.75÷3.97	0.83	0.17÷1.49	-	-	-	-
29-Apr	3.50	2.00÷5.00	0	*0÷0.54*	-	-	0	*0÷1.31*
30-Apr	1.85	0.58÷3.12	1.54	0.81÷2.27	1.51	0÷4.46	0	*0÷3.30*
1-May	4.08	1.60÷6.56	1	0.38÷1.62	0	*0÷8.11*	0	*0÷5.66*
2-May	2.84	0.60÷5.08	0	*0÷0.67*	0	*0÷5.00*	0	*0÷2.56*
3-May	3.55	0.97÷6.13	1.41	0.37÷2.45	0	*0÷3.90*	0	*0÷2.44*
4-May	1.35	0.18÷2.52	0.21	0÷0.62	1.01	0÷2.98	-	-
5-May	3.64	1.30÷5.98	1.86	0.58÷3.14	-	-	-	-
6-May	0.63	0÷1.87	0.90	0.31÷1.49	-	-	0	*0÷2.11*

7-May	1.15	0÷3.39	2.43	1.38÷3.48	0	*0÷4.11*	0	*0÷1.55*
8-May	5.22	1.16÷9.28	1.09	0.14÷2.04	0	*0÷9.37*	0	*0÷0.93*
9-May	2.48	0.08÷4.88	0.36	0÷1.07	0	*0÷3.33*	0	*0÷1.64*
10-May	-	-	0.63	0.08÷1.18	1.89	0÷3.66	0	*0÷2.94*
11-May	6.98	2.58÷11.38	1.16	0.48÷1.84	0	*0÷7.14*	-	-
12-May	4.17	0÷9.82	0.77	0.20÷1.34	-	-	-	-
13-May	0	*0÷7.32*	0.43	0÷1.02	-	-	0	*0÷3.26*
14-May	0	*0÷7.50*	-	-	0	*0÷5.77*	0	*0÷2.54*
15-May	6.90	0÷16.54	0.29	0.27÷0.85	0	*0÷6.52*	0	*0÷4.48*
16-May	-	-	-	-	2.33	0÷6.83	0	*0÷3.80*
17-May	-	-	0.63	0.13÷1.13	0	*0÷10.71*	0.83	0÷2.44
18-May	0	*0÷6.67*	-	-	2.38	0÷6.99	-	-
19-May	2.5	0÷7.34	1.89	0.83÷2.95	0	*0÷11.11*	-	-
20-May	4	0÷12.09	1.43	0.38÷2.48	4.65	0÷10.94	2.13	0.57÷3.69
21-May	13.33	0÷32.16	-	-	1.55	0÷3.68	-	-
22-May	0	*0÷15.00*	0.46	0÷1.36	0.92	0÷2.19	1.26	0÷2.99
23-May	-	-	1.52	0.04÷3.00	3.65	1.00÷4.30	3.09	0÷6.54
24-May	-	-	1.13	0.03÷2.23	3.68	0.52÷6.84	0	*0÷2.07*
25-May	-	-	-	-	2.43	0.77÷4.09	0	*0÷2.31*
26-May	5.88	0.29÷11.47	0.96	0÷2.29	-	-	-	-
27-May	0	*0÷8.33*	-	-	1.6	0÷3.80	0	*0÷0.66*
28-May	-	-	-	-	-	-	0	*0÷2.54*
29-May	-	-	-	-	0.81	0÷2.38	2.27	0÷5.38
30-May	-	-	0	*0÷4.00*	-	-	0.61	0÷1.45
31-May	-	-	0	*0÷5.26*	1.18	0÷2.50	0.47	0÷1.39
1-Jun	-	-	0	*0÷6.12*	0.82	0÷2.42	0	*0÷1.86*
3-Jun	-	-	0	*0÷4.92*	0.68	0÷1.62	0	*0÷3.80*
4-Jun	0	*0÷30.00*	-	-	-	-	-	-
5-Jun	3.33	0÷10.03	0	*0÷5.36*	1.37	0÷2.91	0	*0÷2.68*
7-Jun	2.17	0÷6.38	0	*0÷0.91*	0.87	0÷2.57	0.68	0÷2.00
8-Jun	0	*0÷2.61*	-	-	-	-	-	-
9-Jun	0	*0÷9.68*	0	*0÷0.50*	0	*0÷9.68*	-	-
11-Jun	2.33	0÷6.83	-	-	0	*0÷75.00*	-	-

Figures

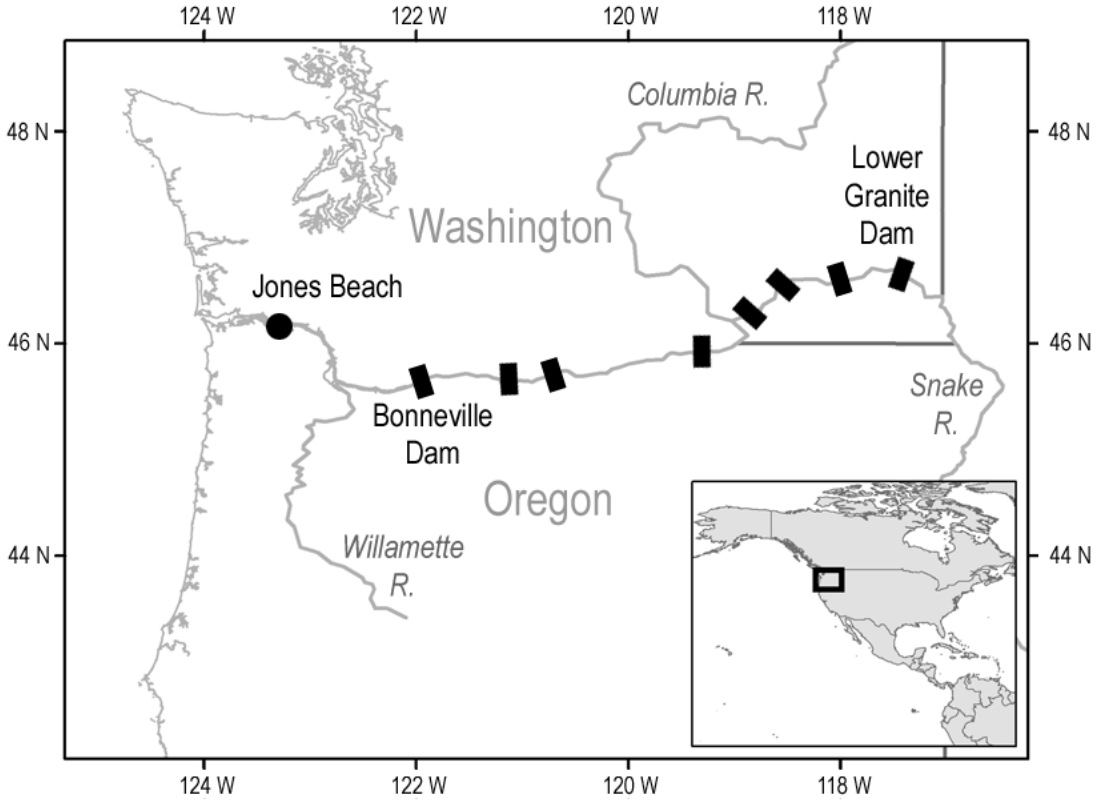

Figure 3.1 - The Columbia River basin. Shown are the locations of the tagging site, Lower Granite Dam, where smolts are loaded on barges for transportation through the dam system, and of Bonneville Dam, downstream of which fish are released back into the river.

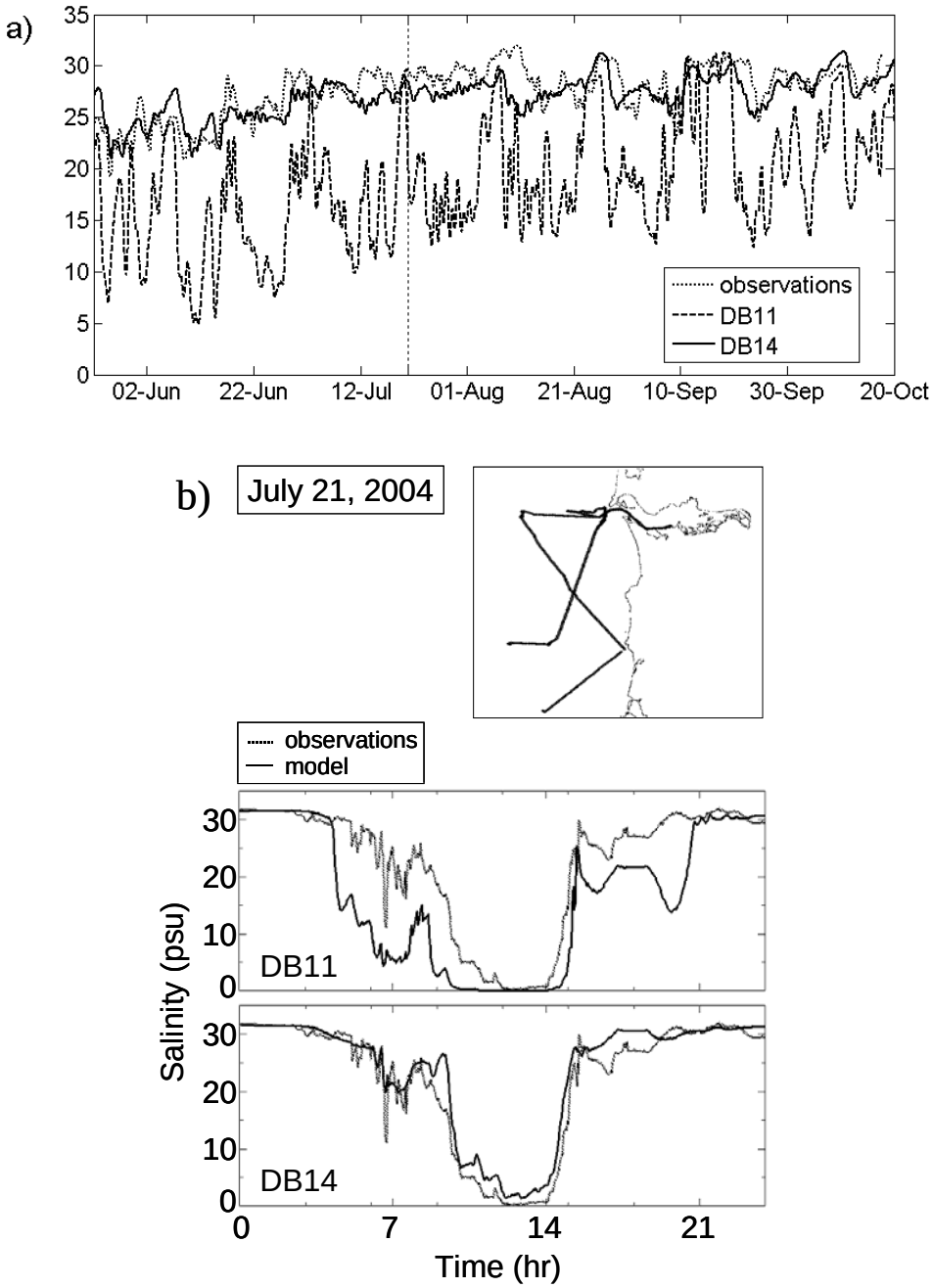

Figure 3.2 - The quality of CORIE simulations is routinely assessed through comparisons with real-time observations from the network of sensors deployed in the CR estuary and on buoys off the river mouth, as well as with data collected by cruises of opportunity. Shown are model-data comparisons, for salinity simulations from DB11 and DB14 respectively: a) at the OGI02 buoy (reference position 46 10.407 N 124 7.630 W), at 1 m depth, offshore the river mouth (time series are low-pass filtered); and b) along a cruise path (July 21, 2004). The dotted vertical line in (a) identifies the day of the same cruise in the OGI02 time series.

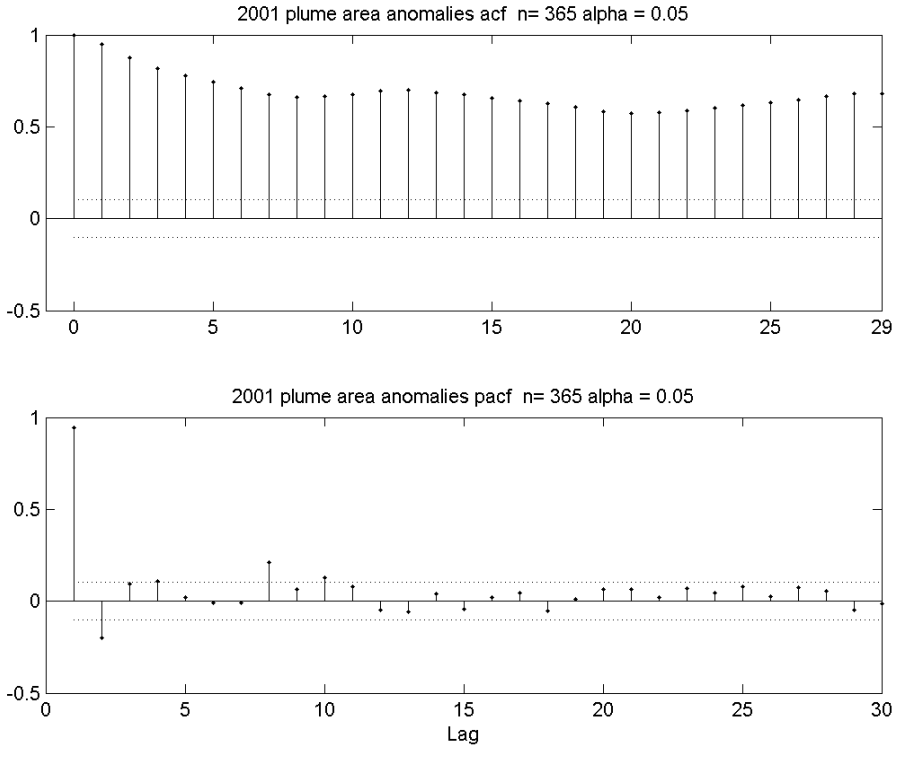

a)

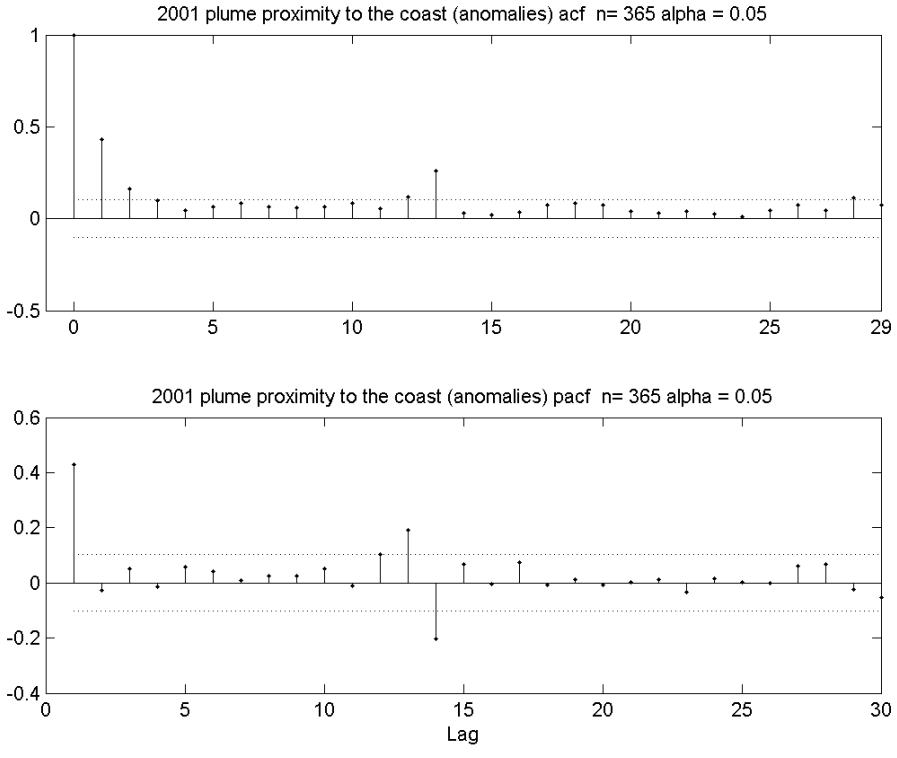

b)

Figure 3.3 - ACF and PACF for the anomalies in: a) plume surface area in 2001; b) plume proximity to the coast in 2001. The 95% confidence interval is shown. The x-axis indicates the number of lags. The shape of the ACF in (a)

reveals the non-stationarity exhibited by the plume surface area, as well as volume, both in 2001 and in 1999. First differencing did not eliminate the autocorrelation, suggesting more complex autoregressive integrated moving average (ARIMA) models. Even where there was no indication of non-stationarity for the same metrics in other years, differencing once was not enough to eliminate autocorrelation because of the higher order autoregressive properties of the time series. Isolated spikes at higher lags in the PACF of the plume proximity to the coast (b), in particular in a year of low river discharge such as 2001, revealed the periodicity linked to the fortnight tidal signal (spring-neap cycle).

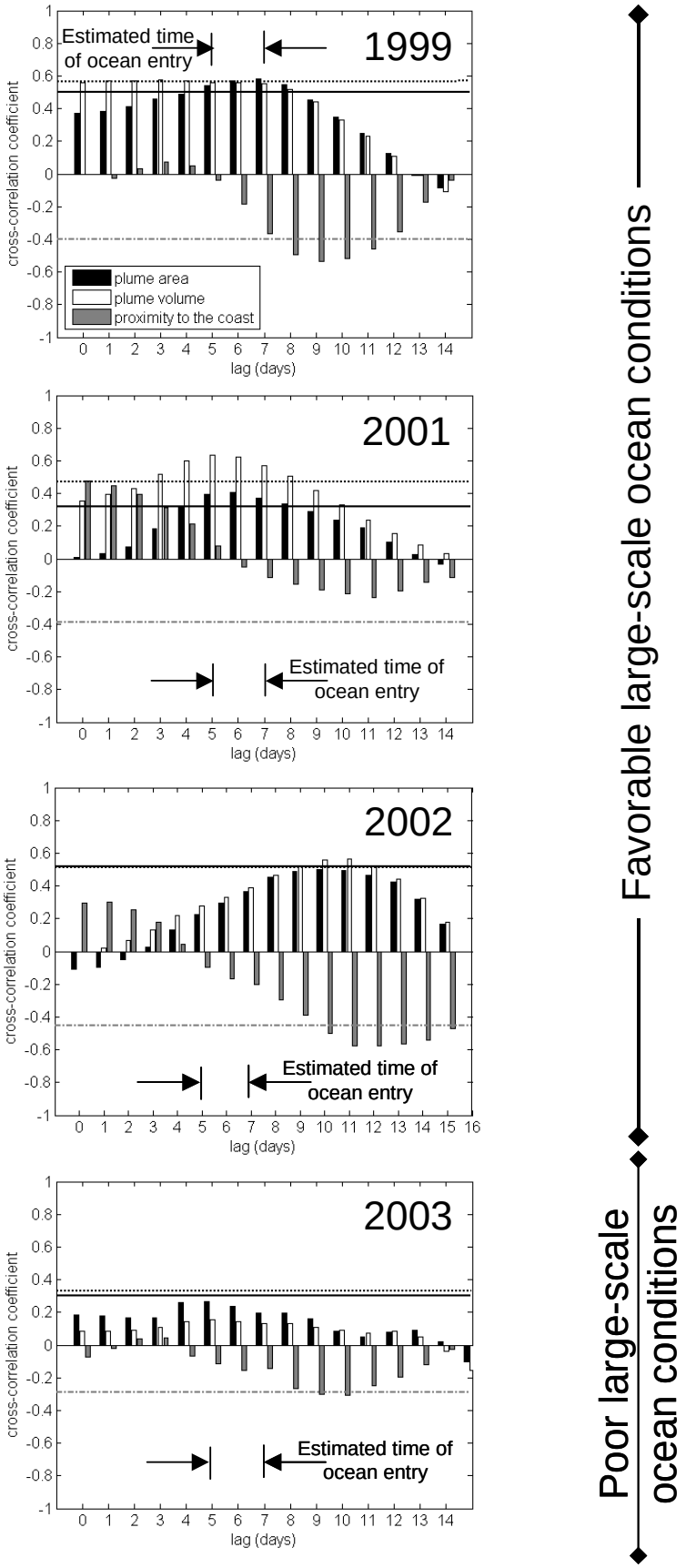

Figure 3.4 (continued)

Figure 3.4 – Cross-correlations between anomalies in steelhead SARs and plume metrics, as a function of the lag by which the plume time series are imposed to trail the SARs in the correlation. Lag zero corresponds to the day of fish tagging and collection upriver. The figure shows the approximate lag at which SARs are being correlated with the plume conditions existing at the estimated time of ocean entry of juveniles. At shorter lags the fish is still in river, either being transported through the dam system or migrating through the estuary. Horizontal lines show critical values for statistical significance at the 5% nominal level (significance of peak correlations is tested; solid line: plume area; dotted line: plume volume; dot-dashed: proximity to the coast). Total number of lags considered was chosen based upon the length of the available SAR dataset.

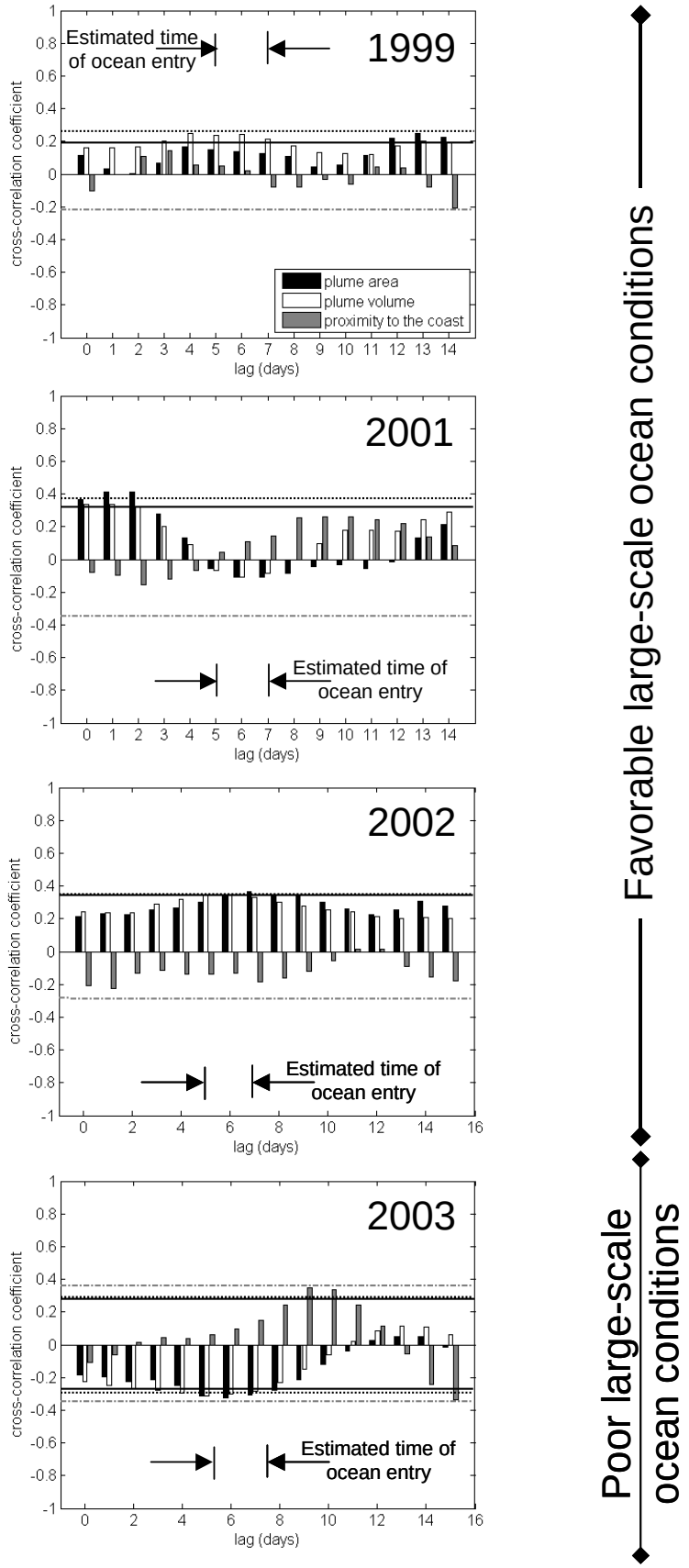

Figure 3.5 - Correlogram for the Chinook case. See Fig. 3.4 for details.

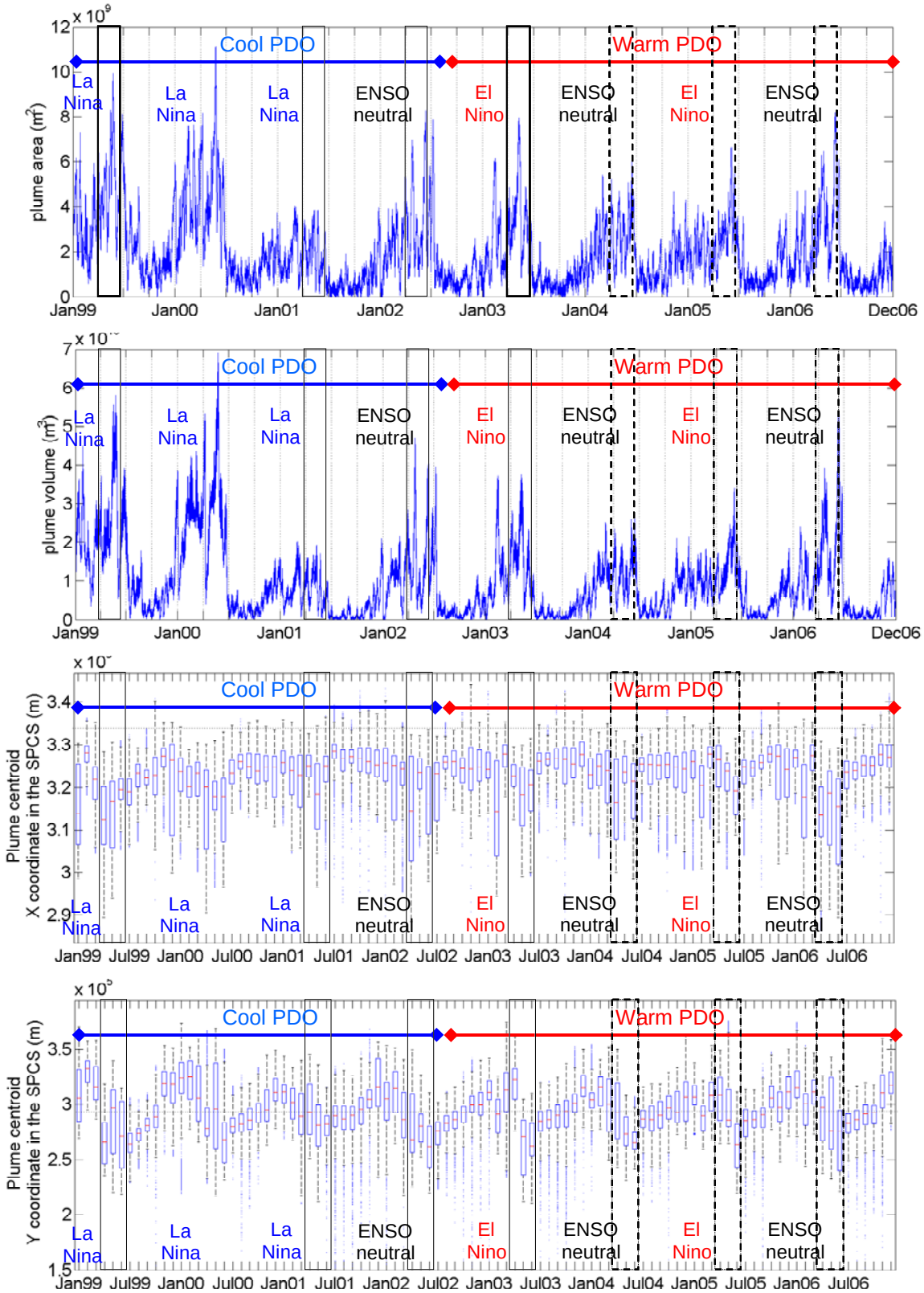

Figure 3.6 - 1999-2006 time series for the CR plume metrics computed from our model simulations. While salmon survival rates from return counts for years

following 2003 were not available at the time of the study, plume metrics from model simulations were generated through 2006. Model simulations for years prior to 1999 could not be generated because of the lack of consistent datasets for ocean conditions to force the model. Shaded boxes indicate the salmon outmigration seasons (April to mid-June). From top to bottom: a) area of the surface plume; b) plume volume; c) monthly distribution of the x coordinate of the centroid of the surface plume in the State Plane Coordinate System (SPCS), which represents the plume proximity to the coast (the dotted horizontal line identifies the location of the coast in the same coordinate system); d) monthly distribution of the Y coordinate of the centroid in the SPCS, representing the plume location along the North-South direction relative to the river mouth (the dotted horizontal line identifies the location of the mouth).

Chapter 4

Salmon habitat opportunity in the Columbia River estuary: Modeling the physical environment to inform management decisions

Authors: Michela Burla, António M. Baptista, Yinglong Zhang, Charles Seaton, Edmundo Casillas, Daniel L. Bottom, and Charles A. Simenstad

To be submitted to Coasts and Estuaries

Abstract:

Long-term variability and abrupt changes in the physics of the Columbia River (CR) estuary-plume-shelf ecosystem are believed to modulate salmon survival and life histories. Flow regulation, navigational improvements, and diking and filling have profoundly modified the CR estuary over the past century, with extensive loss of wetland habitat. Using the high-resolution modeling capabilities of a multi-purpose, cross-scale coastal-margin observatory developed over the past decade for the CR, we investigated the impact of natural variability and anthropogenic change on estuarine physical habitat opportunity (PHO) for salmon. With multi-year simulations and scenario comparisons between the modern and predevelopment conditions, we found that only strategies aimed at re-establishing some connectivity between the river and its floodplain through modification of both flow and bathymetry can significantly restore PHO in the CR estuary. The simulations also provided insight into the role of salinity and temperature on PHO in different regions of the contemporary and predevelopment estuary.

Keywords: Columbia River estuary, salmon, habitat, modeling, seasonal and inter-annual variability, anthropogenic change

4.1 Introduction

Long-term variability and abrupt changes in the physics of the Columbia River (CR) estuary-plume-shelf ecosystem are believed to modulate salmon survival and life histories. However, no clear understanding exists on specific cause-effect relationships, which hinders informed decision-making on sustainable development issues, such as hydropower regulation, bathymetric changes in the estuary for navigational purposes, land use changes and restoration projects.

By draining a basin of 660,500 km^2, the CR (Fig. 4.1) discharges in the Northeast Pacific a daily flow that, during a typical year, ranges from 3,200 to 10,500 $m^3 s^{-1}$ (USGS, http://waterdata.usgs.gov/or/nwis, last accessed January 26, 2009), but with recent extremes of 1,800 $m^3 s^{-1}$ in September 2001 and of 24,500 $m^3 s^{-1}$ in February 1996. The high annual discharge, second only to the Mississippi River in the continental United States, makes the circulation in the CR estuary river-dominated (Chawla et al. 2008). The estuary shifts from highly to weakly stratified conditions under high flow and low flow respectively, with rapid transitions (a few days or one flushing time) between the two stratification regimes, so that the intermediate, partially mixed state is unstable and only transient (Jay and Smith 1990b). When river flow is low, internal mixing due to strong tidal forcing turns the system to weakly stratified. Salinity intrusion is largest during neap tides and low flows, and its length varies approximately between 15 and 50 km. Tidal influence, instead, extends upriver to Bonneville Dam, at r-km 234. The two main channels that cut the shallow estuary, merging about 15 km upstream of the mouth, differ significantly in their dynamics (Jay and Smith 1990a; Chawla et al. 2008). Freshwater outflow is strongest in the South channel, while the North Channel has more tidal transport. While most of water transport is confined in the main channels, important biological and sedimentary processes occur in the four shallow peripheral bays: Baker Bay, Youngs Bay, Grays Bay and Cathlamet Bay (Jay and Smith 1990a).

In the past century, the morphology of the CR estuary has profoundly changed, due to navigational improvements (channel dredging, jetties, pile dikes) and diking and filling of much of the wetland area (Sherwood et al. 1990). Natural shoaling has also contributed but to a much lesser extent, and it has been often accelerated still by human

factors, as is the case of Baker Bay, due to the jetty construction at the river mouth (Thomas 1983). Extensive loss of shallow water habitat, in particular tidal swamps and marshes, occurred in all four lateral bays and in the upper estuary due to diking and filling (Thomas 1983; Bottom et al. 2008). Total wetland area decreased by slightly more than 50%, with high loss of forested wetlands particularly in the tidal freshwater portion of the estuary above Cathlamet Bay (Bottom et al. 2008). Shallow-water estuarine habitats provide important rearing habitat for juvenile salmon during their migration to the ocean.

Flow regulation, due to hydropower production and flood control, and water diversion for irrigation have significantly modified the annual hydrograph for the CR. The most intense flows were historically observed in the system between May and July, due to snowmelt mainly from the interior subbasin. The peak of the spring freshet has now shifted earlier because of flow regulation and has decreased by more than 40% (rarely exceeding now 15,000 m^3s^{-1}), with flow regulation being responsible for about 70% of this loss (Bottom et al. 2005). At the same time, winter flows, characterized by high-flow events associated with storms that bring precipitation in the low-elevation subbasin west of the Cascade Range, have become moderately higher (Sherwood et al. 1990; Bottom et al. 2005). These changes in the seasonal variability of river flow are superimposed to a more moderate but steady decline in annual discharge over the long term equally due to climate change and irrigation depletion (Sherwood et al. 1990; Bottom et al. 2005).

It was already in the 30's and based upon studies in the CR that Rich (1939) observed that each salmon species is composed of a diversity of geographically discrete and locally-adapted populations. These salmon populations from throughout the river basin intermingle in the estuary, where they reside and grow for varying periods of time before entering the ocean. Nonetheless, a view of the estuary as a corridor for a single, homogeneous group of salmon has long prevailed in the management of the CR system (Bottom et al. 2005; Fresh et al. 2005). Viewing the estuary as a bottleneck for the number of adults that could be produced, the focus has been on controlling predators and promoting rapid salmon seaward migration. Critical to the resilience of salmon populations in changing environments is, instead, a diversity of salmon life history

strategies (Healy 2009; Waples et al. 2009). Diverse habitat opportunities throughout a watershed, including those in the estuary, allow for expression of such diversity of salmon life histories. Expression of subyearling life histories among juvenile salmon species, including fry and fingerling migrants that often rear in estuaries for extended periods before entering the ocean, has been linked to the availability of wetlands and other shallow estuarine rearing habitats (e.g. Healey 1991; Bottom et al. 2005). Despite the extent to which the CR estuary has been modified by development in the past century and evidence of reduced diversity of juvenile life histories, Chinook salmon have been still observed in the estuary throughout the entire year, but with highest abundance of subyearlings from March through July (Bottom et al. 2008). To sustain or restore the resilience that has allowed salmon to perform well in a changing environment for millions of years, management practices need to look at maintaining habitat quality and diversity to allow for expression of those life histories (Healey 2009). Important data gaps have been identified that hinder interpretation of the effects of CR estuarine modifications on historical salmon populations and inferences about the responses of threatened and endangered stocks to restoration actions in the estuary (Bottom et al. 2005; Bottom et al. 2008). Recovery goals, strategies and expectations for CR salmon must also take into account natural variability determined by shifts in climatic and oceanic conditions (Bottom et al. 2005), which have been shown to produce fluctuations in salmon production across the North Pacific Ocean (e.g. Mantua et al. 1997).

The physical attributes of estuarine habitats that allow for expression of subyearling life histories can be modeled. Over the last decade, a multi-purpose, cross-scale coastal-margin observatory –CORIE/SATURN (Baptista et al. 1998; Baptista et al. 1999; Baptista 2002; 2006)– was developed for the CR estuary-plume-shelf system. With observation, modeling and information sub-systems, CORIE focuses on physical properties–water depth, velocity, salinity and temperature– and their ecosystem implications. CORIE simulations have already proven successful in advancing understanding of the seasonal and interannual variability of the CR plume (Burla et al. in press), in developing hypotheses regarding the role of the plume as salmon habitat (Burla et al. in review), and in assisting research cruises with short-term quality forecasts (Zhang et al. in review).

Collaboration among biologists and physical oceanographers has led to the development and use of semi-empirical metrics of *physical habitat opportunity (PHO)* for juvenile salmon in the estuary environment (Bottom et al. 2005). Through these metrics, in the present study we have used CORIE simulations of estuarine circulation to (a) understand seasonal and inter-annual variability of habitat opportunity in the CR estuary from 1999 to 2006; and (b) analyze alternative management scenarios, comparing habitat opportunity under modern and predevelopment conditions for river flow and estuarine bathymetry. The purpose is ultimately to separate natural and anthropogenic sources of variability in PHO for juvenile salmon in the CR estuary and to inform restoration and management strategies. The analysis also explores the impact of different modeling choices on the estimated PHO.

4.2 Methods

4.2.1 Physical habitat opportunity

Bottom et al (2005) defined habitat opportunity (a concept first introduced by Simenstad and Cordell (2000)) as availability of habitat that, based upon physical factors, physiological constraints, and ecological interactions, salmon can access and which salmon can benefit from occupying. We translated CORIE simulations of water levels, velocities, salinity and temperature in the CR estuary in terms of PHO, using criteria that fishery biologists suggested looking at the estuary for its role as a rearing environment for ‘ocean-type’ salmon life histories. The analyses emphasized subyearling ‘ocean-type’ Chinook salmon, because this life history type makes maximum use of estuarine habitats, in particular of the shallow water habitats most affected by the flow and bathymetric changes occurred in the CR system (Bottom et al. 2005). Results should, however, apply likewise to other ‘ocean-type’ salmon life histories, in particular chum salmon.

Based upon literature, results of laboratory experiments and expert judgment, water levels between 10 cm and 2 m and velocities smaller than 30 cm/s identify suitable shallow and low-velocity habitats that subyearlings prefer (USACE 2001; Bottom et al. 2005). Salmon access to shallow habitats is limited by temperature: recent studies in the Columbia River estuary (Bottom et al. 2008; Roegner et al. 2009) and in Washington’s

Snohomish River estuary (Kurt Fresh, NOAA Fisheries, pers. comm.) reveal that most individuals move out of shallow wetland areas as temperatures approach 19ºC, which we therefore adopted as an upper limit for the PHO criteria. We further selected a salinity range between 0 and 5 psu to assess the amount of transitional habitat available for subyearling migrants that may choose to acclimate gradually to salt water, before moving to more saline portions of the estuary.

4.2.2 Model simulations and PHO estimates

Bottom et al (2005) used the estuarine PHO metrics for depth and velocity with an early, two-dimensional generation of the CORIE modeling system to simulate the effects of flow regulation and bathymetric change on the opportunity for subyearling salmon to access preferred habitats. Three-dimensional baroclinic circulation models (ELCIRC and SELFE) have since then been developed for the CORIE modeling system, which have significantly and progressively advanced its ability to correctly simulate the dynamics of the CR estuary-plume-shelf system (Zhang et al. 2004; Baptista et al. 2005; Zhang and Baptista 2008; Burla et al. in press). In this study we used the most recent model, SELFE (Zhang and Baptista 2008), a 3D shallow-water circulation model that uses a semi-implicit, Eulerian-Lagrangian, finite element framework. Discretization of the model domain relies on unstructured grids in the horizontal and, in the vertical, on terrain-following S-coordinates (Song and Haidvogel 1994), placed on top of (optional) unstretched Z-coordinates.

In addition to relying on significantly improved simulation capabilities and a 3D representation, we have taken the approach, used early on in (USACE 2001; Bottom et al. 2005), further by:

- extending the analysis to salinity and temperature;
- refining the computation of PHO as described below;
- generating a multi-year database of simulations to investigate seasonal and inter-annual variability in PHO; and

- generating ad-hoc, 3-month long scenarios, with an improved historical bathymetry, to compare modern and predevelopment conditions in the CR estuary and inform management options.

To apply the estuarine PHO criteria in the 3D model representation of the velocity, salinity and temperature fields, we separately considered the minimum, maximum and average values along the water column for these parameters. Due to the stratification of the water column, saltier and colder water is generally found near the bottom. Not to be overly conservative or permissive, most of the results reported herein are based upon depth-averaged metrics.

Based upon the estuarine PHO criteria, the simulated water levels, velocities, salinity and temperature, available at 15-minute intervals, were translated in terms of:

- PHO maps, integrating over time the number of hours during which each criterion was satisfied within a week time period (hence out of a total of 168 hours) at each grid point of the computational domain;
- PHO accumulated per week over a specified region (hours*m^2), through integration in space and time; and
- PHO averaged within the inundated area (hours/week) in a region, to separate the effect of wetting and drying from the constraints to habitat opportunity placed by physical parameters other than water depth (velocity, S, T). Only by parsing out the separate contributions of the different physical parameters it was possible to understand the forcing mechanisms (how river flow and ocean tides interact to modify PHO in the CR estuary).

4.2.3 PHO across estuarine regions

To investigate the differential response of different areas of the estuary, we computed PHO integrating results over the following regions (Fig. 4.2):

- The region between the river mouth and Tongue Point (r-km 30), where the influence of seawater intrusion is dominant; we will also refer to this region as lower estuary;

- The middle estuary, approximately to the upper limit of salinity intrusion (r-km 50);
- The tidal freshwater region approximately between r-km 50 and r-km 80 (note that the tidal signal propagates further upriver, up to r-km 234 where Bonneville Dam is located);
- The four peripheral bays: Baker Bay and Youngs Bay, which are adjacent to the mouth; and Grays Bay and Cathlamet Bay, in the middle estuary.

4.2.4 Seasonal and inter-annual variability

To investigate inter-annual and seasonal variability in PHO in the CR estuary, we used a long-term (1999-2006) database of simulated circulation to generate weekly PHO climatologies and anomalies. Along with a catalogue of anomaly maps (to capture also spatial variability), we generated time series of weekly PHO climatologies (to reveal seasonal variability) and anomalies (to reveal interannual variability).

The eight years encompassed by our long-term simulation database covered a broad range of river flow characteristics (Fig. 4.3). During the eight-year period, flow conditions ranged from the high river discharges of 1999 to the record drought observed in 2001. Both these extremes preceded a climatic regime shift that occurred in late 2002, when the Pacific Decadal Oscillation transitioned back to a ‘warm’ phase after several years of a ‘cool’ pattern.

4.2.5 Scenarios

To compare estuarine PHO under modern (2004) and predevelopment (1880) conditions and isolate the effect, respectively, of flow regulation and bathymetric changes (navigational improvements and diking/filling) that occurred in the CR estuary over the past century, we simulated circulation in the following scenarios:

Scenario 1: predevelopment (1880) bathymetry and flow;

Scenario 2: predevelopment flow over the predevelopment bathymetry modified with the introduction of modern dikes in portions of

Cathlamet Bay and Tenasillahe Island (Fig. 4.4), near r-km 50; the extent of the diked area is 18.5 km^2;

Scenario 3: predevelopment flow over modern bathymetry;

Scenario 4: modern flow (2004) over predevelopment bathymetry; and

Scenario 5: modern flow (2004) over modern bathymetry.

The simulations for these scenarios were run for the months of April through June (calendar weeks 14 through 26, with weeks 12 and 13 used to ramp up the model simulations), to cover the spring freshet and the months of highest abundances of subyearling salmon observed in the modern CR estuary.

The predevelopment bathymetry was reconstructed by digitizing late 19^{th} century hydrographic and topographic survey data (Bottom et al. 2008). In spite of the higher resolution relative to previous analyses, the reconstructed bathymetry probably still does not represent with adequate detail the type of tidal connectivity that was lost with the introduction of the dikes in Scenario 2 above. Hence the impact of the introduction of those dikes was probably underestimated in our analysis.

4.2.6 Implications of model skills on PHO estimates

Two different simulation databases were used in this study, both generated with the SELFE model. The analysis of inter-annual and seasonal variability in PHO was based upon the multi-year simulations of database DB14, currently the most extensive CORIE database. DB14 simulations focused on the plume-estuary continuum and used a full, river-to-ocean domain, extending over the shelf from California to the Strait of Georgia in British Columbia. In the scenario analysis we used instead database DB17, a more recent configuration that uses a domain limited to the estuary, from the mouth to Beaver Army Terminal (r-km 87), and is driven by DB14 results at the mouth boundary. DB17 simulations, which cover only year 2004 for the modern estuary, have brought improvements particularly at depth and in the middle estuary in the representation of salt intrusion and temperature.

Modeling choices and data sources for the atmospheric and ocean forcings adopted for the two databases are summarized in Table 1. Model skills for the two

simulation databases and implications for the PHO estimates are discussed with the results below.

4.3 Results

Under modern flow conditions and in the modern bathymetry, a tidal signal associated with the spring-neap cycle dominates in the entire middle and lower estuary the variability in salmon habitat opportunity determined by the elevation and velocity constraints (Figg. 4.5a, b and 4.6). Overall throughout the modern middle and lower estuary, more extensive shallow and slow environments become available to salmon during particularly weak neap tides.

Individual regions in the estuary, however, respond differently to ocean and river forcing. According to the simulations, increased PHO (under the elevation criterion) is observed, for example, during particularly weak neap tides in Grays Bay and lower Cathlamet Bay (Fig. 4.7a). During spring tides, PHO is lost in these same regions, while in upper Cathlamet Bay and areas upriver there is a moderate gain in the availability of shallow and low-velocity environments (Fig.4.7b).

In the upper estuary, instead, variability in river flow is the dominant signal in the seasonal and inter-annual variability in PHO (Fig. 4.8). Only more extreme flows, however, have an appreciable impact on PHO in the modern bathymetry. The simulations indicated that the high river discharge during 1999 led to above-average extent of shallow water habitat for salmon in the tidal freshwater zone between approximately r-km 50 and r-km 80. Even more pronounced was conversely the loss of shallow water habitat in the same region during the 2001 drought. Even in such cases of more extreme modern flow regimes, however, the change in PHO was relatively modest.

Indeed, when we forced the system with predevelopment flows over the modern bathymetry, PHO remained substantially flat in the tidal freshwater zone even as river flow reached the higher levels of the historical spring freshets (Fig. 4.9). In the predevelopment bathymetry, instead, PHO increased linearly and steadily with flow and the river flows historically observed in the system during the freshet brought a considerable gain in shallow water habitats, through access to the floodplain (Fig. 4.9).

Introduction of modern dikes on Tenasillahe Island and in portions of Cathlamet Bay, downstream of the tidal freshwater region, in the predevelopment bathymetry, reduced PHO but did not modify the linear response to increasing flows.

In addition, in the modern bathymetry, as flow increases, the moderate gain in shallow water habitat in the stretch of the tidal river we examined tends to be canceled out by the loss of PHO due to velocity constraints (Fig.4.10). The simulations showed that this was not the case in the predevelopment bathymetry. When flows reached levels higher than 15,000 m^3s^{-1}, the loss in PHO due to increasing velocities stopped and the inundated floodplain provided suitable slow and shallow environments for juvenile salmon to rear (Fig.4.11).

Seasonal and inter-annual variability in river discharge have a clear influence on how salinity affects PHO for salmon in the middle and lower estuary. Salinity constrains PHO only to a very limited extent in the middle estuary and mainly during the low-flow months following the spring freshet, during the summer and through the fall. The effect of salt intrusion is particularly modest in lower Cathlamet Bay (Fig. 4.12a), to some degree more apparent in Grays Bay (Fig. 4.12b), according to the multi-year simulations in database DB14. Some modest loss in PHO in these regions was observed in our simulations in a drought year like 2001, while some gain was detected in higher river discharge years like 1999.

The simulations also suggested a deeper salt intrusion in the modern bathymetry, where salinity continues to limit PHO at times in the middle estuary also at higher flows (Fig. 4.13). Estimated loss in habitat opportunity due to salt intruding further into the estuary was, however, modest overall in the modern middle estuary, mainly confined to the lower Cathlamet Bay. It was also of an order of magnitude not very dissimilar from the loss determined by extreme low flows within the natural variability of the modern system (Fig. 4.12a).

Salinity becomes more an important constraint in the region closer to the mouth. According to the simulations, habitat opportunity for subyearling salmon in Baker Bay is modest for most of the year in the modern system (not shown), because of salinity above the range that identifies transitional habitat suitable for subyearling migrants to gradually acclimate to salt water. Habitat opportunity steadily increases there, however, with

increasing flows. Could river discharge reach levels observed in the system before hydropower development, salinity would no longer be a significant constraint, even in the modern bathymetry (Fig. 4.14). Salinity is not as limiting in Youngs Bay (Fig. 4.15). It is not a limiting factor there during the spring freshet, while it becomes increasingly limiting as river discharge decreases in the late summer and fall. This shift occurred much earlier in a drought year like 2001.

Correct representation of salt intrusion into the estuary is an area where we seek continuous improvement in our model simulations. Comparisons of model results against observations indicated that the modeling choices used to generate the multi-year simulations in database DB14 fell short at reproducing the extent of the intrusion. CORIE/SATURN observations indicate that, under low river flow conditions and during neap tide, salt penetrates, at depth, past Elliott Point, in the navigation channel. The modeling choices adopted in database DB17, which we used instead in our study of predevelopment scenarios, significantly improved the skill of our simulations in reproducing salt penetration that far into the South Channel. Fig. 4.16 shows the resulting different patterns of maximum intrusion near the bottom of the estuary as simulated in DB14 and DB17 respectively, during low flow conditions in the fall. The impact of this difference in skill on PHO estimates, however, results to be minimal in Grays Bay and Cathlamet Bay (Fig. 4.17d, g). Intrusion within the deeper channels minimally affects PHO in the shallower areas that salmon uses for rearing.

The deeper salt intrusion in DB17 simulations results from a stronger stratification and a more developed salt wedge than in DB14. This stratification, however, also results, closer to the mouth, in underestimating salinity in the surface layers, particularly during neap tides and low river flows in late summer and fall. Under these conditions, DB14 simulations generally exhibit better skill closer to the surface (Fig. 4.17b). Weaker stratification in DB14 simulations still translates in a slight overprediction of salinity at the surface, and underprediction at depth, where DB17 outperforms DB14 also closer to the mouth (Fig. 4.17c). Upwelling events, which move plume waters, fresher than ocean waters, in front of the river mouth, heighten the latter bias in DB14. These differences impact the way salinity affects habitat opportunity in Youngs Bay (Fig. 4.17a). During the low flow season of late summer and fall, salt

penetrates the shallow Youngs Bay in DB14 simulations, limiting habitat opportunity. It does not, at least not to the same extent, in DB17 simulations. The above comparisons with observations suggest that salt may indeed be significantly limiting in Youngs Bay in case of low river discharge, although not to the extent indicated by DB14 simulations.

The modeling choices adopted in DB17 have dramatically improved the skill of the simulations to represent temperature, at least in the mid-estuary region (Fig. 4.18). In these simulations of the modern system (which cover only the year 2004), temperatures above 19ºC started to limit habitat opportunity for salmon in the middle estuary in mid-June (week 25; see Fig. 4.19). By mid-July, and through the first week of September, substantially no habitat remained available in 2004 to juvenile salmon in the middle estuary because of excessively warm temperatures.

Our simulations cannot provide for a comparison between the predevelopment and modern system in terms of the effect of temperature on habitat opportunity. Initial and boundary conditions imposed for T in the predevelopment model runs were, in fact, the same as for the modern runs. Hence, comparisons of the predevelopment and modern scenarios cannot account for the effect on temperature of hydropower regulation and reservoirs upriver.

4.4 Discussion

The results of our study indicate that changes both in the bathymetry of the system and in the river flow combined to determine reduced opportunity for subyearling salmon to access rearing habitat in the CR estuary before their migration to the ocean. This is particularly evident in the tidal freshwater portion of the estuary above Cathlamet Bay, where even restoring the natural hydrograph and the high historical spring freshet flows would not appreciably increase habitat opportunity for salmon, if access to the floodplain were not restored. At the same time, only flows above those typically observed in the CR during the spring freshet since the development of the dam system could provide a significant increase in habitat opportunity for salmon in the tidal fluvial zone, after restoring access to the floodplain.

Using a nonstationary tidal model together with a one-dimensional river stage model, Kukulka and Jay (2003b) also showed extensive loss of shallow water habitat in the reach between r-km 50 and r-km 90, caused by dikes and flow alteration (a 62% total loss relative to virgin conditions). Contrary to our findings, however, their results suggested that dike removal could, by itself, provide a substantial increase in shallow water habitat, and more than what flow restoration could provide without removal of dikes. They recognized, though, that restoration of a natural flow regime would increase the duration of inundation. Time during which rearing habitat is accessible to salmon in the estuary is embedded in our definition of PHO, being it a cumulative measure in time (and in space, when we integrated over specific regions). While Kukulka and Jay (2003a; 2003b) focused on water elevations resulting from the interaction of ocean tides and river flow, in our study we further showed that re-establishing access to the tidal freshwater reaches is also necessary to re-create low-velocity rearing environments. Consistently with our results, Kukulka and Jay (2003b) also noted the stronger influence of tides on variability in shallow water habitat in the modern CR system because of reduced modern flows.

Our finding that salt may penetrate deeper in the modern CR system, at times limiting habitat opportunity in Cathlamet Bay and off Grays Bay also at higher flows, is contrary to early modeling studies (Sherwood et al. 1990). It is, though, consistent with

an increased length of the salinity intrusion over the past century because of decreased flows –particularly during the spring freshet–, deepened channels, and changes in bathymetry and in the tidal prism (Bottom et al. 2005). How salinity intrusion is changing relative to historical conditions, however, is yet not fully understood. Larger tides due to deeper channels, reduced bottom friction and increasing ocean tides along the coast (Jay 2008) bring more energy for mixing into the system (potentially reducing intrusion length), but also more advective transport deeper into the estuary, particularly with reduced spring freshet flows. Estimated loss in PHO due to deeper salt intrusion into the modern middle estuary, based on our simulations, was, anyway, modest, and of an order of magnitude not dissimilar from the loss determined by extreme low flows within the natural variability of the modern system.

Our simulations confirmed that, by mid-July (and through September), habitat is scarcely available for salmon to rear in the middle estuary because of excessively warm temperatures. A drop in salmon densities within the CR estuarine wetlands was observed to coincide with high water temperatures approaching or exceeding 19°C by July (Bottom et al. 2008).

Our analysis spanned a broad spectrum of temporal scales, from seasonal, to inter-annual and to historical, to capture both natural variability and the substantial modification that the CR estuarine system has undergone during the last century because of hydropower development upriver and other anthropogenic activities. Short-term, sharp fluctuations in river flow, on a daily and weekly scale, are determined in the modern system by “power-peaking” operations at river dams, which respond to variations in electrical power demand (Kukulka and Jay 2003a). Power-peaking operations were shown to affect upriver spawning habitat through shoreline fluctuations, stranding of emerged fry, and reduction in the diversity and productivity of the salmon food web (ISAB 1998). Power peaking also determines a pseudodiurnal tide that propagates seaward from Bonneville Dam (r-km 234) and contributes to damping ocean tides (Kukulka and Jay 2003a). During high-flow periods, however, water is spilled when power demand drops and power peaking is suppressed. The irregular power-peaking cycles generates more event-like fluctuations. In addition, Kukulka and Jay (2003a) found that the influence of these discharge waves becomes weak downstream of

Columbia City at r-km 135 (with an excursion of 0.05 m at Columbia City). For these reasons, we did not attempt to discern, with a time series analysis, effects of power-peaking operations to broaden the spectrum of temporal scales considered in our study.

While it is ultimately the interplay of all physical parameters (constraints from the combined effect of elevation, salinity, velocity and temperature) to determine habitat opportunity, we focused on an analysis that separately looked at the effect of individual parameters, both to enable an understanding of cause-effect relationships and a better appreciation of what gains different restoration strategies may bring. These strategies require identifying the limiting factors to PHO in different regions and seasons and understanding how river flow and ocean tides interact to modify PHO in the CR estuary in different bathymetric scenarios. We noted, however, that, at times, only the concurrent consideration of multiple parameters could shed full light on the response of the system to change. This was the case in the tidal fluvial zone, where the changes in PHO determined by water depth and velocity, as flow increases, tend to cancel out in the modern bathymetry, because of lack of connectivity with the floodplain, which provided both shallow and low-velocity habitats in the predevelopment system.

Our study looked at the overall PHO within key regions in the estuary, without consideration of the spatial connectivity between habitats. Size, shape, location within the estuary, composition of surrounding habitat, and connectivity with other habitats, all determine habitat function and importance (Turner 1989; Fresh et al. 2005). Isoline maps of weekly PHO (such as those in Figure 4.7) can provide only a limited visual appreciation of how available habitats are distributed and connected. We suggest a landscape analysis of habitat opportunity as a focus for future investigation, to answer such questions as: to what extent are pockets of opportunity linked among each other? How large are they? For how many hours are they linked?

While we seek continuous improvements in the quality of the CORIE/SATURN simulations, the robust skills of the simulations archived in database DB14, which we used in this study to investigate seasonal and inter-annual variability in PHO, have been proven in studies of the CR plume (Zhang et al. in review; Burla et al. in press). By focusing on the estuary domain and adopting the modeling choices described in Table 1, further improvements, in terms of length of the salinity intrusion and, dramatically, in

terms of temperature representation, were achieved in DB17 simulations, which we adopted in the scenario simulations. While improved skill in representing salt intrusion had minimal impact on PHO estimates in the middle estuary peripheral bays, DB17 skill in representing temperature changes in that region has been transformative. Yet, DB17 simulations of salinity in the surface layers are still outperformed by DB14, particularly closer to the mouth during neap tides and low flows. The generation of a new database, which extends the model domain further out from the river mouth, is currently under way (DB20, available online at http://www.stccmop.org/CORIE/hindcasts/database/base_frame.html). DB20 further improves simulation of salinity at depth in the mouth region but it is outperformed by DB14, as was DB17, closer to the surface. We noted that skill in representing salinity in the surface layers in the mouth region has implications on the PHO estimates in Youngs Bay. In addition, DB20 degrades skill in representing temperature during the critical summer months in the middle estuary relative to DB17. We do not expect, therefore, that DB20 will advance our understanding of PHO variability in the CR estuary.

To examine restoration alternatives that account for site-specific bathymetric and topographic conditions and selected flow management scenarios, finer-scale modeling will be necessary (Bottom et al. 2008). This will require further refinement (through surveys) of the bathymetric and topographic detail of the model grid, particularly in the channels and flats. The predevelopment bathymetry reconstructed through digitization of historical maps has achieved higher resolution than previous analyses, but we suspect that the tidal connectivity that was lost with the introduction of modern dikes is still not captured in full detail. The impact of diking in specific areas was, therefore, probably underestimated in our analysis.

Only an estuary-wide restoration strategy, however, which considers the diversity of habitat pathways and salmon life-histories along the continuum from the tidal river to the ocean, can be successful in meeting salmon recovery goals (Bottom et al. 2008). A modeling approach like the one proposed in this study can be instrumental in such a strategy. It has already shown, as we reported here, how only a combination of flow and habitat modification, to re-establish some connectivity between the river and its floodplain, will serve the goal of restoring access to critical rearing habitat for salmon in

the estuary. Contrary to the early notion that high-resolution models are not optimal for simulations on time scales (seasons to years to a century) relevant to understand climate and human impacts on estuarine habitats (Kukulka and Jay 2003b), we have demonstrated here how the high-resolution capabilities of the CORIE/SATURN modeling system can be used to address these very scales. Only by investigating and separating natural from anthropogenic sources of variability in the CR estuary we can inform decision-making and sustainable development in the system.

4.5 Acknowledgments

Funding for this research was provided in part by the National Oceanic and Atmospheric Administration (AB133F-04-CN-0033) and the National Science Foundation (OCE-0622278; OCE-0424602). The study relied on results from the CORIE/SATURN modeling system. Thanks are due to the additional following members of the CORIE/SATURN team: to Paul Turner for his contributions to generating the circulation databases and related information products, and for creating Figure 4.1; and to Mike Wilkin and other field crew for their effort in maintaining the CORIE/SATURN observational network. We also would like to thank Jen Burke (School of Aquatic and Fisheries Science, UW) for providing the data for the reconstructed historical bathymetry. Any statements, opinions, findings, conclusions or recommendations expressed in this material are those of the authors and do not necessarily reflect the views or policies of the federal sponsors, and no official endorsement should be inferred.

4.6 Literature Cited

Baptista, A. M. 2002. Environmental observation and forecasting systems. In: R. A. Meyers, Ed. *Encyclopedia of Physical Science and Technology*. Academic Press, New York. 5**:** 16.

Baptista, A. M. 2006. CORIE: the first decade of a coastal-margin collaborative observatory. In: *Ocean '06*. Boston, MA: MTS/IEEE.

Baptista, A. M., M. Wilkin, P. Pearson, P. Turner, C. McCandlish, P. Barrett, S. Das, W. Sommerfield, M. Qi, N. Nangia, D. Jay, D. Long, C. Pu, J. Hunt, Z. Yang, E. Myers, J. Darland and A. Farrenkopf. 1998. Towards a multi-purpose forecast system for the Columbia River estuary. In: *Ocean Community Conference '98*. Baltimore, Maryland

Baptista, A. M., M. Wilkin, P. Pearson, P. J. Turner, C. McCandlish and P. Barrett. 1999. Coastal and estuarine forecast systems: a multi-purpose infrastructure for the Columbia River. *Earth System Monitor (NOAA)* 9(3): 1-2, 4-5, 16.

Baptista, A. M., Y. Zhang, A. Chawla, M. Zulauf, C. Seaton, E. P. Myers, J. Kindle, M. Wilkin, M. Burla and P. J. Turner. 2005. A cross-scale model for 3D baroclinic circulation in estuary-plume-shelf systems: II. Application to the Columbia River. *Continental Shelf Research* 25: 935-972.

Bottom, D. L., G. Anderson, A. M. Baptista, J. Burke, M. Burla, M. Bhuthimethee, L. Campbell, E. Casillas, S. Hinton, K. Jacobson, D. A. Jay, R. A. McNatt, P. Moran, G. C. Roegner, C. A. Simenstad, V. Stamatiou, D. Teel and J. E. Zamon. 2008. *Salmon life histories, habitat, and food webs in the Columbia River estuary: an overview of research results, 2002-2006*. 45 pp.

Bottom, D. L., C. A. Simenstad, A. M. Baptista, D. A. Jay, J. Burke, K. K. Jones, E. Casillas and M. H. Schiewe. 2005. *Salmon at River's End: The Role of the Estuary in the Decline and Recovery of Columbia River Salmon*, U.S. Dept. of Commerce NOAA Technical Memorandum NMFS-NWFSC-68.

Burla, M., A. M. Baptista, E. Casillas and J. G. Williams. In review. The influence of the Columbia River plume on the survival of steelhead (*Oncorhynchus mykiss*) and chinook salmon (*O. tshawytscha*): a numerical exploration. *Submitted to Canadian Journal of Fisheries and Aquatic Sciences*.

Burla, M., A. M. Baptista, Y. Zhang and S. Frolov. In press. Seasonal and interannual variability of the Columbia River plume: A perspective enabled by multi-year simulation databases. *Journal of Geophysical Research: Oceans*.

Chawla, A., D. A. Jay, A. M. Baptista, M. Wilkin and C. Seaton. 2008. Seasonal variability and estuary-shelf interactions in circulation dynamics of a river-dominated estuary. *Estuaries and Coasts* 31: 269-288.

Fresh, K. L., E. Casillas, L. L. Johnson and D. L. Bottom. 2005. *Role of the estuary in the recovery of Columbia River basin salmon and steelhead: an evaluation of the effects of selected factors on salmonid population viability.* U.S. Dept. Commerce, NOAA Tech. Memo NMFS-NWFSC-69, 105 pp.

Healey, M. C. 1991. Life history of Chinook salmon (Oncorhynchus tshawytscha). In: C. Groot and L. Margolis, Eds. *Pacific salmon life histories.* UBC Press, Vancouver, BC: 576.

Healey, M. C. 2009. Resilient salmon, resilient fisheries for British Columbia, Canada. *Ecology and Society* 14(1): 2 [online].

ISAB. 1998. *Recommendation for stable flows in the Hanford Reach during time when juvenile Fall Chinook are present each spring.* Report to the Northwest Power Planning Council and National Marine Fisheries Service. Portland, OR. ISAB 98-5, pp.

Jay, D. A. and J. D. Smith. 1990a. Circulation, density distribution and neap-spring transitions in the Columbia River estuary. *Progress in Oceanography* 25: 81-112.

Jay, D. A. and J. D. Smith. 1990b. Residual circulation in shallow estuaries: 2. Weakly stratified and partially mixed, narrow estuaries. *Journal of Geophysical Research* 95(C1): 733-748.

Kukulka, T. and D. A. Jay. 2003a. Impacts of Columbia River discharge on salmonid habitat: 1. A nonstationary fluvial tide model. *Journal of Geophysical Research* 108(C9): 3293, doi:10.1029/2002JC001382.

Kukulka, T. and D. A. Jay. 2003b. Impacts of Columbia River discharge on salmonid habitat: 2. Changes in shallow-water habitat. *Journal of Geophysical Research* 108(C9): 3294, doi:10.1029/2003JC001829.

Mantua, N. J., S. R. Hare, Y. Zhang, J. M. Wallace and R. C. Francis. 1997. A Pacific interdecadal climate oscillation with impacts on salmon production. *Bulletin of the American Meteorological Society* 78(6): 1069-1079.

Rich, W. H. 1939. Local populations and migration in relation to the conservation of Pacific salmon in the western states and Alaska. *Publications of the American Association for the Advancement of Science* 8: 45-50.

Sherwood, C. R., D. A. Jay, R. B. Harvey, P. Hamilton and C. A. Simenstad. 1990. Historical changes in the Columbia River estuary. *Progress in Oceanography* 25: 299-352.

Simenstad, C. A. and J. R. Cordell. 2000. Ecological assessment criteria for restoring anadromous salmon habitat in Pacific Northwest estuaries. *Ecological Engineering* 15: 283-302.

Song, Y. and D. Haidvogel. 1994. A semi-implicit ocean circulation model using a generalized topography-following coordinate system. *Journal of Computational Physics* 115: 228-244.

Thomas, D. W. 1983. *Changes in Columbia River estuary habitat types over the past century*. Astoria, OR, Columbia River Estuary Data Development Program.

Turner, M. G. 1989. Landscape ecosystem: The effect of pattern on process. *Annual Review of Ecology and Systematics* 20: 171-197.

USACE. 2001. *Biological assessment - Columbia River channel improvements project: An internal report to the National Marine Fisheries Service and U.S. Fish and Wildlife Service.* U.S. Army Corps of Engineers, Portland, OR

Waples, R. S., T. Beechie and G. R. Pess. 2009. Evolutionary history, habitat disturbance regimes, and anthropogenic changes: what do these mean for resilience of Pacific salmon populations? *Ecology and Society* 14(1): 3 [online].

Zhang, Y. and A. M. Baptista. 2008. SELFE: A semi-implicit Eularian-Lagrangian finite-element model for cross-scale ocean circulation, with hybrid vertical coordinates. *Ocean Modelling* 21(3-4): 71-96.

Zhang, Y., A. M. Baptista, B. M. Hickey, B. C. Crump, D. A. Jay, M. Wilkin and C. Seaton. Daily forecasts of Columbia River plume circulation: a tale of spring/summer cruises. *Submitted to Journal of Geophysical Research*.

Zhang, Y., A. M. Baptista and E. P. Myers. 2004. A cross-scale model for 3D baroclinic circulation in estuary-plume-shelf systems: I. Formulation and skill assessment. *Continental Shelf Research* 24: 2187-2214.

4.7 Sources of Unpublished Materials

Jay, D. A. 2008. The Columbia River estuary: structure and function. In: *Proceedings of the Columbia River Estuary Conference on Ecosystem Restoration.* Astoria, OR

Tables

Table 4.1 – Key differences between the databases of circulation used in the study. Resolution for the forcing sources is indicated in parenthesis. ELM: Eulerian Lagrangian Method; NRL NCOM: Navy Coastal Ocean Model of the Naval Research Laboratory; ETA: NOAA National Centers for Environmental Prediction (NCEP)'s mesoscale model; NARR: NCEP North American Regional Reanalysis.

	DB14	**DB17**
Model	SELFE v1.4a	SELFE v1.5h (discontinuous velocity at nodes with Shapiro filter)
Domain	Estuary (Beaver Army to mouth) and shelf (CA-BC)	Estuary only (Beaver Army to mouth)
Grid	Horizontal grid: 39133 elements; ~2.5 mil. faces Vertical: 18 Z-levels + 37 S-levels, with transition depth between SZ hs=100m, and transition depth between S and sigma hc=30m Min & max equivalent radius= 19m, 12km	Horizontal grid: 16741 elements Vertical: 26 pure S-levels Min & max equivalent radius= 19m, 333m
Numerical solution for S, T transport	Finite-volume upwind method	Upwind for T and ELM for S
Drag coefficient	From 0.002 (at the Astoria Megler bridge) to 0.005 (r-km 30)	From 0.003 (r-km 13) to 0.007 (at the Astoria Megler bridge)
Ocean conditions	NRL NCOM (1/8 degree; daily), with weak nudging in extensive shelf region	Same as DB14
Atmospheric forcing	1999-2003: NARR (32 km resolution; 6-hourly) 2004: ETA (12km; 3-hourly)	Same as DB14

Figures

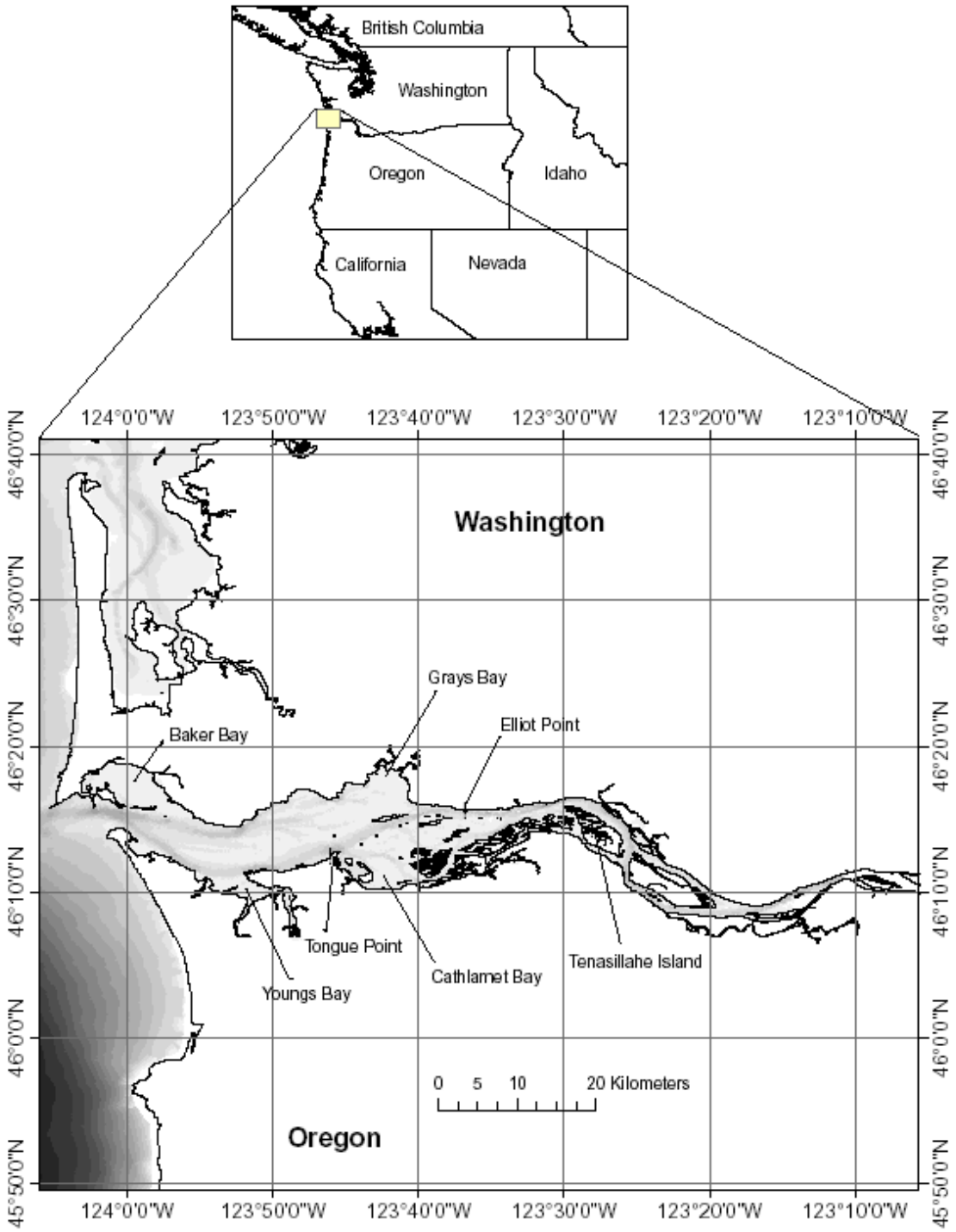

Figure 4.1 – The study location: the Columbia River estuary.

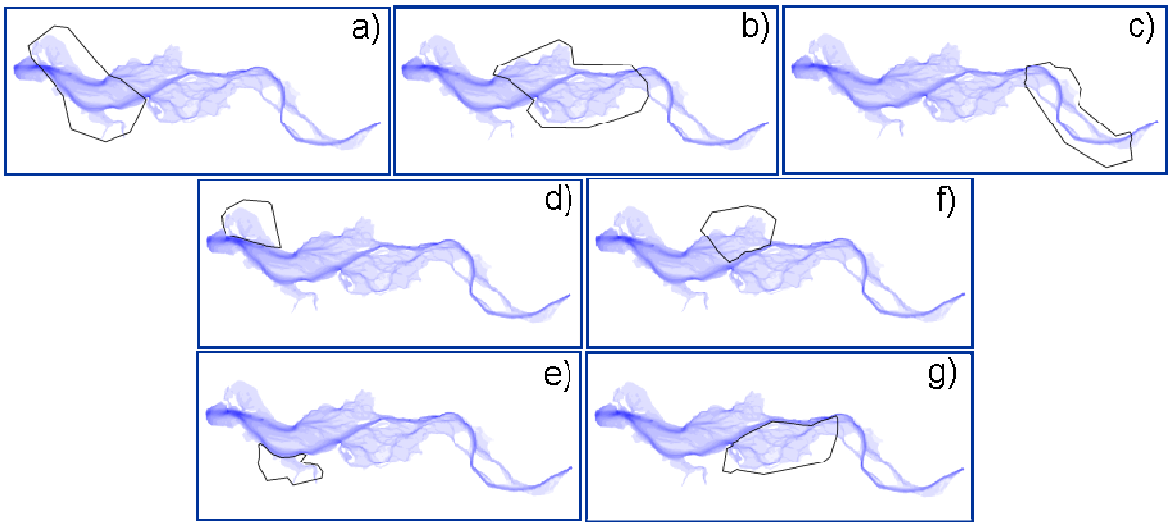

Figure 4.2 - Region boundaries used in the study to integrate PHO within: a) the mouth region; b) the middle estuary; c) the tidal freshwater region; d) Baker Bay; e) Youngs Bay; f) Grays Bay; and g) Cathlamet Bay.

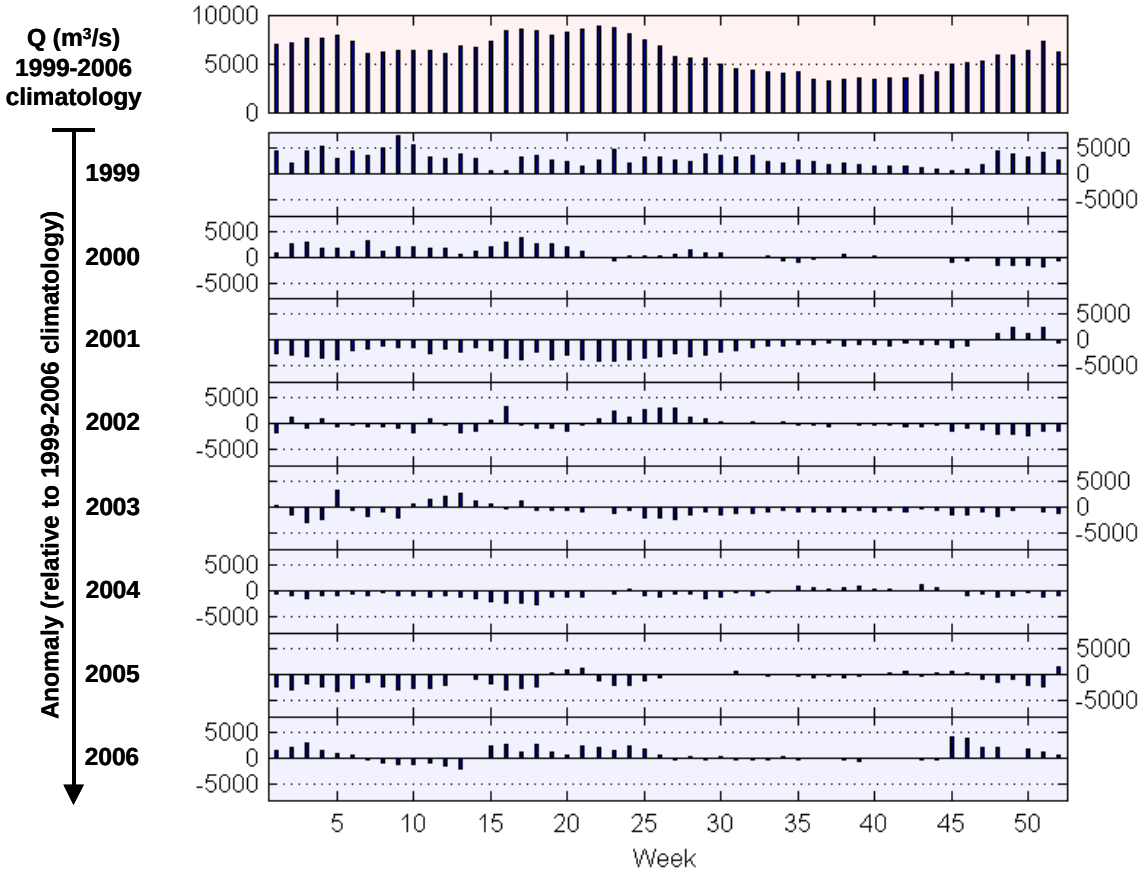

Figure 4.3 – 1999-2006 climatology and anomalies for the Columbia River flow at Beaver Army Terminal ($m^3\ s^{-1}$).

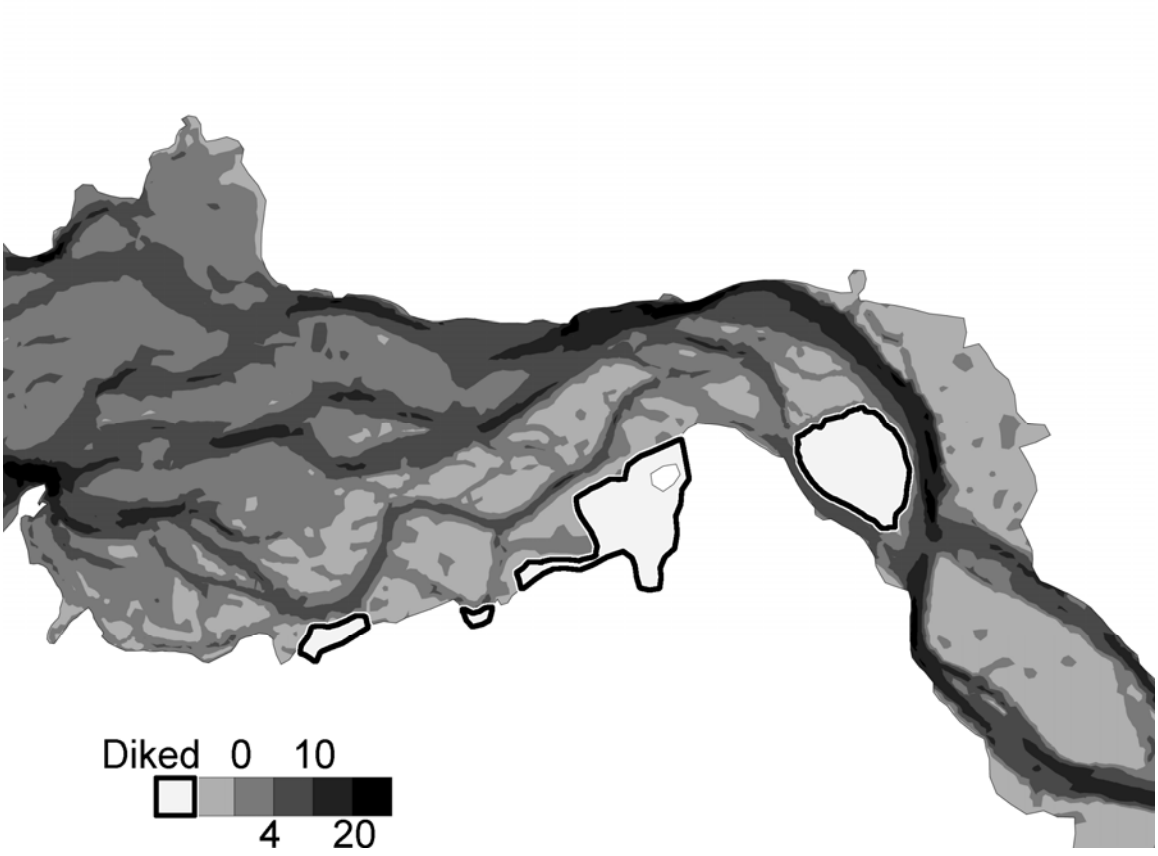

Figure 4.4 – Location of the dikes introduced in Scenario 2.

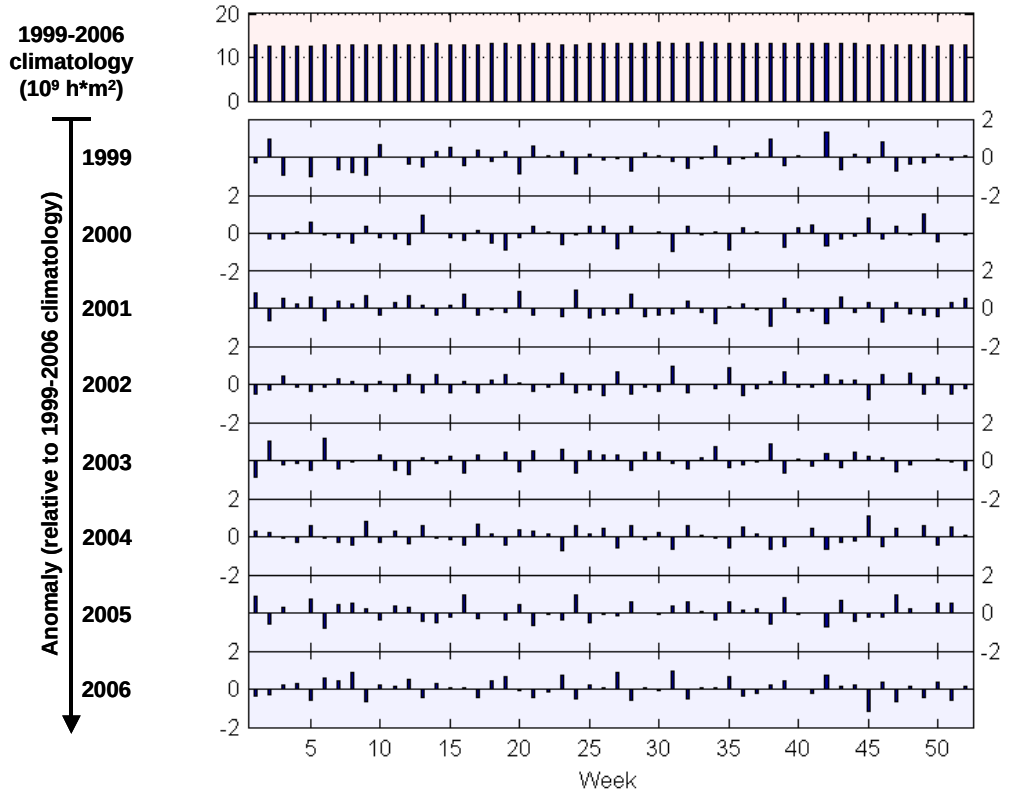

a)

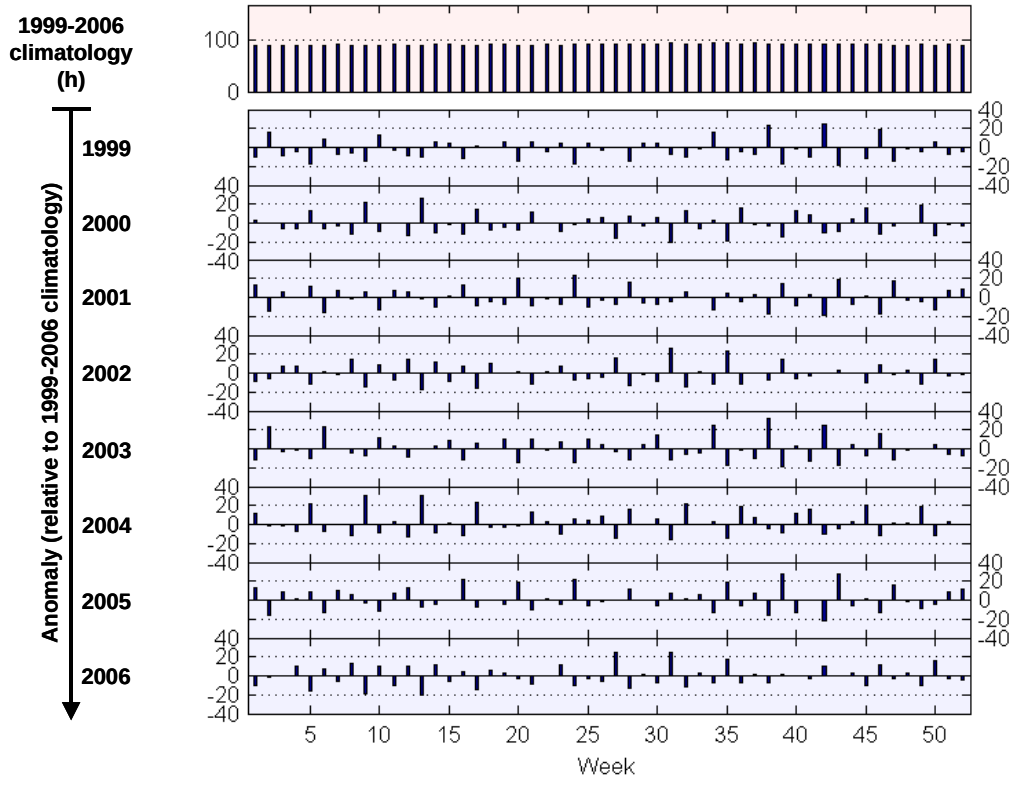

b)

Figure 4.5 – Climatology and anomalies for PHO in the estuary below r-km 50 (middle and lower estuary), under modern bathymetric and flow conditions, based

upon: a) the elevation criterion (10^9 h*m^2); and b) the (depth-averaged) velocity criterion (hours per week of PHO within the inundated area). PHO exhibits here a tidal signal associated with the spring-neap cycle. See, for example, weeks 38 and 42 in 1999 associated with the weaker neap tides shown in the elevation time series in Figure 4.6.

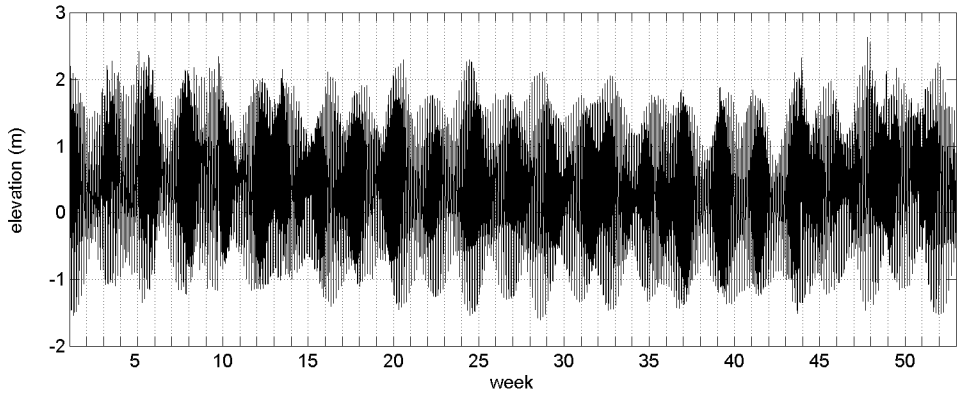

Figure 4.6 – Elevation time series at Tongue Point in 1999.

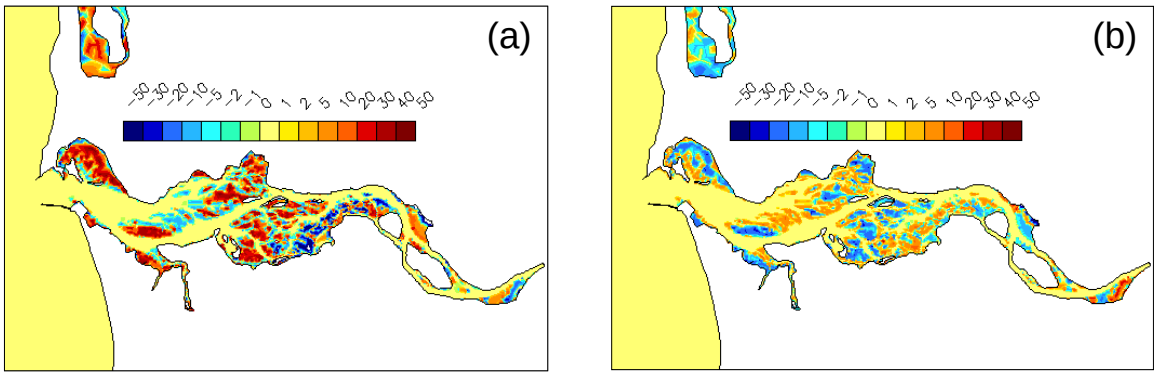

Figure 4.7 – Isoline map for PHO (hours) in the estuary under the elevation criterion: a) during an extreme neap tide (week 42, 1999) and b) during the following spring tide.

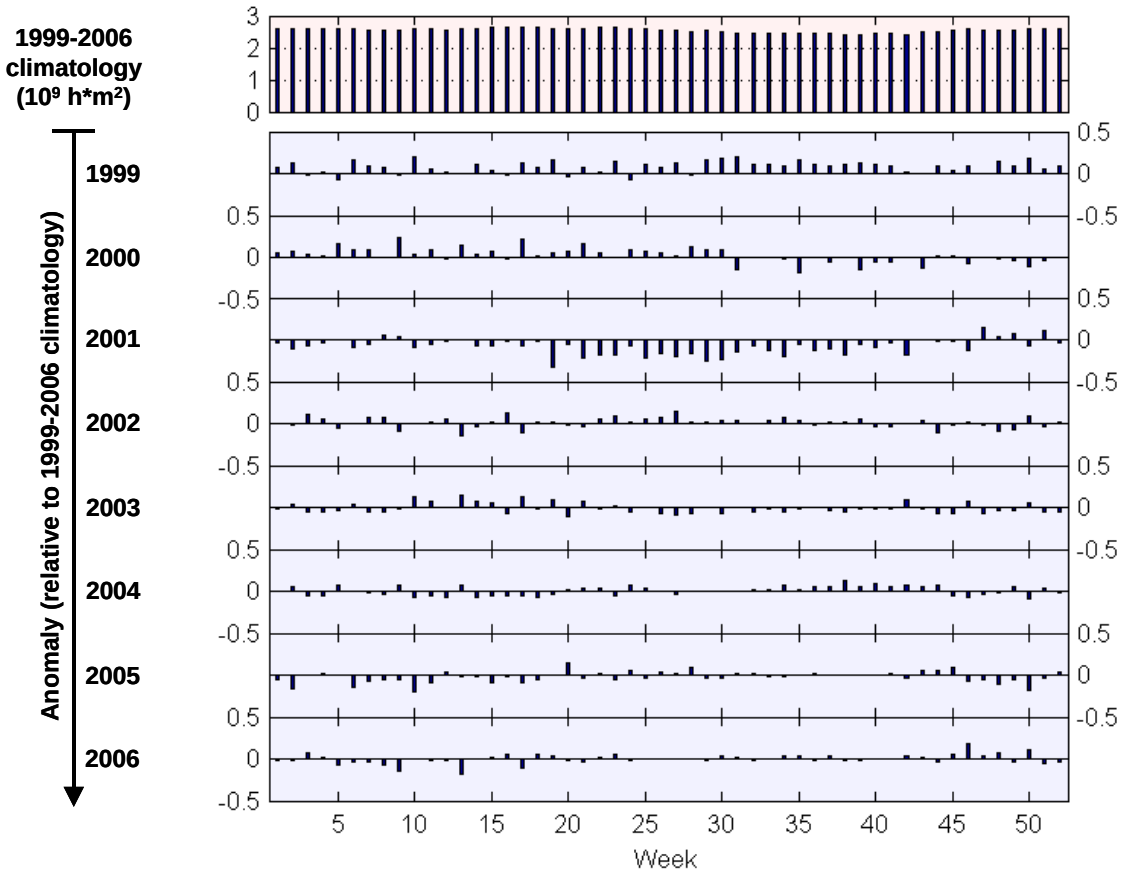

Figure 4.8 – Climatology and anomalies for PHO in the tidal freshwater zone between r-km 50 and r-km 80, based upon the elevation criterion (10^9 h*m^2 per week).

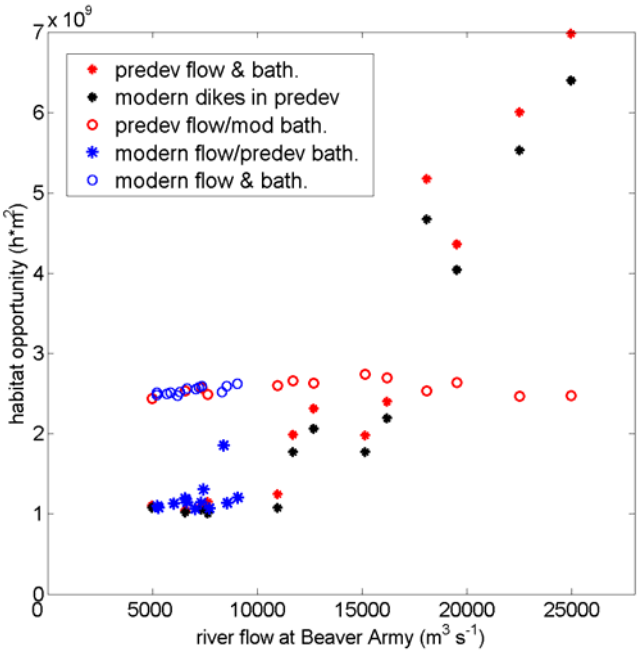

Figure 4.9 - PHO in the tidal freshwater zone between r-km 50 and r-km 80, based upon the elevation criterion (10^9 h*m^2 per week), in the different scenarios considered in the study to compare the effect of modern and predevelopment bathymetric and flow conditions.

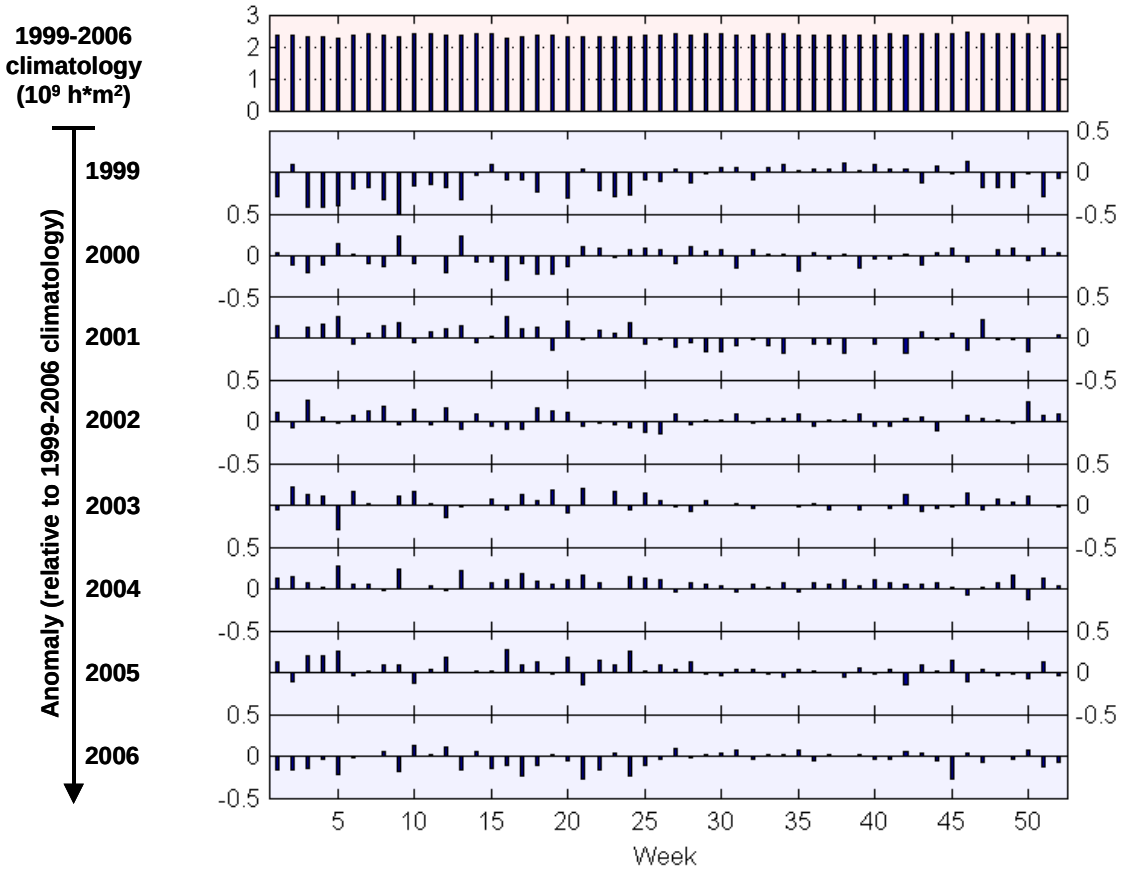

Figure 4.10 - PHO in the tidal freshwater zone between r-km 50 and r-km 80, under modern bathymetric and flow conditions, combining the constraints imposed by elevation and velocity conditions (10^9 h*m^2 per week).

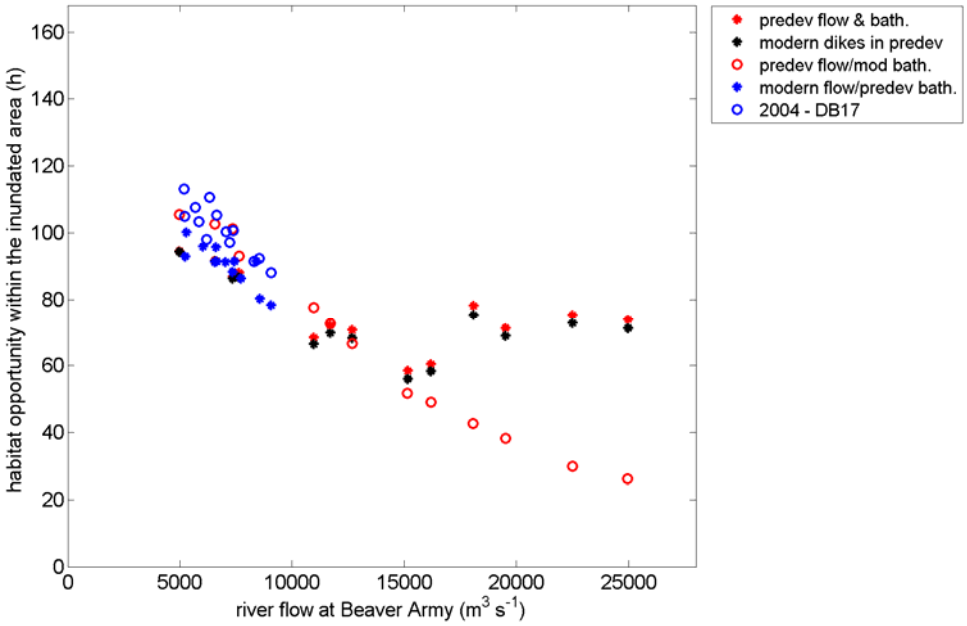

Figure 4.11 - PHO in the tidal freshwater zone between r-km 50 and r-km 80, based upon the (depth-averaged) velocity criterion, in the different scenarios considered in the study to compare the effect of modern and predevelopment bathymetric and flow conditions. Unit is hours of PHO within the inundated area per week.

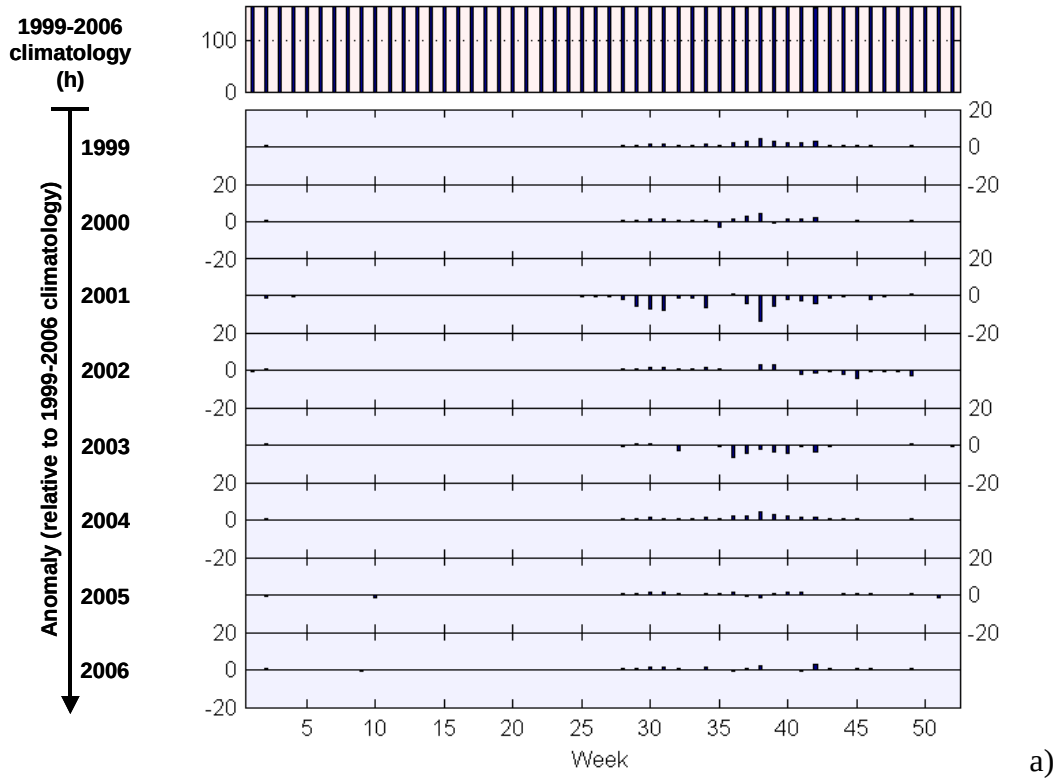

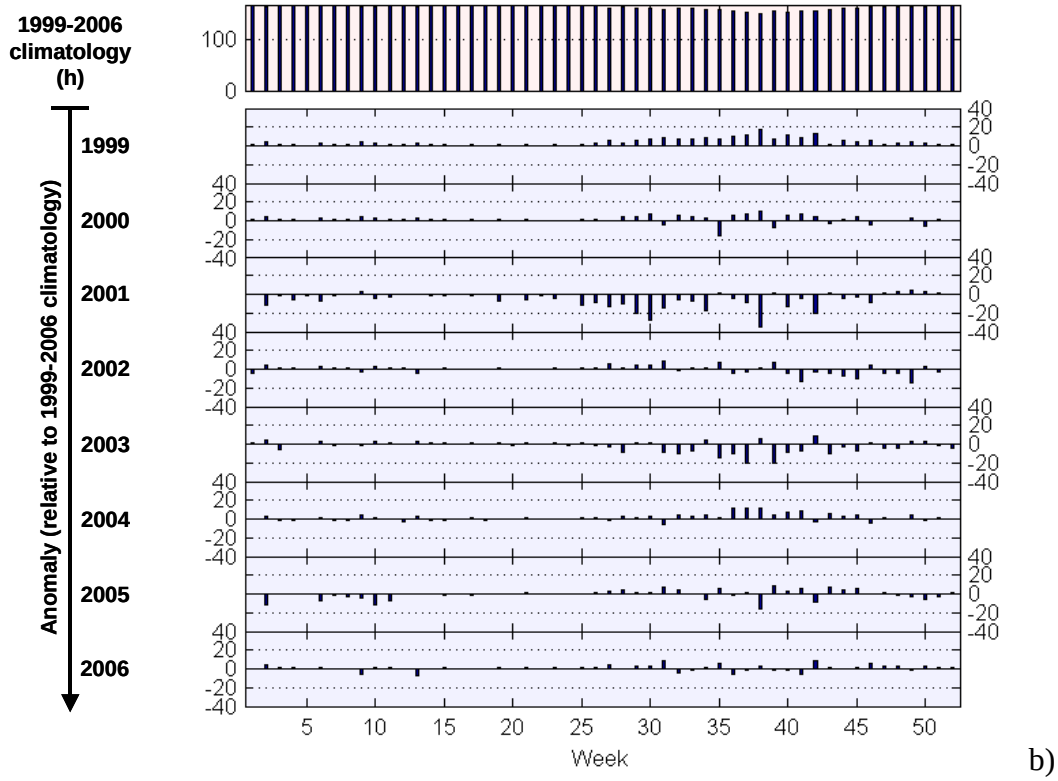

Figure 4.12 - PHO (hours within the inundated area per week) in (a) lower Cathlamet Bay and in (b) Grays Bay based upon the (depth-averaged) salinity criterion, under modern bathymetric and flow conditions.

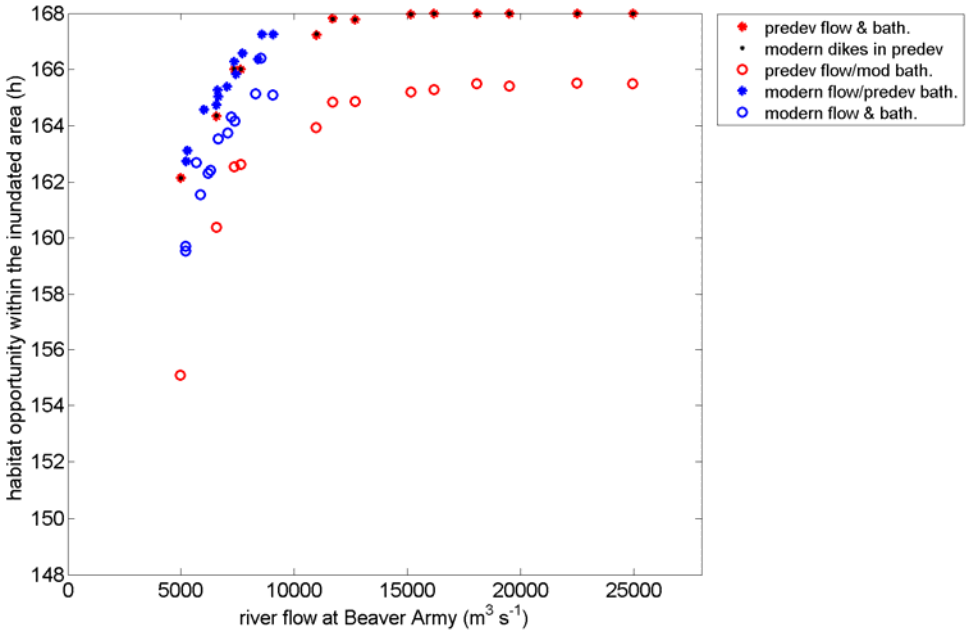

Figure 4.13 - PHO in the middle estuary, based upon the (depth-averaged) velocity criterion, in the different scenarios considered in the study to compare the effect of modern and predevelopment bathymetric and flow conditions.

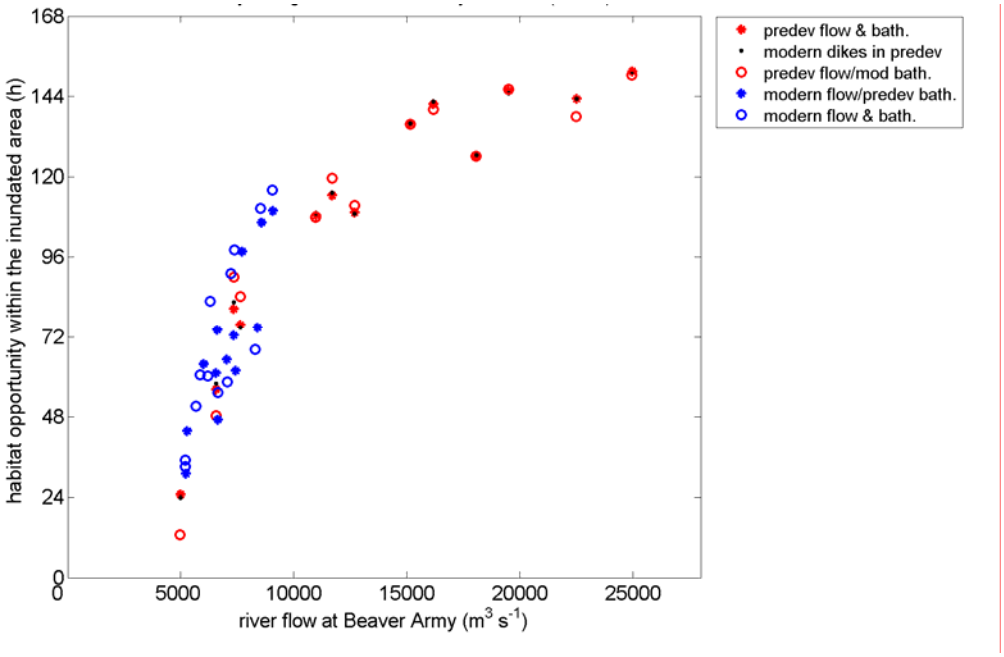

Figure 4.14 - PHO in Baker Bay, based upon the (depth-averaged) velocity criterion, in the different scenarios considered in the study to compare the effect of modern and predevelopment bathymetric and flow conditions.

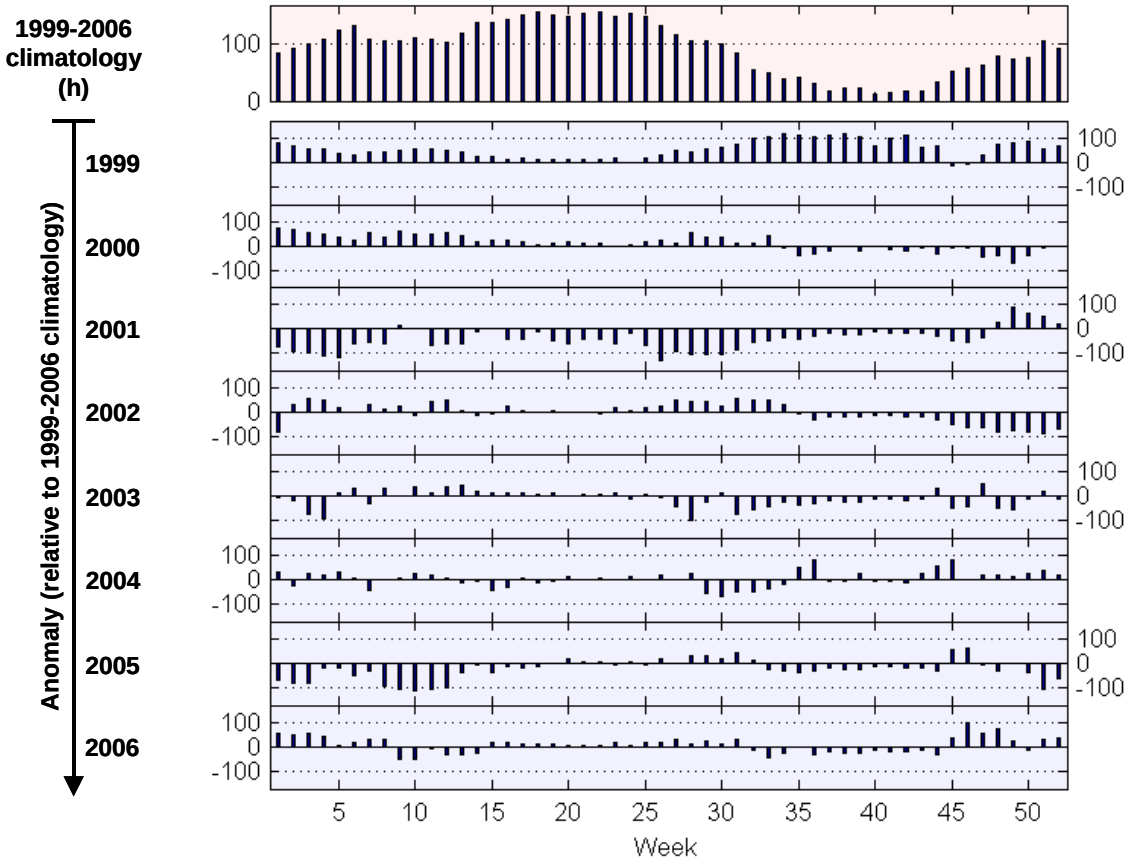

Figure 4.15 - PHO (hours within the inundated area per week) in Youngs Bay based upon the (depth-averaged) salinity criterion, under modern bathymetric and flow conditions.

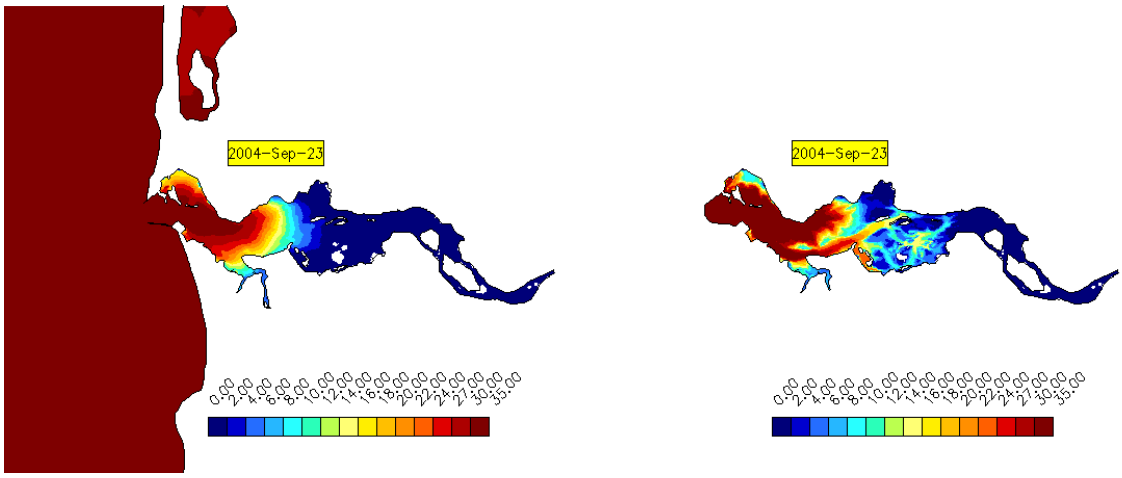

a) b)

Figure 4.16 - Isoline maps of salinity intrusion near the bottom as simulated in: a) database DB14, and b) database DB17.

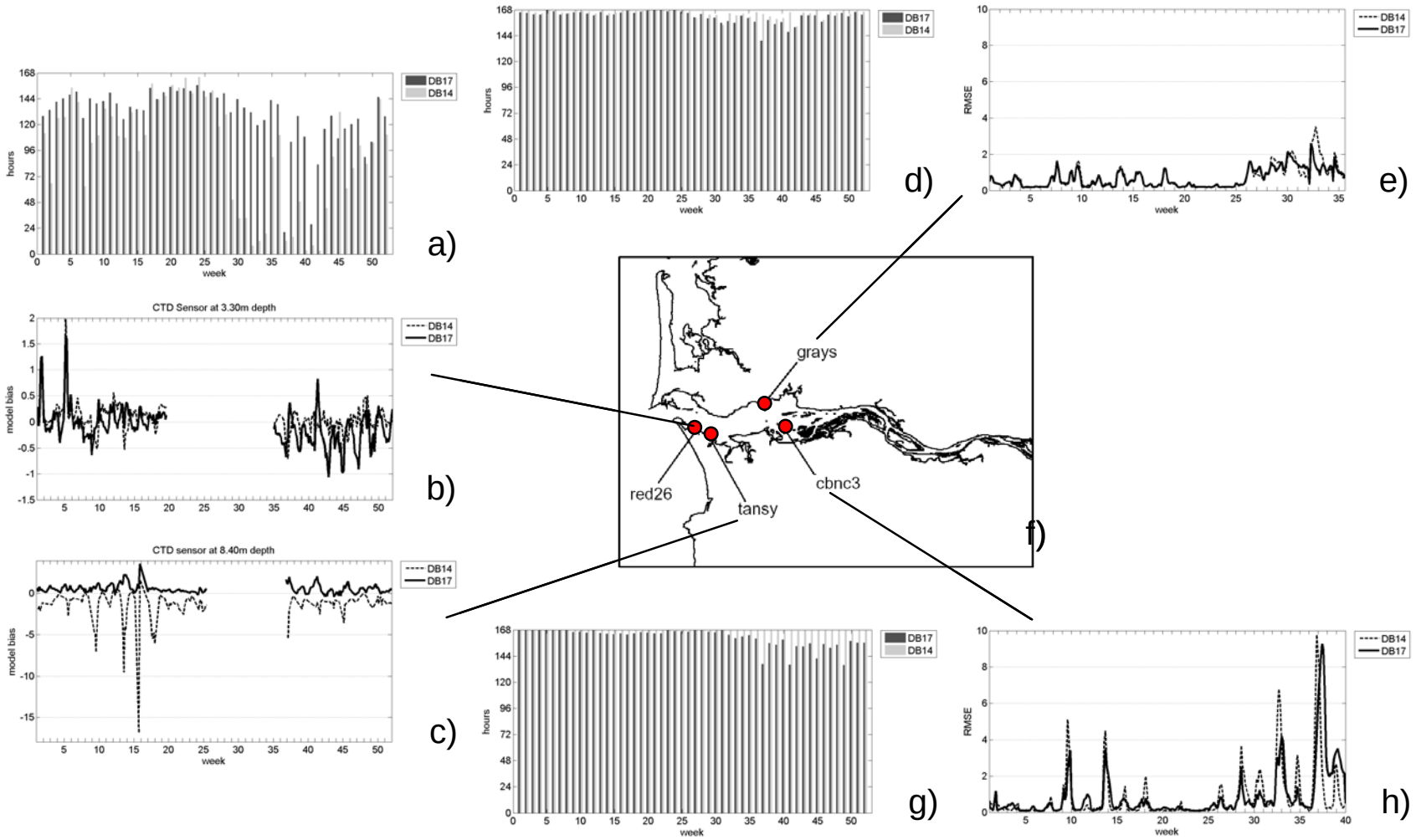

Figure 4.17 - a) PHO in Youngs Bay, based upon the (depth-averaged) salinity criterion, estimated respectively from DB17 and DB14 simulations (in hours of opportunity within the inundated area per week); b) model bias for the two sets of simulations measured relative to the salinity observed with a CTD sensor deployed at 3.3 m depth at station *red26* (the closest

station to Youngs Bay active in the CORIE/SATURN network with a near-surface sensor); c) model bias measured relative to the salinity observed with a CTD sensor deployed at 8.4 m depth at *tansy* (a station located just outside the mouth of Youngs Bay); d) PHO based upon the same criterion in Grays Bay; e) model root mean square error (RMSE) relative to the salinity observed at the *grays* station with a CTD sensor deployed at 1.6 m depth; f) location of the CORIE/SATURN stations g) PHO based upon the same criterion in Cathlamet Bay; h) model RMSE relative to the salinity observed at station *cbnc3* in the North Cathlamet Bay Channel with a CTD sensor deployed at 6.5 m depth.

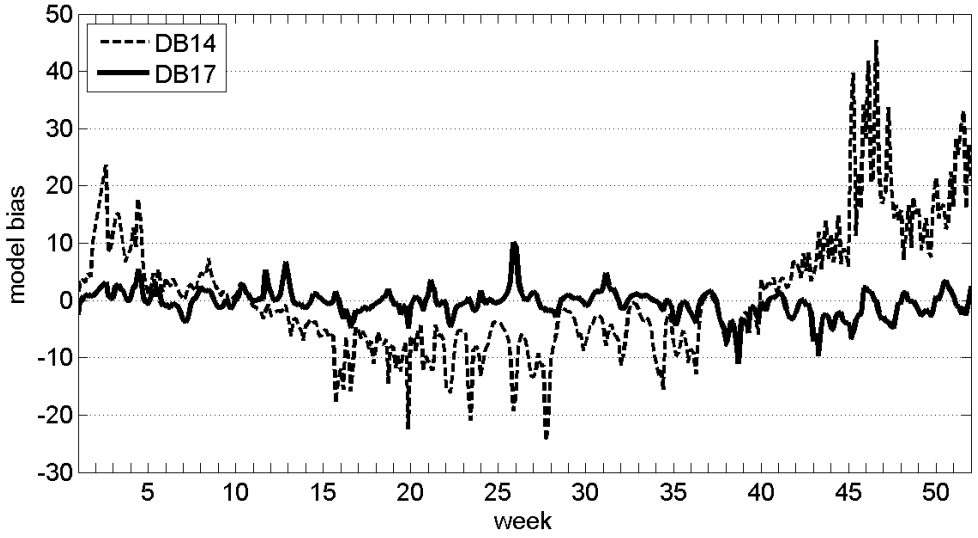

Figure 4.18 - Model bias for DB14 and DB17 simulations relative to the temperature observed at station *cbnc3* in the North Cathlamet Bay Channel with a CTD sensor deployed at 6.5 m depth.

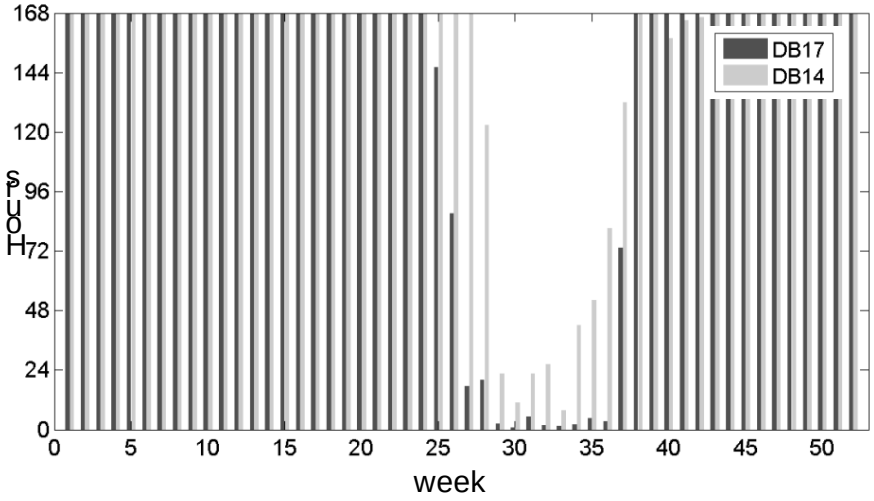

Figure 4.19 - Weekly hours of PHO in the middle estuary based upon the temperature criterion, under modern bathymetric and flow conditions, estimated respectively from DB17 and DB14.

Chapter 5

Conclusions and Future Work

5.1 Summary of findings

The research presented in this dissertation has demonstrated how high-resolution numerical models like SELFE and ELCIRC, providing the modeling capabilities of coastal-margin observatories, can be successfully used, either in a diagnostic or in a predictive mode, to:

- Address temporal scales that are relevant to investigate and separate anthropogenic change and natural (seasonal and interannual) variability;
- Help formulate hypotheses for the mechanisms that link performance of biological species to their physical environment;
- Inform natural resource management strategies, enabling investigation of alternative management scenarios.

The specific accomplishments of the research can be summarized as follows.

5.1.1 Demonstration of the high performance of CORIE/SATURN simulations in reproducing known dynamics of the CR plume

We proposed a systematic approach based upon a suite of integrative metrics, climatologies and anomalies of surface salinity, and a EOF analysis, using a simulation database of eight years of 3D baroclinic circulation in the CR estuary-plume-shelf system, to study variability in the plume dynamics at the interannual, seasonal and event scale.

We demonstrated that the modeling capability of the CORIE/SATURN coastal-margin observatory, which relies on the SELFE and ELCIRC numerical models, produces high-quality simulations that capture key features of the CR plume dynamics and its variability around two known seasonal patterns (Barnes et al. 1972; Hickey et al. 1998; Garcia-Berdeal et al. 2002; Hickey et al. 2005; Thomas and Weatherbee 2006).

The success of the approach in verifying the quality of the CORIE/SATURN simulations provided a rationale for using integrative metrics of the CR plume structure, from model simulations, to investigate the ecological implications of plume dynamics.

5.1.2 Improved understanding of the seasonal and interannual variability in the CR plume dynamics

The high-resolution, multi-year CORIE/SATURN simulations, which now extend even beyond the eight years we used in this analysis, showed the significant inter-annual variability of the CR plume orientation and extent, with potential implications on the variability of productivity over the Washington and Oregon shelf. The only other long-term simulation of the circulation in the CR estuary-plume-shelf system to date (Liu et al. 2008a; Liu et al. 2008b; MacCready et al. 2008) covered a period of solely three months (June-August) of 2004 and could only look at intraseasonal variability.

With these long-term simulations, we demonstrated, through a EOF analysis, the generality of earlier results obtained by observational studies based on a single survey year, in relation to winter patterns of plume variability (Hickey et al. 1998). We also showed that the finding of a prevalent bi-directional structure for the CR plume in the

summer months (Hickey et al. 2005; Liu et al. 2008a) holds true regardless of inter-annual variability.

In addition, we found that a bi-directional plume, with branches both north and south of the river mouth, while prevalent in the summer, can episodically occur also in the winter season.

5.1.3 Formulation of a hypothesis for the role of the CR plume in the survival of steelhead (*Oncorhynchus mykiss*)

Using the integrative plume metrics developed in the first part of this body of work, we examined whether the *intraseasonal* variability in smolt-to-adult survival rates (SARs) for steelhead and Snake River spring/summer Chinook salmon is dependent upon changes in the CR plume at the time the juvenile migrants enter the ocean. Previous studies relating salmon survival to regional and local ocean conditions looked at variability only at an interannual (e.g. Koslow et al. 2002; Logerwell et al. 2003; Scheuerell and Williams 2005) or decadal scale (Francis and Hare 1994; Mantua et al. 1997; Beamish et al. 1999).

Lagged cross-correlations between SARs and metrics of plume size and location suggested that steelhead benefit from the plume environment at a narrow window of time around their ocean entry. The result was robust to interannual variability of local ocean conditions. The influence of local (plume) conditions on the overall variability in steelhead survival became modest, however, when large-scale ocean conditions turned unfavorable.

The analysis did not indicate a role for the plume in the intraseasonal variability in Chinook survival. The differential response between the two species is consistent with observed and previously reported behavioral characteristics they exhibit. It corroborates our hypothesis that steelhead mainly use the plume to move quickly away from coastal habitats and the predation pressures associated with this environment, for a more direct migration to ocean habitats in the Gulf of Alaska. This hypothesis should be further pursued through continuation of focused observational studies.

Studies relating salmon survival to other coastal and ocean environmental processes have succeeded in explaining higher proportions of its variability than found in our analysis (Koslow et al. 2002; Logerwell et al. 2003; Scheuerell and Williams 2005). To increase the predictive power of their forecasting models, those studies employed multiple predictors, covering processes affecting different stages of the fish life history. If we establish that plume conditions influence steelhead survival in the very early stage of marine residence, metrics of plume structure, as predicted by the CORIE/SATURN models, could participate in similar multivariate forecasting models.

5.1.4 Simulations made directly relevant to salmon recovery and restoration strategies in the CR estuary

With multi-year simulations and scenario comparisons between modern and predevelopment flow and bathymetric conditions, we found that only strategies aimed at re-establishing some connectivity between the river and its floodplain through modification of *both* flow and bathymetry can restore access to shallow and low-velocity rearing habitats for salmon in the CR estuary.

We also found a deeper salt intrusion in the modern CR estuary, but the estimated consequent loss in physical habitat opportunity in the middle estuary was modest. How salinity intrusion is changing relative to historical conditions will need to be, however, a focus of further investigation.

Contrary to the early notion that high-resolution models are not optimal for simulations on time scales (seasons to years to a century) relevant to understand climate and human impacts on estuarine habitats (Kukulka and Jay 2003b), we demonstrated how the high-resolution capabilities of the CORIE/SATURN modeling system can be used to address these very scales.

5.1.5 Evaluation of model skills with the end question in mind

Evaluation of model skills has to go hand in hand with the science and management questions being posed. In Chapter 2, we performed a comprehensive evaluation of the skill of the CORIE/SATURN modeling system to reproduce CR plume dynamics and its

variability at multiple temporal and spatial scales. Duplicative realizations of multi-year simulations –generated, respectively, with the SELFE and ELCIRC models– were used to that purpose. In particular:

- We adopted an array of aggregated scores and concluded that no one score is adequate by itself to fully evaluate the skill of a model.
- We also found that no modeling solution outperforms others in all regards, a consideration we drew also from our work on estuarine physical habitat opportunity for salmon in Chapter 4.
- While we confirmed an overall superiority of SELFE over ELCIRC, and its improved ability to represent specific features of plume dynamics, we revealed that, to a certain extent, SELFE simulations achieved better performance in terms of RMSE –even when exhibiting a weaker correlation with the observations than ELCIRC simulations– by producing results that are conservatively less variable than the corresponding observations.
- We obtained this result by plotting distributions of modeled salinities, conditional on the value of observed salinity, which proved to be an effective way to synthesize many aspects of individual and relative model skills.
- An EOF analysis suggested a leading role for the river over winds in forcing the variability in the surface salinity field generated by the CR plume off the Washington and Oregon coasts, in simulations generated with SELFE. In contrast, the seasonal oscillation between upwelling- to downwelling-favorable winds resulted to be the leading forcing mechanism for simulations generated with ELCIRC. The relative importance of the two forcing mechanisms in the SELFE simulations continues to be subject of investigation, to verify whether it is determined by specific modeling choices.

Differences between simulations generated with the two models did not affect the results that informed our hypothesis for a role of the CR plume in the survival of juvenile steelhead. We assessed on a case-by-case basis the implications of model error and different modeling choices on our estimates of salmon habitat opportunity in the CR estuary, as determined by its physical environment.

5.1.6 Management implications

The research illustrated, through modeling, how different species and life history types of salmon respond independently to physical variations at a couple of different life stages (juvenile steelhead and Snake River spring/summer yearling Chinook in their utilization of the plume as they migrate from the river to the ocean environment; and subyearling Chinook salmon rearing in the estuary before their transition to the ocean). Different and independent responses among salmon species and life history types imply that no single optimum condition exists at any one life stage that will always maximize production of all species. The intent of modeling the plume and estuarine physical environments was not to support the unlikely proposition of finding a single "optimal" flow condition that supports both steelhead optimal utilization of the plume that enhances its overall survival and habitat opportunity in the estuary for subyearling Chinook salmon. Efforts to manage towards such as single optimum, disregarding the diversity of salmon life history strategies, may erode opportunities for life history expression and diminish population and ecosystem resilience, as discussed in Chapter 4. In fact, such a management paradigm, focused on boosting fish production by controlling or removing limiting factors for a single, homogeneous group of salmon, has long prevailed in the CR basin but has proven ineffective to reverse the sharp salmon decline in the CR (Lichatowich 1999; Bottom et al. 2005; Williams 2006). A recovery strategy aimed at sustaining or restoring salmon resilience by preserving the diversity of salmon life histories must consider the entire continuum of habitats (river, estuary, ocean) that salmon must navigate to complete their life cycles and return to spawn. Modeling provides a useful way to identify sources of variation and opportunities for life history expression at each salmon life stage that management may seek to emulate or restore. It also provides a useful tool to examine the responses or sensitivities of the salmon ecosystem to different variables and to variability both of natural and anthropogenic origin.

5.2 Future work

Another question that may be of interest to fishery biologists and inform salmon recovery strategies is how variability in river, ocean and atmospheric forcings may modify migration paths and residence times in the CR estuary and plume, potentially affecting survival success for outmigrating juvenile salmon.

Using the velocity field generated by ELCIRC simulations, we have conducted numerical tracking experiments of passive particles released at different times, depths and locations to compute residence times in the CR estuary-plume system. Neutrally buoyant conservative particles were seeded every fourth of an M2 tidal period (approximately 3 hours), over the entire span of a multiyear circulation database, at the locations shown in Figure 5.1. At each location, particles were seeded, typically, near the surface, at mid-depth and near the bottom. The database covered the three years 1999, 2001 and 2002, representative of a broad range of river flows (Figure 5.2a). Particles were tracked numerically for five consecutive weeks (using a Runge-Kutta tracking algorithm) and residence times were computed by detecting the time at which each particle left the domain of interest (for the first time). Two different domains were used: the first limited to the estuary; the second domain also including the shelf region shown in Figure 5.3a. In the case of the domain extending offshore, the direction from which particles left the domain was also recorded (and color-coded in the time series).

Long-term time series of residence times were so generated from the multi-year circulation database, to explore their inter-annual and seasonal variability in response to changes in river discharge and coastal winds. By seeding at different locations, we investigated the differential response of different types of environments (shallow regions versus channels).

The experiments have so far revealed that:

- Shallow regions are areas of longer retention (Figure 5.2);
- Shallow environments and well-connected channels exhibit a differential response to changes in river discharge, both seasonally and interannually (Figure 5.2).

- While residence times in the estuary are clearly influenced by river flow regimes, dominant processes affecting residence times in the domain extending over the plume region are wind-driven, and not necessarily linked to the presence of the plume (Figure 5.3).

Given the overall superiority we demonstrated for SELFE over ELCIRC, we are currently validating and expanding results from these experiments with simulations generated with SELFE.

5.3 Conclusions

The long-term, multi-year databases of simulated circulation produced by the CORIE/SATURN coastal margin observatory open unparalleled data mining opportunities to continue investigating the dynamics of the CR estuary and plume at multiple temporal and spatial scales, and its ecological implications. They truly enable a paradigm shift in the way we investigate seasonal and interannual variability and anthropogenic change, and offer capabilities that can become integral, but at the same rethink, adaptive management approaches.

5.4 References

Barnes, C. A., A. C. Duxbury and B.-A. Morse. 1972. Circulation and selected properties of the Columbia River effluent at sea. In: A. T. Pruter and D. L. Alverson, Eds. *The Columbia River estuary and adjacent ocean waters*. University of Washington Press, Seattle, WA**:** 41-80.

Beamish, R. J., D. J. Noakes, G. A. McFarlane, L. Klyashtorin, V. V. Ivanov and V. Kurashov. 1999. The regime concept and natural trends in the production of Pacific salmon. *Canadian Journal of Fisheries and Aquatic Sciences* 56: 516-526.

Bottom, D. L., C. A. Simenstad, A. M. Baptista, D. A. Jay, J. Burke, K. K. Jones, E. Casillas and M. H. Schiewe. 2005. *Salmon at River's End: The Role of the Estuary in the Decline and Recovery of Columbia River Salmon*, U.S. Dept. of Commerce NOAA Technical Memorandum NMFS-NWFSC-68.

Francis, R. C. and S. R. Hare. 1994. Decadal-scale regime shifts in the large marine ecosystems of the Northeast Pacific: a case for historical science. *Fisheries Oceanography* 3: 279-291.

Garcia-Berdeal, I., B. M. Hickey and M. Kawase. 2002. Influence of wind stress and ambient flow on a high discharge river plume. *Journal of Geophysical Research* 107 (C9): 3130.

Hickey, B. M., S. Geier, N. Kachel and A. MacFadyen. 2005. A bi-directional river plume: the Columbia in summer. *Continental Shelf Research* 25: 1631-1656.

Hickey, B. M., L. J. Pietrafesa, D. A. Jay and W. C. Boicourt. 1998. The Columbia River Plume Study: Subtidal variability in the velocity and salinity fields. *Journal of Geophysical Research* 103(C5): 10339-10368.

Koslow, J. A., A. J. Hobday and G. W. Boehlert. 2002. Climate variability and marine survival of coho salmon (*Oncorhynchus kisutch*) in the Oregon production area. *Fisheries Oceanography* 11(2): 65-77.

Lichatowich, J. A. 1999. *Salmon Without Rivers: A History of the Pacific Salmon Crisis*. Island Press, Washington, DC

Liu, Y., P. MacCready and B. M. Hickey. 2008a. Columbia River Plume Patterns as Revealed by a Hindcast Coastal Ocean Circulation Model in Summer 2004. *Submitted to Geophysical Research Letters*.

Liu, Y., P. MacCready, B. M. Hickey, E. P. Dever, P. M. Kosro and N. S. Banas. 2008b. Evaluation of a coastal ocean circulation model for the Columbia River plume in summer 2004. *Submitted to Journal of Geophysical Research*.

Logerwell, E. A., N. J. Mantua, P. W. Lawson, R. C. Francis and V. N. Agostini. 2003. Tracking environmental processes in the coastal zone for understanding and predicting Oregon coho (*Oncorhynchus kisutch*) marine survival. *Fisheries Oceanography* 12(6): 554-568.

MacCready, P., N. S. Banas, B. M. Hickey, E. P. Dever and Y. Liu. 2008. A model study of tide- and wind-induced mixing in the Columbia River estaury and plume. *Continental Shelf Research* doi:10.1016/j.csr.2008.03.015.

Mantua, N. J., S. R. Hare, Y. Zhang, J. M. Wallace and R. C. Francis. 1997. A Pacific interdecadal climate oscillation with impacts on salmon production. *Bulletin of the American Meteorological Society* 78(6): 1069-1079.

Scheuerell, M. D. and J. G. Williams. 2005. Forecasting climate-induced changes in the survival of Snake River spring/summer Chinook salmon (*Oncorhynchus tshawytscha*). *Fisheries Oceanography* 14(6): 448-457.

Thomas, A. C. and R. A. Weatherbee. 2006. Satellite-measured temporal variability of the Columbia River plume. *Remote Sensing of Environment* 100: 167-178.

Williams, R. N., Ed. 2006. *Return to the River: Restoring Salmon to the Columbia River*, Elsevier Academic Press.

Figures

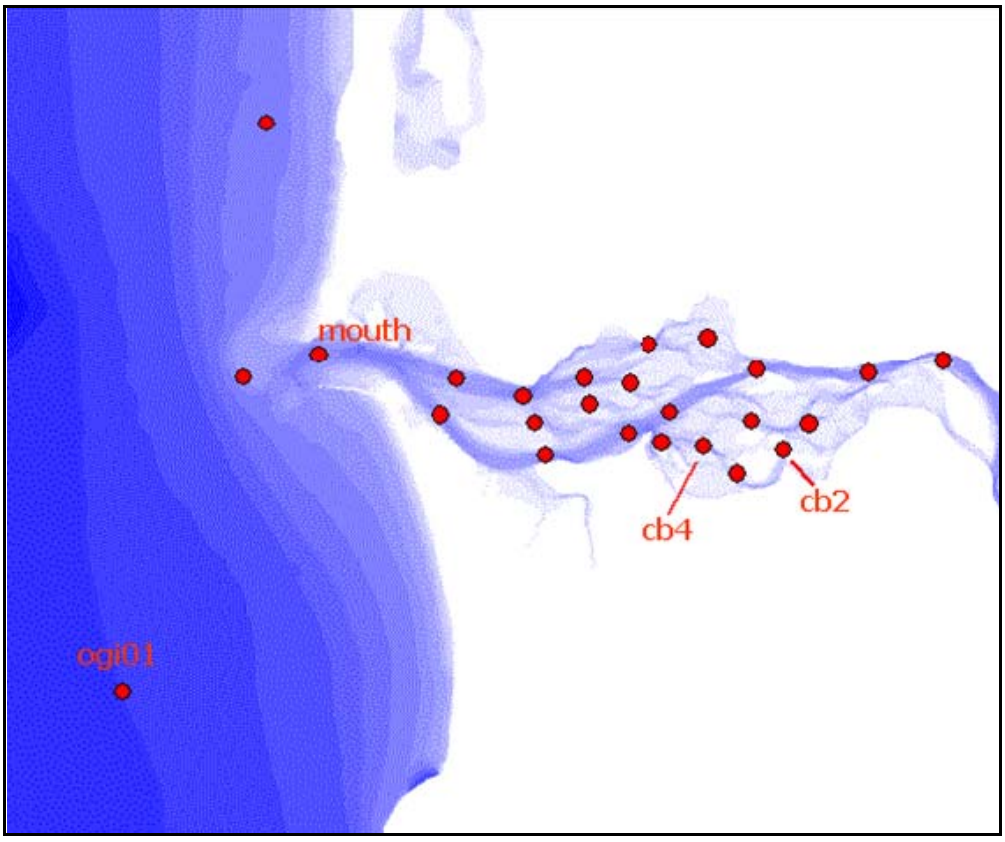

Figure 5.1

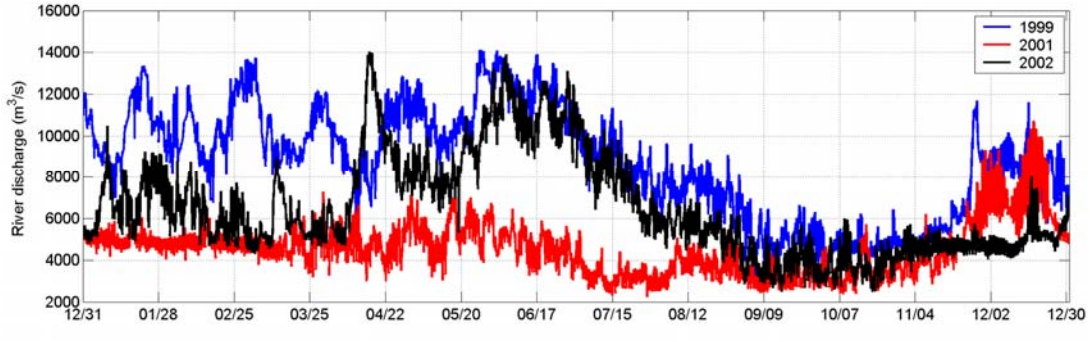

a)

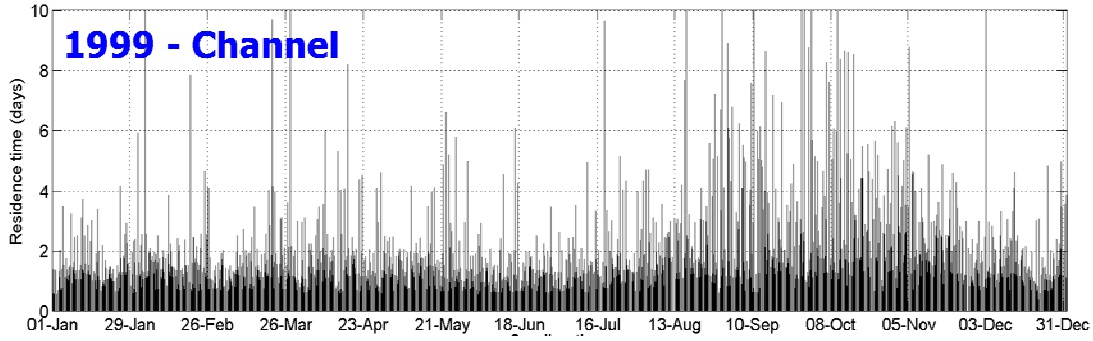

b)

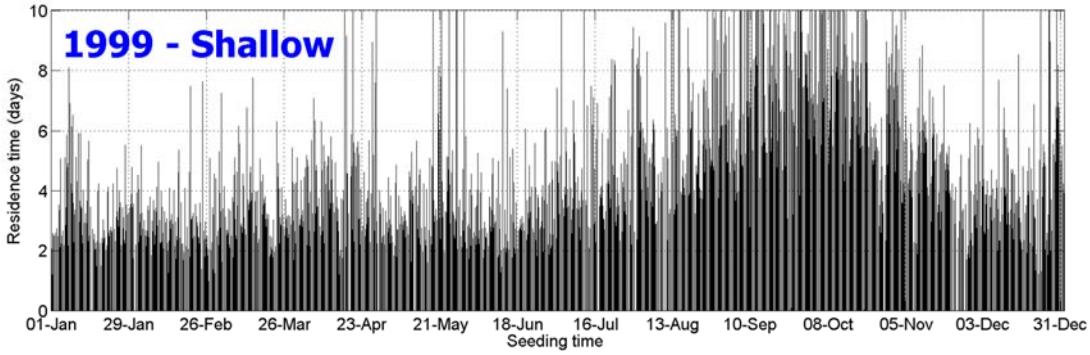

c)

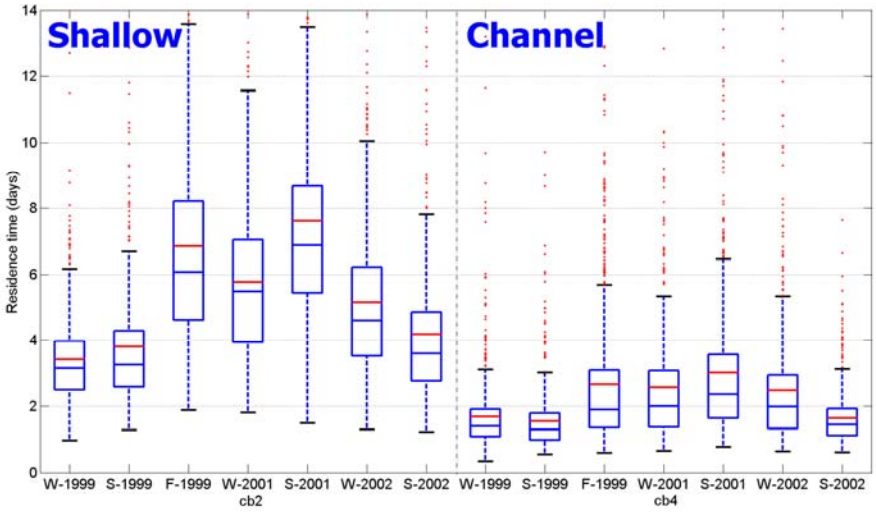

d)

Figure 5.2

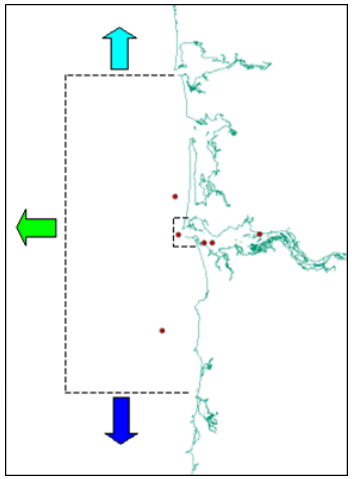

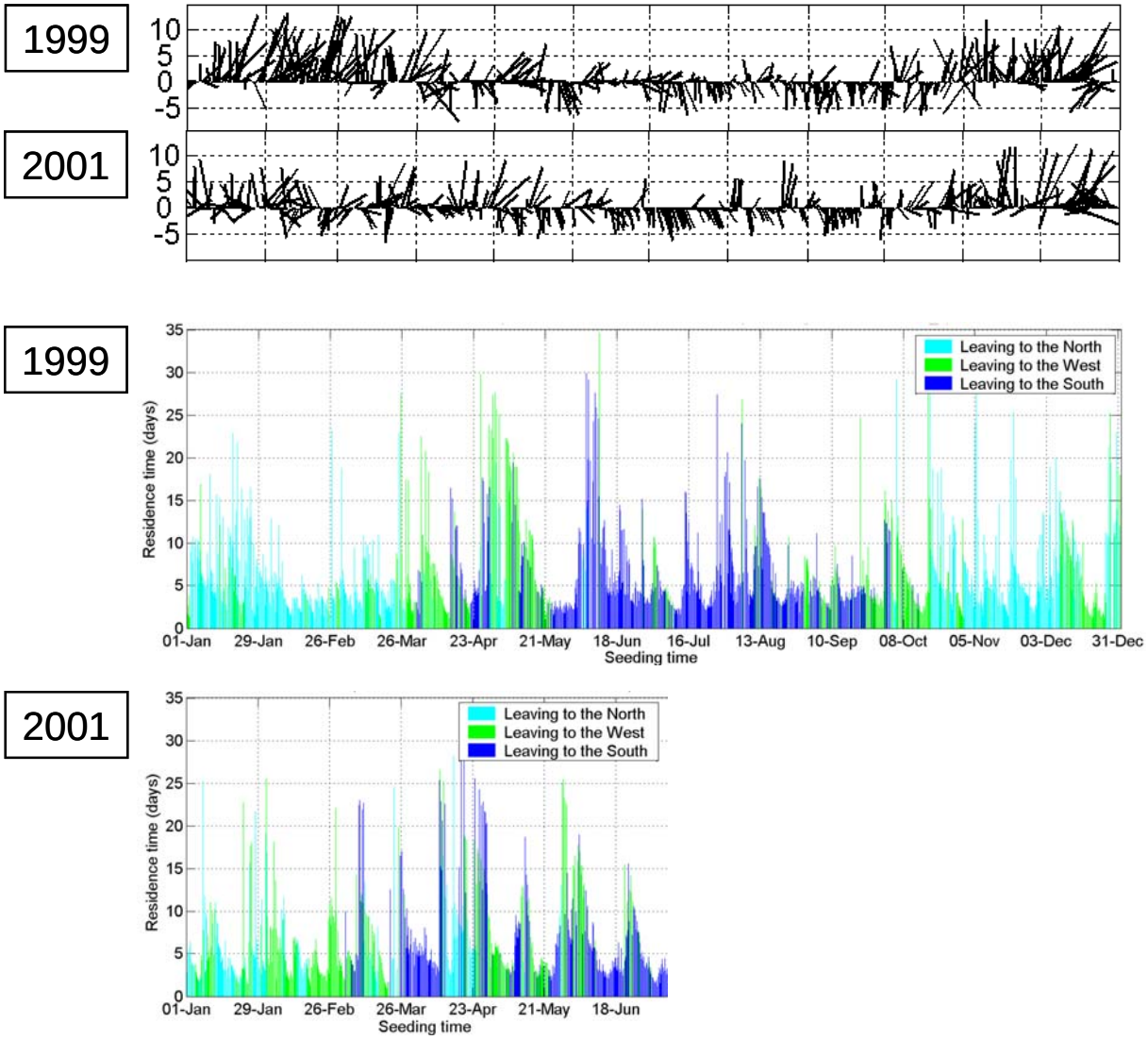
1999
2001
10
5
0
-5
1999
Leaving to the North
Leaving to the West
Leaving to the South
Residence time (days)
35
30
25
20
15
10
5
0
01-Jan
29-Jan
26-Feb
26-Mar
23-Apr
21-May
18-Jun
16-Jul
13-Aug
10-Sep
08-Oct
05-Nov
03-Dec
31-Dec
Seeding time
2001
Leaving to the North
Leaving to the West
Leaving to the South
Residence time (days)
01-Jan
29-Jan
26-Feb
26-Mar
23-Apr
21-May
18-Jun
Seeding time

Figure 5.3